UFL/COEL/MPR-2003/001

PHYSICAL MODELING OF A FLOATING BREAKWATER WITH A MEMBRANE

by

Michael W. Hermanson

2003

PHYSICAL MODELING OF A FLOATING BREAKWATER WITH A MEMBRANE

By
MICHAEL W. HERMANSON

A REPORT PRESENTED TO THE CIVIL AND COASTAL ENGINEERING DEPARTMENT OF THE UNIVERSITY OF FLORIDA IN PARTIAL FULFILLMENT OF THE REQUIREMENTS FOR THE DEGREE OF MASTER OF SCIENCE

UNIVERSITY OF FLORIDA

2003

ACKNOWLEDGMENT

I would like to give a sincere thanks to my Supervisory Committee chair, Dr. William McDougal for his patience, guidance, and selflessness throughout the duration of this project. This project could not have been completed without his professional expertise and personal dedication. Also, I would like to thank Dr. Robert Dean and Dr. Robert Thieke for their participation as members of my supervisory committee.

I would also like to thank Jim Joiner and Sidney Schofield for their assistance in fabrication of the physical model and setting up the equipment used for this project. Additionally, a hearty thanks to my friends and fellow graduate students, Rashmi Patra and Enrique Gutierrez, for taking the time in their busy schedules to assist me with the data collection process of this project. Also, I would especially like to thank my wife, Romina, for her patience and support during my graduate studies.

TABLE OF CONTENTS

page

LIST OF TABLES

LIST OF FIGURES

LIST OF SYMBOLS

d	draft of breakwater
g	acceleration due to gravity
h	still water depth
H_i	incident wave height
H_r	reflected wave height
H_t	transmitted wave height
H_{max}	standing wave envelope maximum height
H_{min}	standing wave envelope minimum height
k	wave number
k_o	deep water wave number
k_p	permeativity
k_s	spring stiffness
K_d	dissipation coefficient
K_e	energy coefficient
K_r	reflection coefficient
K_t	transmission coefficient
L	wavelength
t	breakwater total height
T	wave period
W	breakwater width
π	3.14159265359
Φ	total velocity potential
Φ_o	velocity potential due to incident waves
Φs	velocity potential due to scattered waves
Φj	velocity potential due to radiated waves

Abstract of Engineering Report Presented to the Department of Civil and Coastal Engineering of the University of Florida in Partial Fulfillment of the Requirements for the Degree of Masters of Science

PHYSICAL MODELING OF A FLOATING BREAKWATER WITH A MEMBRANE

By

MICHAEL W. HERMANSON

December 2003

Chair: Dr. William G. McDougal
Major Department: Department of Civil and Coastal Engineering

A physical model study of a floating breakwater with an attached vertical membrane was conducted. The objective was to determine if the wave protection provided by a floating breakwater can be improved by the addition of a membrane. The wave transmission characteristics were analyzed for nine different structural configurations. The different configurations examined the compliance of the moorings and the length, position, and permeability of the membrane. The nine configurations were tested at 8 different wave periods ranging from 0.5 seconds to 1.2 seconds and each test was performed twice. Thus, 72 combinations were examined and approximately 150 flume runs were completed to collect data for this project.

The average transmission coefficient for each of the nine cases ranged from 0.705 to 0.853. In all cases tested, the addition of a membrane to the floating breakwater reduced the transmitted wave height relative to the structure with no membrane. The

average wave transmission coefficient was 0.85 for the structure with no membrane. The average far all the configurations with a membrane was 0.75, or about a 12 % reduction. The most effective membrane configuration gave a reduction of 17 %. For the breakwater configurations and wave conditions tested, the following results were observed:

1) A membrane length that is ¼ of the water depth in length is more effective than membrane lengths of ½ the depth and the full depth.

2) Lower transmission was obtained by placing the membrane at the lee side of the structure rather than the front or center.

3) A permeable membrane is more affective than an impermeable membrane.

4) Elastic mooring lines had a lower transmission than stiff moorings.

CHAPTER 1
INTRODUCTION

1.1 Background

Common applications of floating breakwaters are to protect harbors, marinas, moored vessels, and offshore structures from wave attack. Floating breakwaters provide wave protection by reflecting the incident wave, moving out of phase with incident wave to cause to cancellations, or by dissipating wave energy. In the first two types, wave energy is conserved. Examples are floating pontoon breakwaters and floating docks. Examples of breakwaters that are primarily dissipative are floating tire breakwaters and perforated screens. Advantages of floating breakwaters over conventional structures include low environmental impact, lower initial costs, and structure portability. Their disadvantages include large forces in the moorings and connections, and that floating breakwaters tend to be most effective only for short period waves.

Wave attenuators are often cost-effective where other breakwater solutions may not be feasible. Attenuators are visually unobtrusive allowing for easy viewing of the waterfront. Floating wave attenuators do not encourage scouring as rubble mound or pile supported structure might. Well designed wave attenuators do not restrict water circulation or tidal flow minimizing adverse effects on water quality. Also, floating breakwaters do not block the migration of fish. Wave attenuators can often be designed for multi-purpose usage. They may be used for transient moorage, public access and fishing, or barriers for floating debris.

The cost of construction of a rubble mound breakwater is strongly a function of the design water depth and deeper water often makes their use an expensive solution. The attractiveness of floating type breakwaters is highlighted by their low initial costs, which are relatively independent of water depth. The nature of their design also makes them, rapidly deployable and an alternative for short-term applications.

A possible method of improving floating breakwater performance is the inclusion of an attached vertical membrane. A vertical-membrane floating breakwater consists of three parts: 1) A floatation component providing buoyancy for the breakwater; 2) A vertical membrane that is connected to the floatation component; and 3) A mooring system. These membrane-modified floating breakwaters offer an attractive means of increasing wave protection. Such structures are lightweight, inexpensive, and easily deployed, and are reusable. These membrane-modified structures may also be used as silt curtains to prevent the spread of turbidity-induced sediment suspension caused by marine construction, dredging, or maintenance operations.

1.2 Objectives

The objective of this project is to determine if the wave protection provided by a floating breakwater can be improved by the addition of a vertical membrane. Physical model tests of a floating breakwater with and without an attached vertical membrane were conducted in nine configurations. The configurations examined included changes in the compliance of the moorings and the length, position and permeability of the membrane. The transmission characteristics of the structure were analyzed and the most effective configurations identified.

A particular application of this technology is as a retrofit to existing floating docks. The installation of a membrane on an existing dock can result in an increase in wave protection. With this application in mind, the dimensions in the physical model were selected to be representative of commonly available floating docks sections.

1.3 Diffraction Theory

An analytical model is being developed in conjunction with this experimental project. The analytical model is based on diffraction theory. A brief description introduces terminology that is useful for describing the observed experimental results. Incident waves interacting with a pontoon floating breakwater undergo significant changes. These are scattering, the reflection and transmission which occur if the floating breakwater is fixed and radiation, the waves which are generated by the motion of the breakwater. The flow field in the vicinity of a large fixed structure can be described in terms of the total velocity potential. This consists of the velocity potential due to the incident waves, Φ_o, and the velocity potential due to the wave scattered by the fixed body, Φ_s. The resulting relation is

$$\Phi = \Phi_o + \Phi_s \tag{1.1}$$

When the body is free to move, the motion of the body radiates waves. The velocity potential including body motions is written as

$$\Phi = \Phi_o + \Phi_s + \sum_{j=1}^{6} \Phi_j \tag{1.2}$$

where Φ_j are the radiated potential due to the structure motions. The total velocity potential consists of potentials due to the incident waves, scattered waves, and radiated

waves in each of the six degrees of freedom of structure motion. In general, a body can have six degrees of motion, three translational and three rotational. Each of these could generate a wave as indicated in (1.2). However, in a two-dimensional wave channel such as the flume used for the testing in this project, the motion is restricted to three degrees of freedom. These are surge, heave, and pitch.

The forces and moments on the floating breakwater are determined by using (1.2) in the Bernoulli equation and integrating the pressure over the surface of the breakwater. The resulting forces and moments are used in the equations of motion for the breakwater for each of the six degrees of freedom. Each degree of freedom is a linear mass, spring damper system subjected to harmonic forcing and each degree of freedom will have a natural frequency. Forcing at this frequency will result in resonance. The physical model tests were designed to span the undamped natural heave frequency of the structure.

CHAPTER 2
EXPERIMENTAL FACILITIES AND PROCEDURES

2.1 Testing Facility

Laboratory experiments were performed in the tilting flume located at the University of Florida Coastal and Oceanographic Engineering Laboratory. The tests were conducted by exposing each breakwater to a series of monochromatic waves and then measuring the incident, reflected, and transmitted wave heights and structure displacements.

The tilting flume is constructed of steel and glass and is approximately 0.6 meters wide, 1.0 meters deep, and 15 meters in length. The flume is equipped with a piston-type wavemaker powered by a variable speed 3 phase, 1.5 horsepower electric motor. An empirical relationship was developed relating wave periods and the motor speed settings on the speed controller Measured wave period data were fit with a polynomial trend line (Fig. 2.1) and used to determine the precise motor speed setting for each wave period examined. Wave heights were measured by resistance wave gauges. One gauge was permanently mounted behind the structure. A second gauge was mounted on a movable cart on the seaward side of the structure. The wave envelope method was used to determine the incident and reflected waves. This technique is discussed in section 2.4.2. Waved data were collected at a rate of 20 hertz and recorded using Global Lab software. The recorded data were then downloaded and analyzed using both MATLAB and EXCEL computer programs.

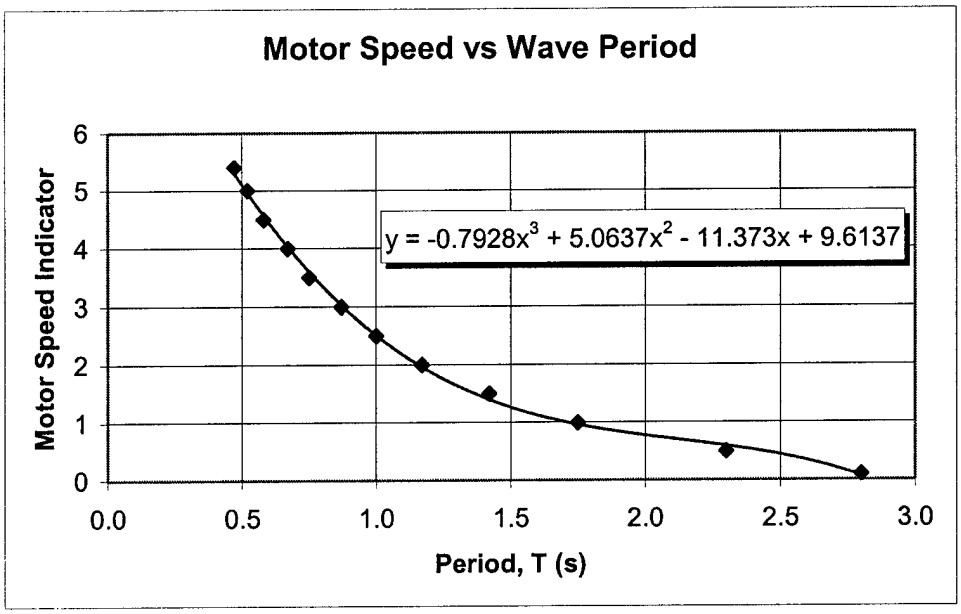

Figure 2.1 Motor speed indicator curve.

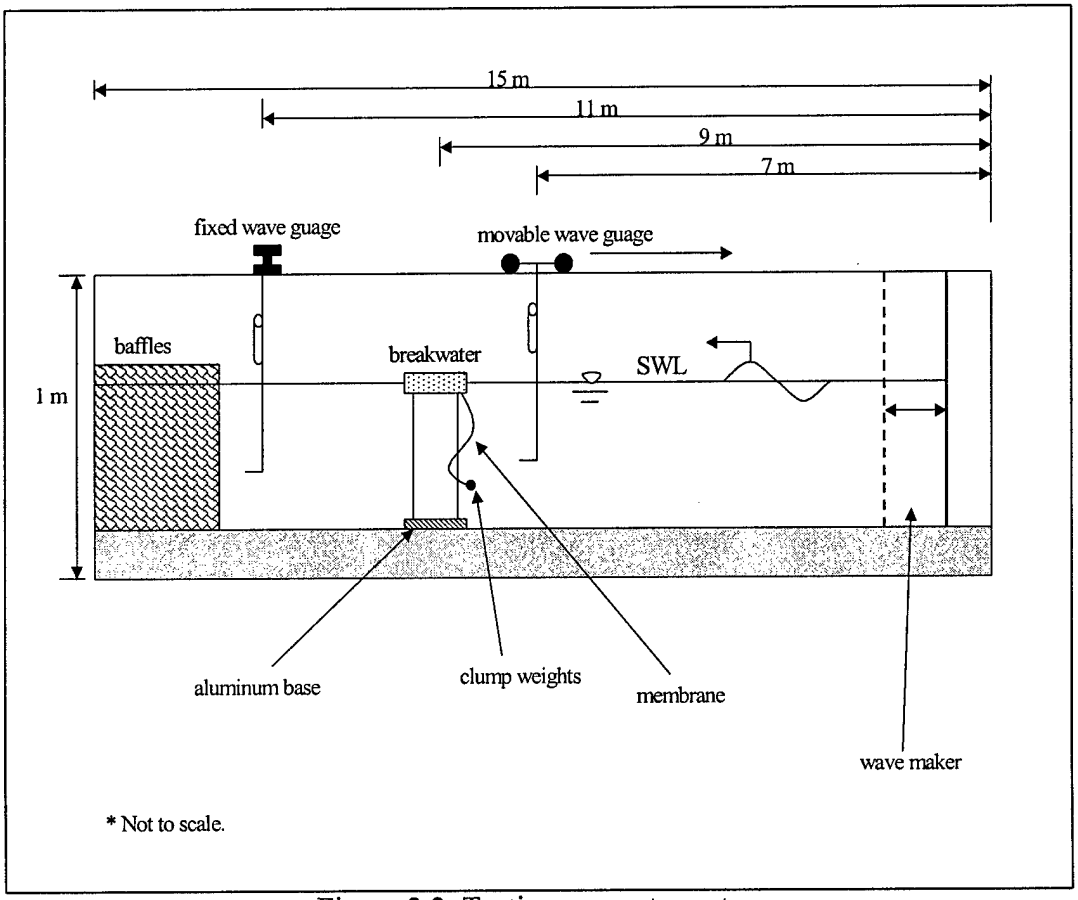

Figure 2.2. Testing apparatus setup.

2.2 Breakwater Construction

2.2.1 Physical Dimensions

To determine the dimensions of the model, the following parameters were assumed for the prototype:

Breakwater width, W_p:	1.2- 2.4 m
Breakwater height, t_p:	76- 81 cm
Wave Period, T_p:	3- 6 seconds
Water depth, h_p:	3- 5 m
Draft, d_p:	31- 39 cm

where t_p is the total height of the breakwater (draft + freeboard). These prototype values were determined primarily from a technical manual provided by Oldcastle which describes the Trus-Channel Concrete Marina System. The float sections used in this system have widths ranging from 1.2 m to 2.4 m and a heights ranging from 76 cm to 81 cm with drafts ranging from 31 cm to 39cm.

The range of wave periods which can be generated in the tilting flume is approximately 0.5 to 2.0 seconds. However, wave periods longer than 1.5 seconds are very difficult to measure using the envelope method and available wave gauges. For a model period of one second and a prototype period of 4.5 seconds Froude similitude yields a scale ratio of 1/20.3

$$\frac{L_m}{L_p} = \left(\frac{T_m}{T_p}\right)^2 = \left(\frac{1}{4.5}\right)^2 = \frac{1}{20.3} \tag{2.1}$$

where the width of the model is the characteristic length.

A parameter which is important in the performance of a floating breakwater is the ratio of the breakwater width to the wavelength. This yields the following scaling

$$\frac{W_m}{W_p} = \frac{L_m}{L_p} \tag{2.2}$$

For deep water conditions, (2.1) and (2.2) yield the same scaling. For the intermediate water depths corresponding to typical prototype applications, the ratio is trivially different. For a prototype wave period , T_p= 4.5 s, and a prototype water depth, $h_{p=}$ 4.0 m, the prototype wave length is 24.4 m. For a model wave period , T_m= 4.5 s, and a prototype water depth, $h_{m=}$ 0.2 ($\approx h_p$/ 20 m), L_p= 1.21 m and the scale ratio is 1/20.2. Unfortunately, the flume in which the tests were conducted is not configured so that large waves can be generated at such a shallow water depth. Therefore, the water depth for the tests was increased to h_m= 0.406 to enable the generation of larger waves.

The final model scale adopted for the tests was appropriately 1/14. This gave a model width of W_p= 129 mm and a model height of 56 mm. The model length was determined based on the flume width of 607 mm minus 25.5 mm clearance on each end for a total of 556 mm. The model dimensions used for the testing are summarized in Figure 2.3. All tests were conducted at a water depth of 406 mm. This corresponds to a water depth of 5.6 m at the prototype scale. Model waves were tested with periods ranging from 0.54 to 1.29 s. This corresponds to a prototype wave period range using Froude similitude of 2.0 to 4.8 s.

The breakwater was moored to a 559 mm x 127 mm x 13 mm thick aluminum plate which was placed at the bottom of the flume and anchored with two lead weights. It was positioned approximately 2/3 the length of the flume (11 m) away from the wave maker. The stationary wave gauge was placed approximately two meters from the model and on the leeside of the model. The movable wave gauge was located on the incident side of the model approximately 2.0 m in front of the model as shown in Fig. 2.2.

Baffling was installed at the end of the tank to dissipate the transmitted waves and to reduce the amount of time between successive flume tests. The baffling was made up of six interconnected plastic cubical crates stuffed with a permeable filter fabric

2.2.2 Model Assembly

The core of the breakwater consists of a 51 mm-thick layer of closed cell polyethylene foam. An aluminum plate was attached to the top and bottom of the foam and connected with six 6 mm diameter bolts each 89 mm in length. An eye bolt in each of the four corners and 2 thru bolts in the mid section of the model were used. Using a specified draft-to- height ratio of 0.46, the model draft was determined to be 23 mm or approximately ½ of the model core thickness.

To achieve the desired draft, short links of lead weights were evenly distributed in the foam core to increase the weight of the model. In total, 32 pieces of lead, each weighing 11.7 g, were used. Many small pieces, instead of fewer larger pieces, were used in an effort to simulate a homogeneous material. The addition of the lead pieces increased the breakwater weight from 1,619 g to 1,996 g resulting in an adjusted relative density of 0.47.

It should be noted that for all cases with an attached membrane (8 of the 9 cases), the relative density of the breakwater core was reduced. This was done to maintain the original draft and keep the breakwater level. To accomplish this, 211 grams of lead were removed from the foam core to compensate from the mass of the clump weights attached to the membrane. This weight decrease resulted in a change in relative density of the breakwater core from 0.47 to 0.37.

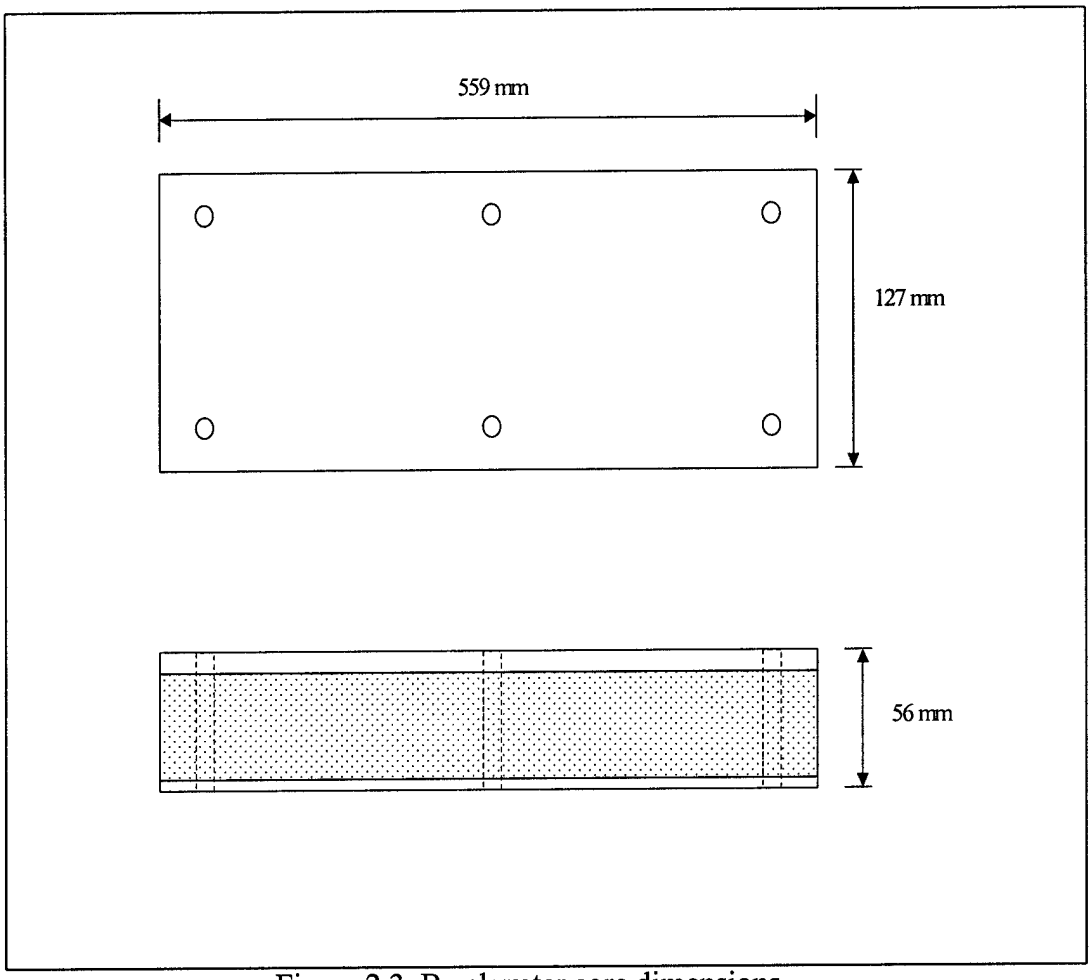

Figure 2.3. Breakwater core dimensions.

2.3 Mooring Construction

2.3.1 Stiff Moorings

For the stiff moorings, 1.6 mm stainless steel cables were used in conjunction with compression fittings and barrel swivels. The swivels allowed 360° rotation of the mooring lines while minimizing the rotation stress in the cable. Figure 2.4 shows the layout of the stiff mooring system.

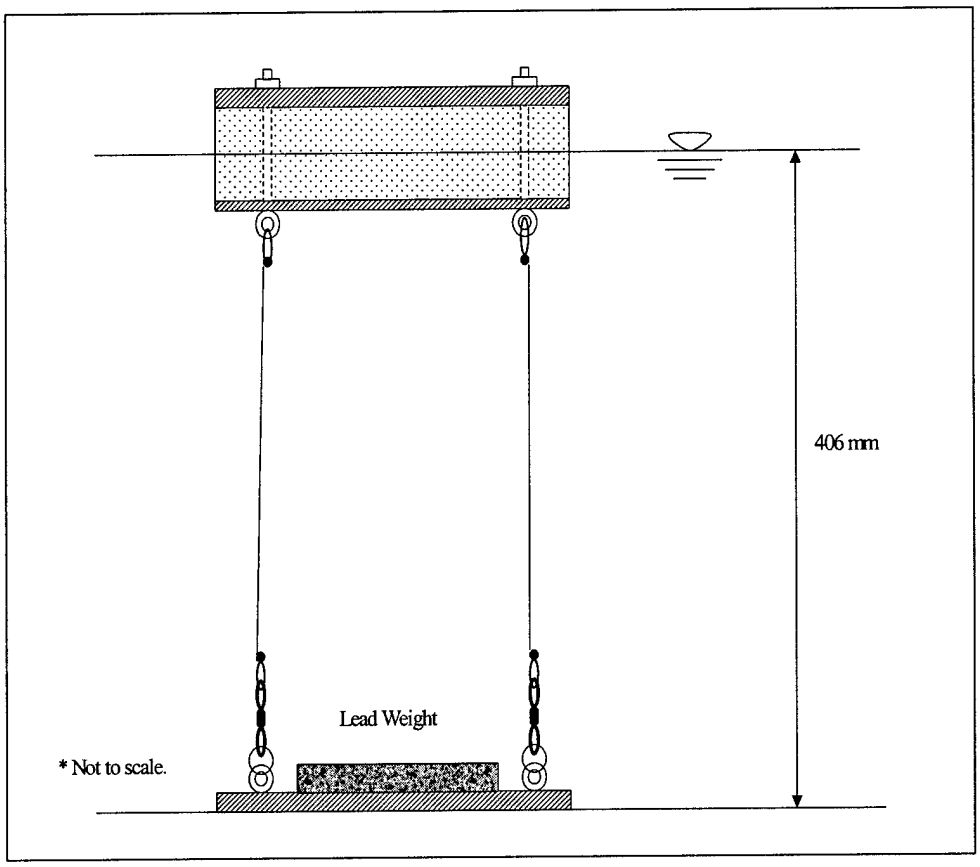

Figure 2.4 Stiff mooring configuration.

2.3.2 Flexible Moorings

For the flexible moorings, 11 mm diameter springs with an overall length of 114 mm were used. These springs have a maximum deflection of 353 mm and a spring constant of 0.02 N/mm. The springs were pre-stressed to a 51 mm initial deflection in static equilibrium prior to performing tests. Figure 2.5 shows the layout of the flexible mooring system.

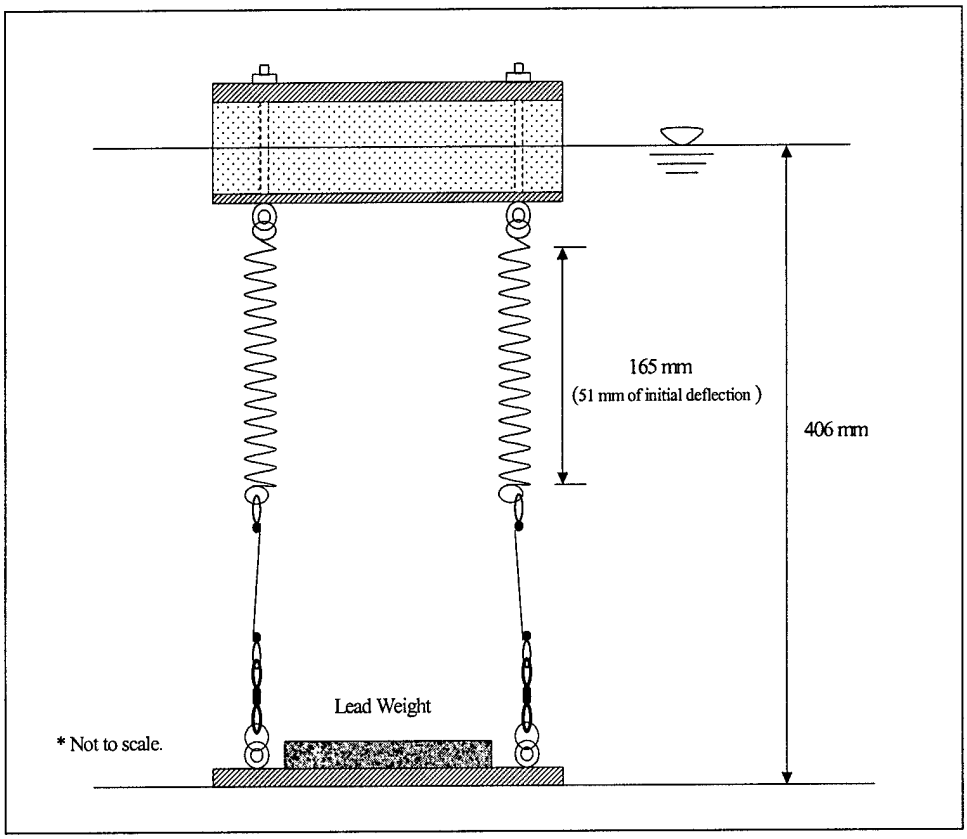

Figure 2.5. Flexible mooring configuration.

2.4 Vertical Membrane

The vertical membrane alternatives were a full-length impermeable material, and full-length, ½- length and ¼–length permeable geo-fabric. The lengths of the full-length, ½- length and ¼–length membranes were approximately 330 mm, 203 mm, and 102 mm, respectively. All membranes had a width of 457 mm. The geo-fabric was determined to have a permeativity coefficient, k_p, of 13.33 cm/s. The permeativity was determined by performing a falling head test. Figure 2.6 shows how the membrane was suspended beneath the breakwater.

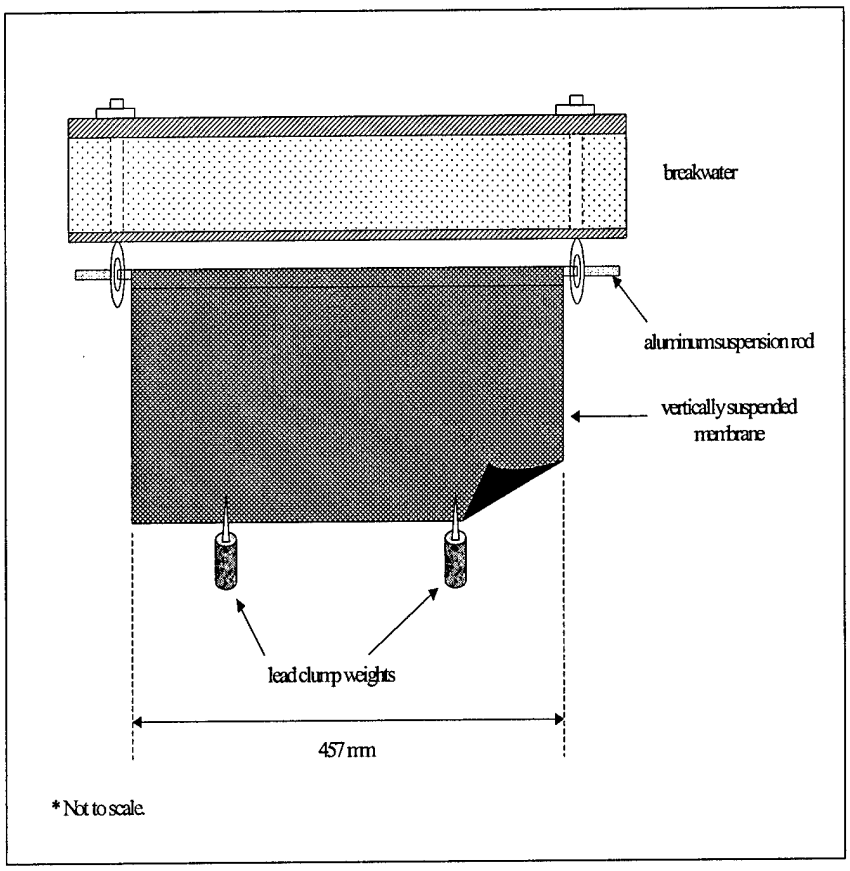

Figure 2.6 Vertical membrane attachment.

2.5 Calibration and Measurement

2.5.1 Calibration

The wave gauges measured the wave fluctuations in volts and calibration factors were used to convert volts to mm. The total displacement recorded in volts was multiplied by the calibration value (mm/volts) to convert from volts the millimeters. The wave gauges were calibrated at the beginning and end of each test day.

2.5.2 Measurement

A partial standing wave envelope was recorded (Fig. 2.7) by appropriately moving the wave gauge on the cart through the incident and reflected wave fields after

the incident waves had reflected from the breakwater. The maximum wave height of the envelope, H_{max}, and minimum wave height of the envelope, H_{min}, of the wave group envelope were used to calculate the incident wave height, H_i, and the reflected wave height, H_r.

$$H_i = \frac{H_{max} + H_{min}}{2} \tag{2.3}$$

$$H_r = \frac{H_{max} - H_{min}}{2} \tag{2.4}$$

The transmitted wave height, H_t, was recorded by the stationary wave gauge located on the leeside of the breakwater.

2.5.3 Coefficient Calculations

The transmission coefficient, K_t, and the reflection coefficient, K_r are given by

$$K_t = \frac{H_t}{H_i} \tag{2.5}$$

$$K_r = \frac{H_r}{H_i} \tag{2.6}$$

Wave energy is a function of the wave heights squared. Wave energy is either reflected, transmitted, or dissipated. The dissipation coefficient, K_d, is a measure of the amount of wave energy dissipated by the breakwater. For a flat bottom, this is given by

$$K_t^2 + K_r^2 + K_d^2 = 1 \tag{2.7}$$

$$K_d = \sqrt{1-(K_t^2 + K_r^2)} \tag{2.8}$$

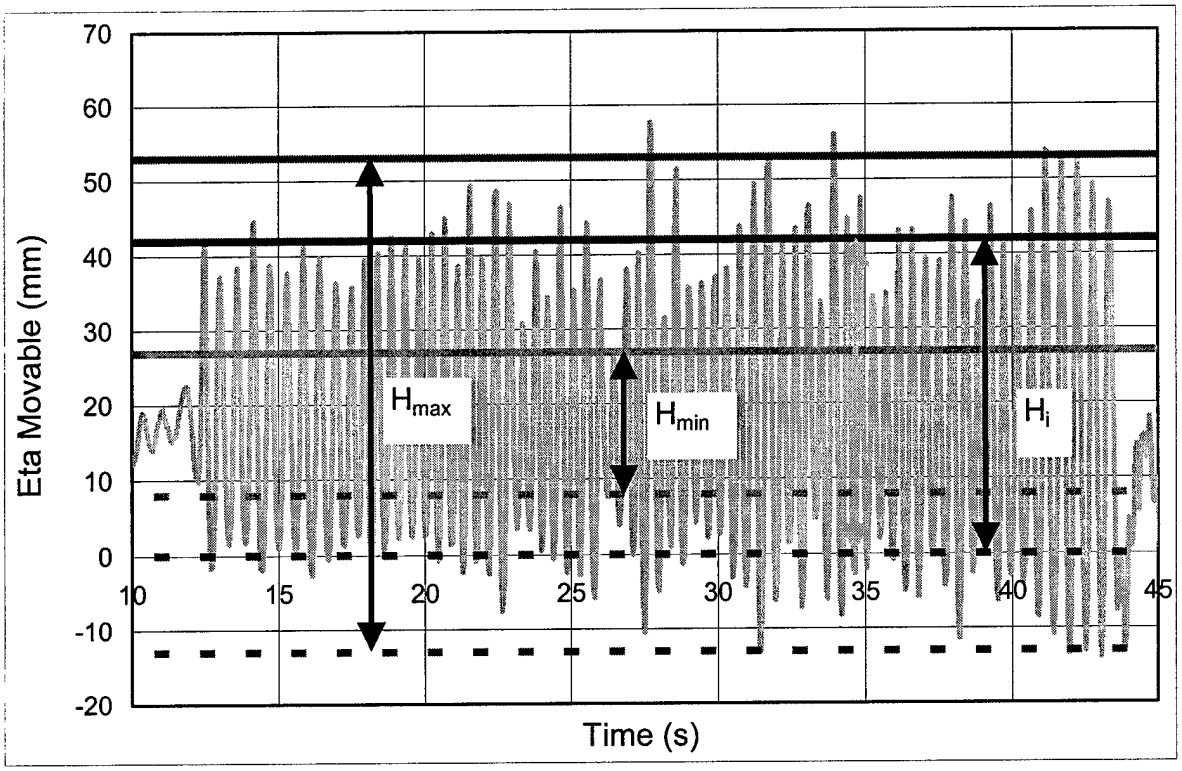

Figure 2.7 Sample wave envelope recorded from movable wave guage.

2.5.4 Model Displacement

The displacement of the model from the static position was recorded visually during each run with the aid of a transparent grid sheet attached to the side of the flume. The maximum displacement of the model was marked with a dry-erase pen in the forward, backward, upward, and downward directions. Although these movements were recorded (see Appendix A), they are not analyzed in this report.

The natural periods of oscillation of the breakwater with stiff and flexible moorings and each membrane length were also measured. The surge, heave, and pitch natural periods are given in Appendix D.

2.6 Model Configurations

Five configurations were examined with stiff moorings, and four configurations with flexible moorings. The nine configurations are listed in Table 2.1.

Each configuration was tested at 8 different wave periods ranging from 0.5 seconds to 1.2 seconds. Thus, 72 combinations were examined. Duplicate runs for each combination were performed. In total, over 150 flume runs were completed to acquire the necessary laboratory data for this project.

Table 2.1 Testing configurations.

Case #	Mooring	Membrane Type	Membrane Length	Membrane Location
1	stiff	none	none	none
2	stiff	impermeable	full depth	front
3	stiff	permeable	full depth	front
4	stiff	permeable	¼ depth	back
5	stiff	permeable	¼ depth	center
6	flexible	permeable	full depth	front
7	flexible	impermeable	full depth	front
8	flexible	permeable	½ depth	front
9	flexible	permeable	¼ depth	front

CHAPTER 3
EXPERIMENTAL RESULTS

3.1 Collected Data

The incident and reflected waves heights were estimated using the envelope method described in Chapter 2. The incident waves were also measured at each wave maker setting with no structure in the flume. It was also attempted to read the incident waves heights from the wave gauge on the seaward side of the structure before reflection occurred. This gave three different estimates for the incident waves height. This was useful for identifying inconsistent measurements.

The reflected wave height was determined from the incident wave height with no structure and the directly measured transmitted wave height assuming conservation of energy. As a result there were two independent estimates for the reflected waves height.

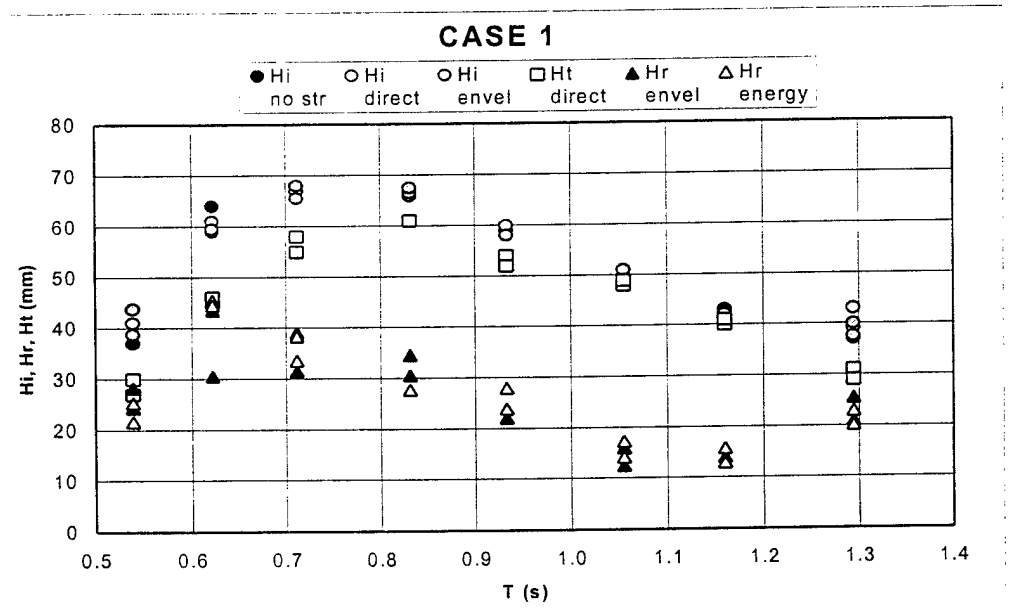

Figure 3.1 Incident, reflected, and transmitted wave height versus time.

Figure 3.1 shows the incident, reflected, and transmitted wave height versus wave period for Case 1. Since tests for each wave period were repeated, there are six estimates for H_i, four for H_r, and two for H_t. In most cases, there was reasonable agreement among the various estimates. However, for Case 9 there was one set of inconsistent data which were eliminated. Figures similar to Figure 3.1 for all nine cases are provided in Appendix B.

3.1.1 Case 1

This case had a stiff mooring and no membrane (Fig 3.2). It corresponds to a pontoon breakwater or floating dock section. With no membrane, Case 1 is the base case against which all other cases are compared to assess the improvement provided by each membrane configuration.

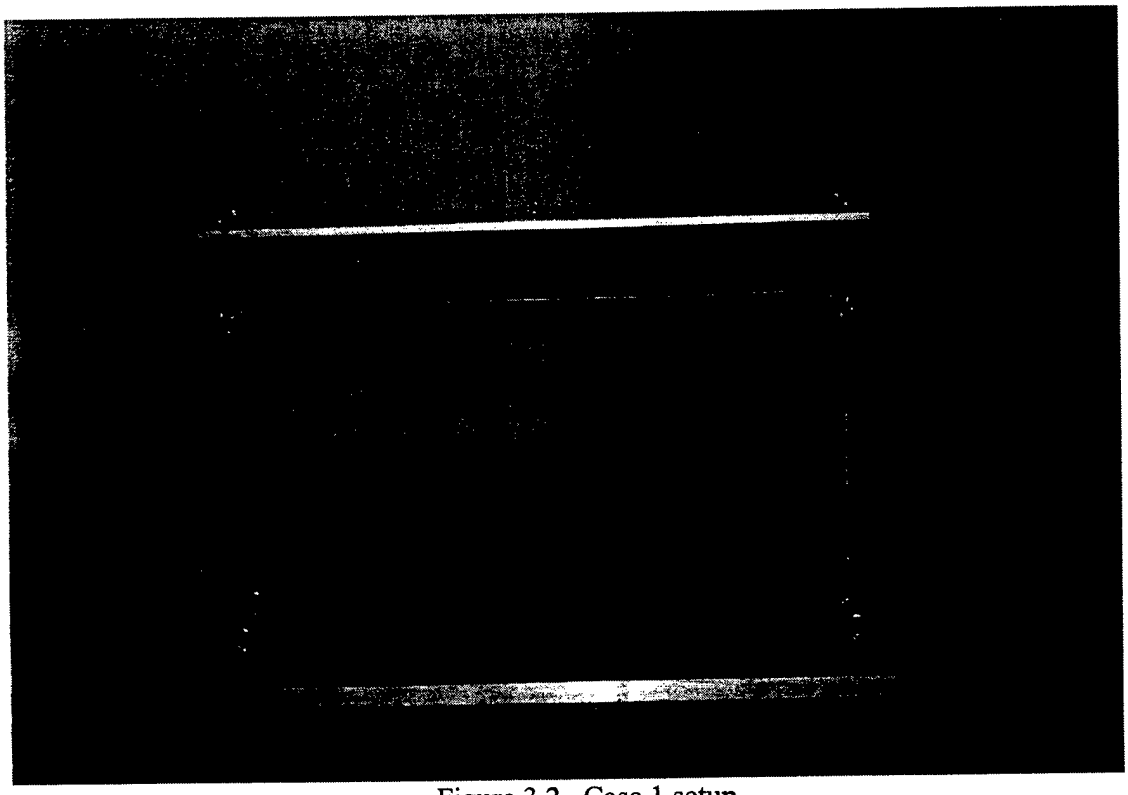

Figure 3.2. Case 1 setup.

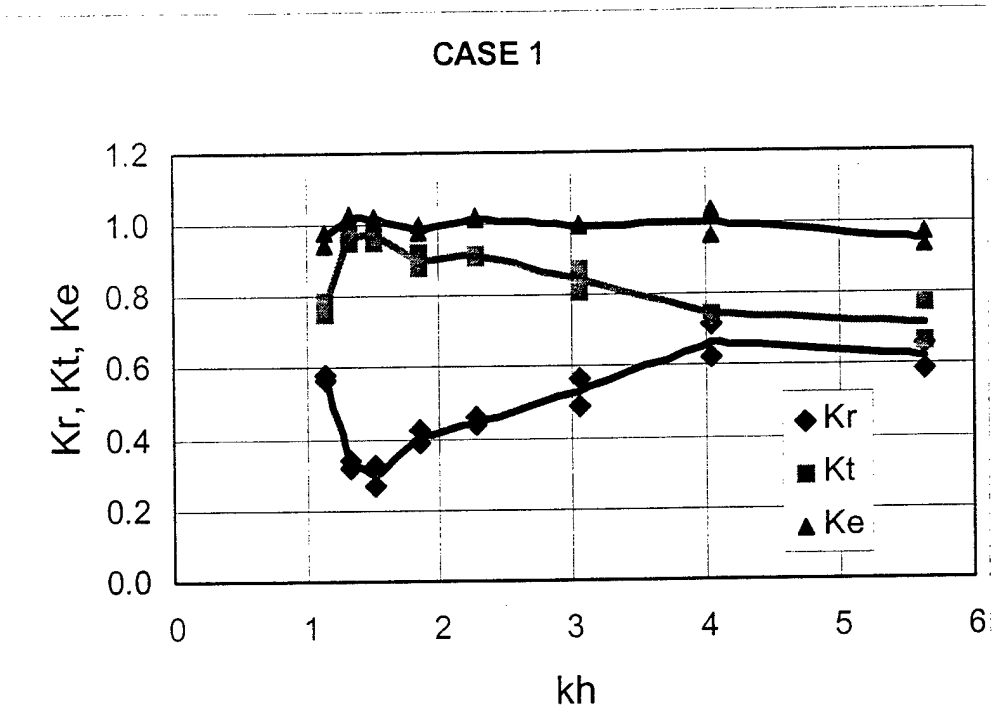

Figure 3.3. Coefficient curves for Case 1.

Figure 3.3 Shows the reflection and transmission coefficients, as defined by (1.6) and (1.7). These are shown as a function of *kh*, where *k* is the wave number and *h* is the water depth. A low *kh* corresponds to a high wave period. In figure 3.3, K_e is an energy coefficient defined as

$$K_e^2 = K_r^2 + K_t^2 \tag{3.1}$$

If energy is conserved, then $K_e = 1.0$. For Case 1, there was no wave breaking or significant turbulence generated by the structure. Therefore, K_e should have a value near 1.0, which it does for all wave periods examined. From Figure 3.3 it is seen that the transmission coefficient varies from approximately 0.7 to almost 1.0. At $kh \approx 1.5$ (T= 1.0 s), the structure is almost transparent and has little influence on reducing the transmitted wave height. This is near the natural frequency of the structure and large displacements were observed. At higher frequencies, the effectiveness of the structure as a wave barrier increases. This occurs for two reasons: 1) At frequencies above the structure's natural frequency the structure inertia

resists motion and 2) A greater proportion of the incident wave height of the shorter waves is disrupted by the fixed draft of the structure. At the low frequencies, the structure acts as a kinematic barrier where its limited displacements interrupts wave transmission less effectively.

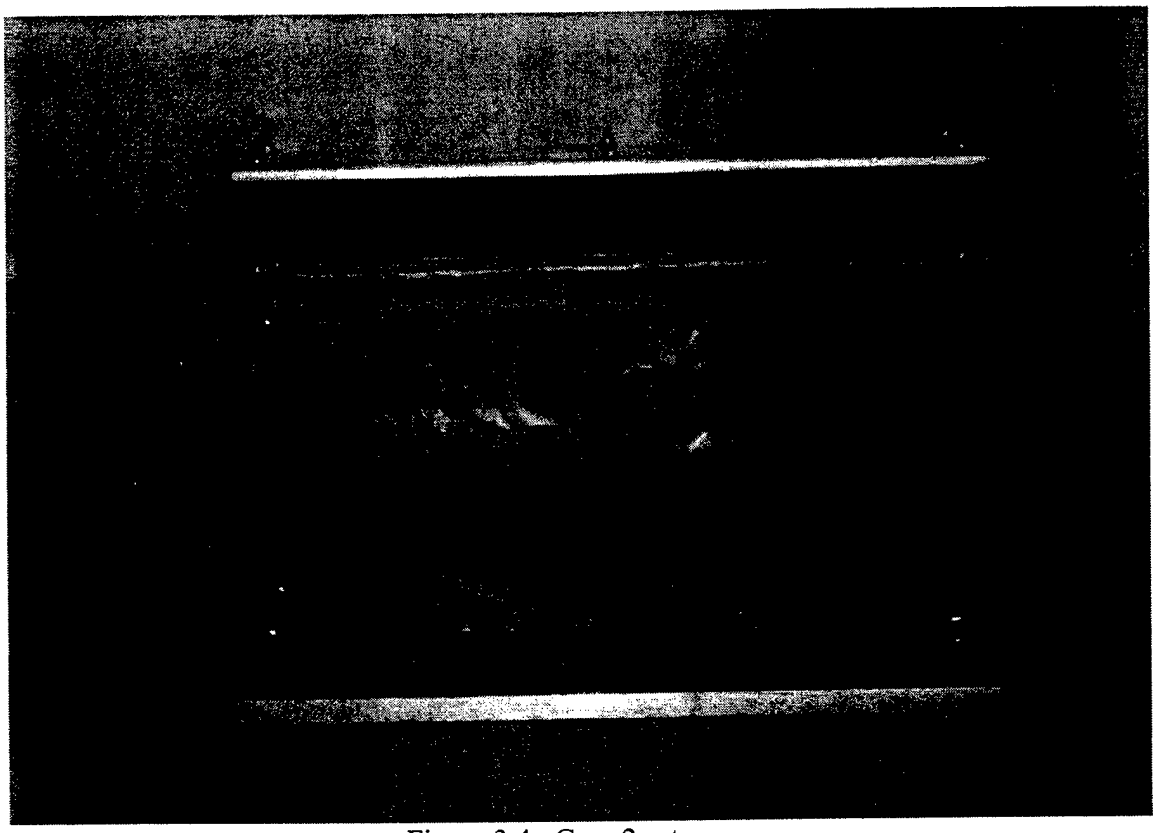

Figure 3.4. Case 2 setup.

3.1.2 Case 2

This case had a stiff mooring and a full-depth, impermeable membrane (Fig 3.4). It corresponds to a pontoon breakwater or floating dock section with an attached, full depth, impermeable membrane. Case 2 was used to compare and evaluate the effect of membrane permeability on wave attenuation.

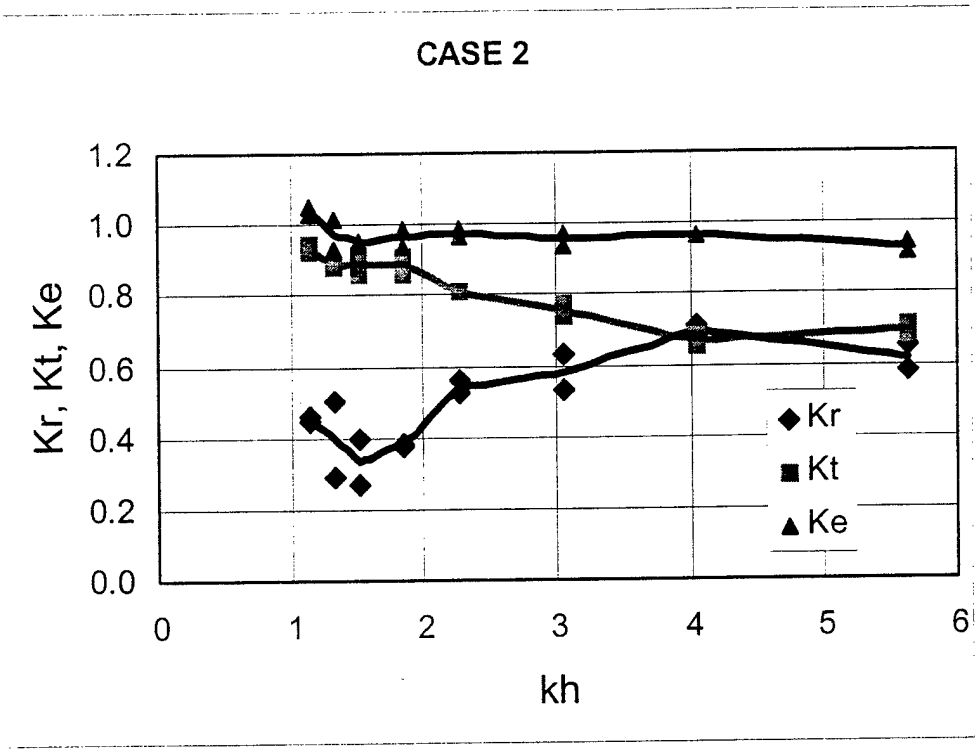

Figure 3.5. Coefficient curves for Case 2.

Figure 3.5 shows the reflection and transmission coefficients for Case 2. As with Case 1, Case 2 has a K_e value near 1.0 for all wave periods examined. From Figure 3.5 it is seen that the transmission coefficient varies from approximately 0.7 to approximately 0.9. At the low frequency range, from $kh \approx 1.2$ (T= 1.2 s) to $kh \approx 1.8$ (T= 0.9 s), the structure appears to have minimal effect on wave attenuation. At higher frequencies, the effectiveness of the structure as a wave barrier increases similarly to Case 1. The reasons for this were discussed in section 3.1.1.

3.1.3 Case 3

Case 3 had a stiff mooring and a full-depth, permeable membrane (Fig 3.6). It corresponds to a pontoon breakwater or floating dock section with an attached, full depth, permeable membrane. This case was used to compare and evaluate the effect of membrane permeability and length on wave attenuation.

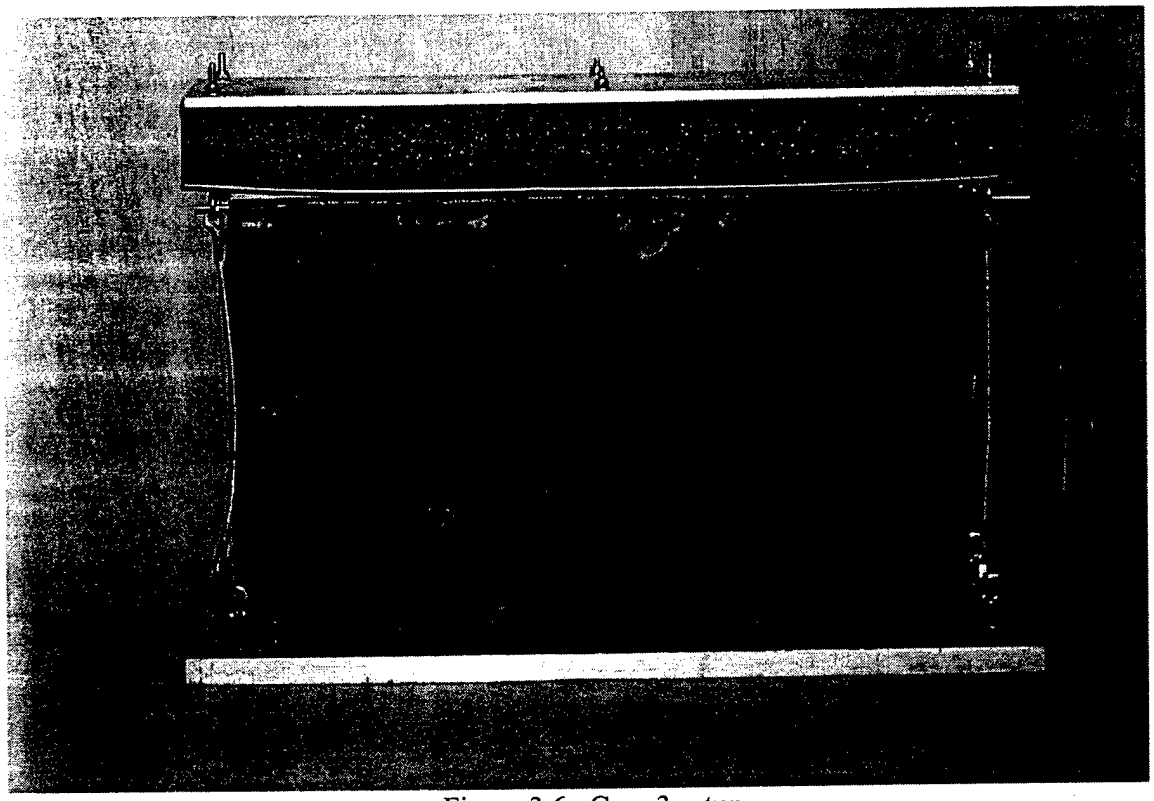

Figure 3.6. Case 3 setup.

Figure 3.7 shows the reflection and transmission coefficients for Case 3. Similarly to the first two cases, Cases 3 has a K_e value near 1.0 for most all wave periods examined. Figure 3.7 shows that the transmission coefficient varies from approximately 0.6 to approximately 0.9. At $kh \approx 5.6$ (T= 0.5 s), the transmission coefficient is at a minimum of approximately 0.6 indicating particularly strong wave attenuation at the high end of the frequency range. This is generally consistent with the first two cases.

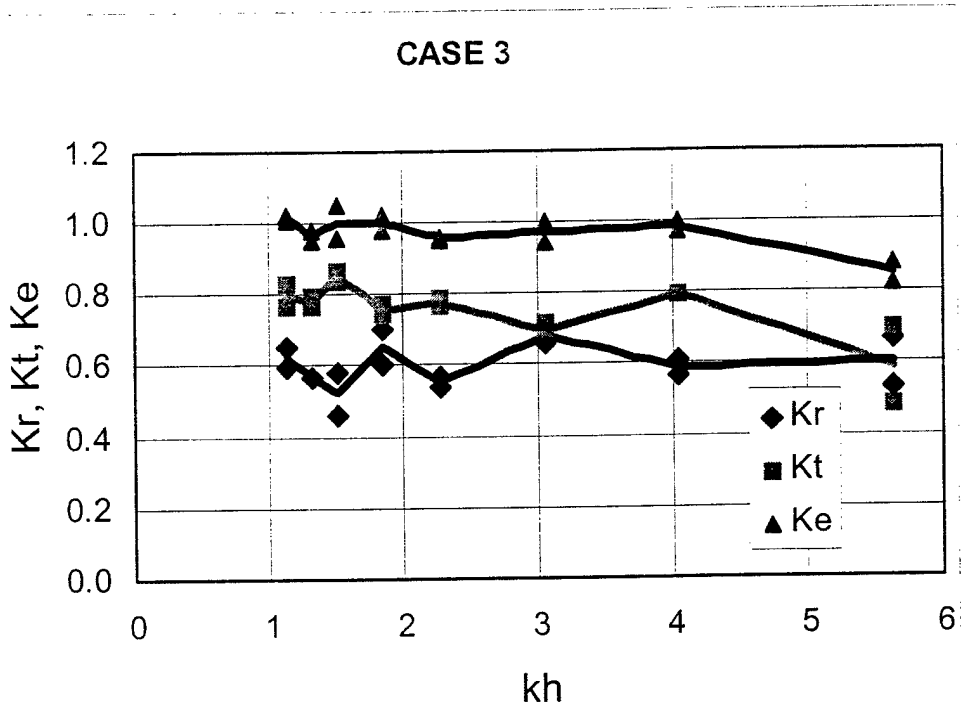

Figure 3.7. Coefficient curves for Case 3.

3.1.4 Case 4

This case had a stiff mooring and a ¼ -depth, impermeable membrane (Fig 3.8). It corresponds to a pontoon breakwater or floating dock section with an attached, partial depth, impermeable membrane. Case 4 was used to compare and evaluate the effect of membrane length on wave attenuation. Figure 3.9 shows the reflection and transmission coefficients for Case 4. As with previous cases, the K_e value was near 1.0 for all wave periods examined. From Figure 3.9 it is seen that the transmission coefficient varies from approximately 0.6 to approximately 0.8. The transmission coefficient seems to be relatively stable from $kh \approx 1.8$ (T= 0.9 s) to $kh \approx 4.0$ (T= 0.6 s). Also, the transmission coefficient is relatively low throughout this range indicating strong wave attenuation for wave periods up to 0.9 seconds.

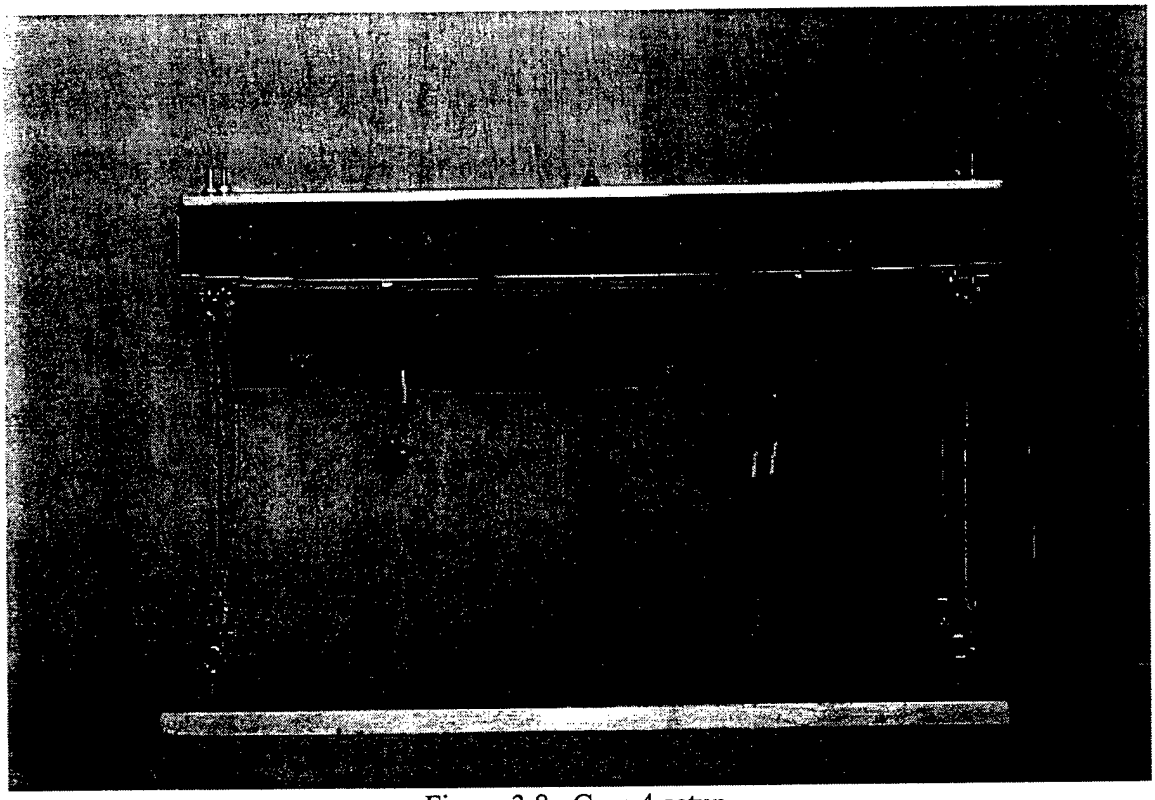

Figure 3.8. Case 4 setup.

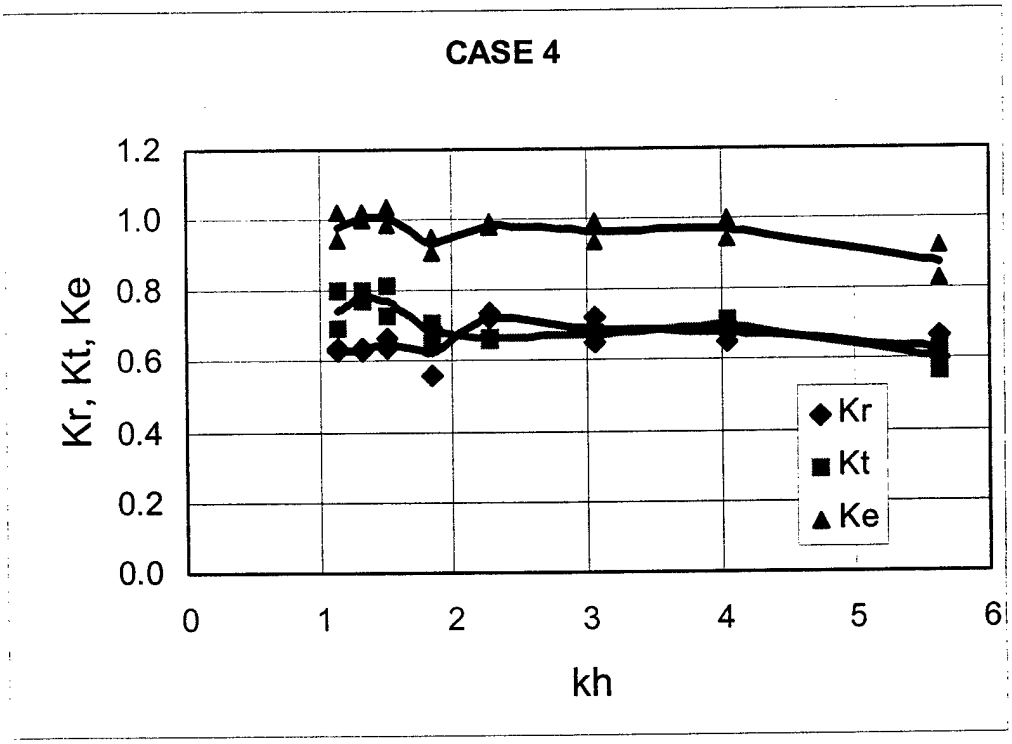

Figure 3.9. Coefficient curves for Case4.

3.1.5 Case 5

Case 5 had a stiff mooring and a ½ -depth, impermeable membrane (Fig 3.8). It corresponds to a pontoon breakwater or floating dock section with an attached, partial depth, impermeable membrane. Case 5 was used to compare and evaluate the effect of membrane length on wave attenuation. Figure 3.11 shows the reflection and transmission coefficients for Case 5. As with previous cases, the K_e value was near 1.0 for all wave periods examined.

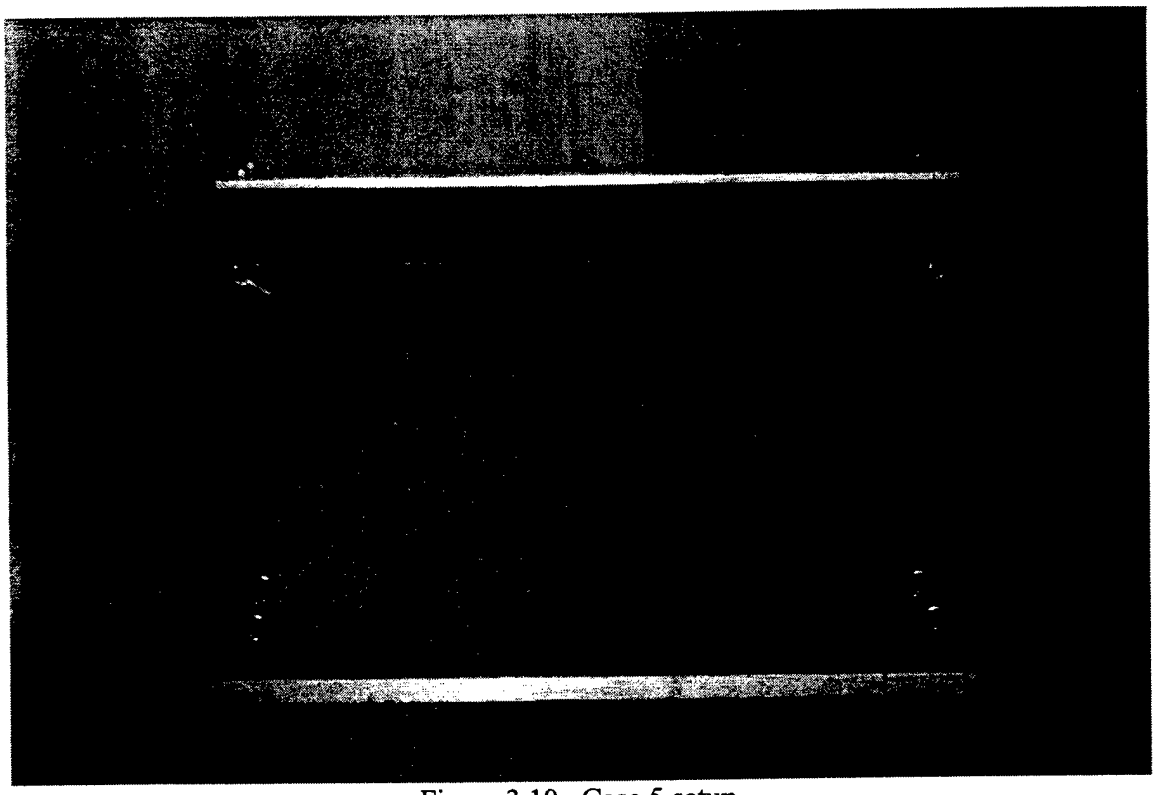

Figure 3.10. Case 5 setup.

From Figure 3.11 it is seen that the transmission coefficient varies from approximately 0.6 to almost 0.8. The transmission coefficient seems to be relatively stable from $kh \approx 2.8$ (T= 0.7 s) to $kh \approx 5.6$ (T= 0.5 s). Since the transmission coefficient is relatively low here, wave attenuation seems to be maximized throughout this range..

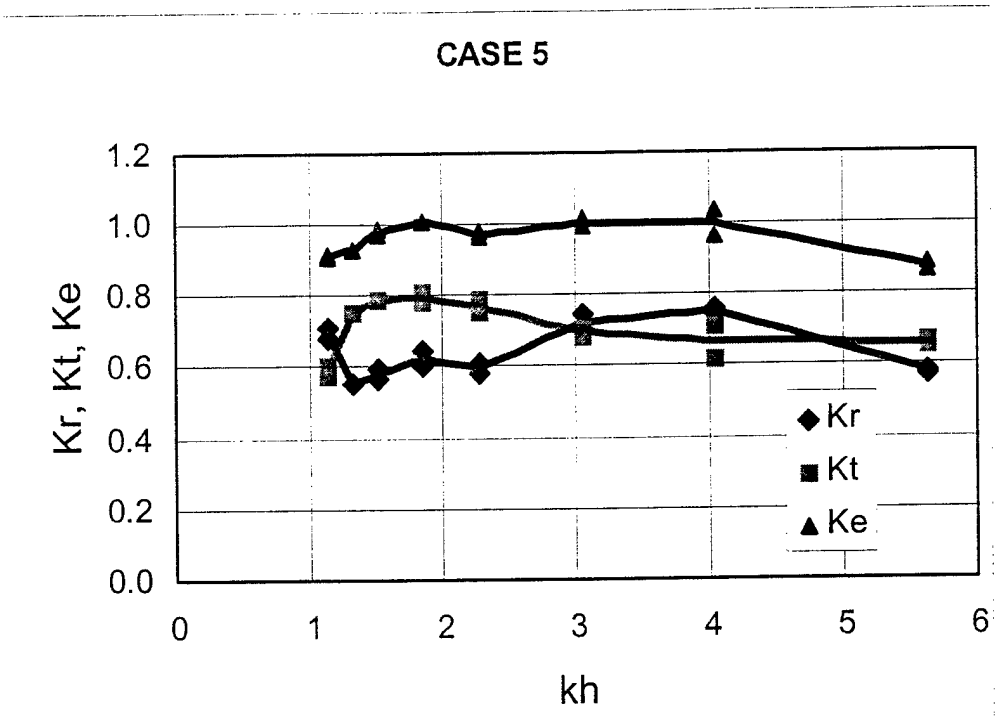

Figure 3.11. Coefficient curves for Case 5.

3.1.6. Case 6

Case 6 had a flexible mooring and a full-depth, permeable membrane (Fig 3.12). It corresponds to a pontoon breakwater or floating dock section with an attached, full depth, permeable membrane. This case was used to compare and evaluate the effect of membrane permeability and membrane length on wave attenuation.

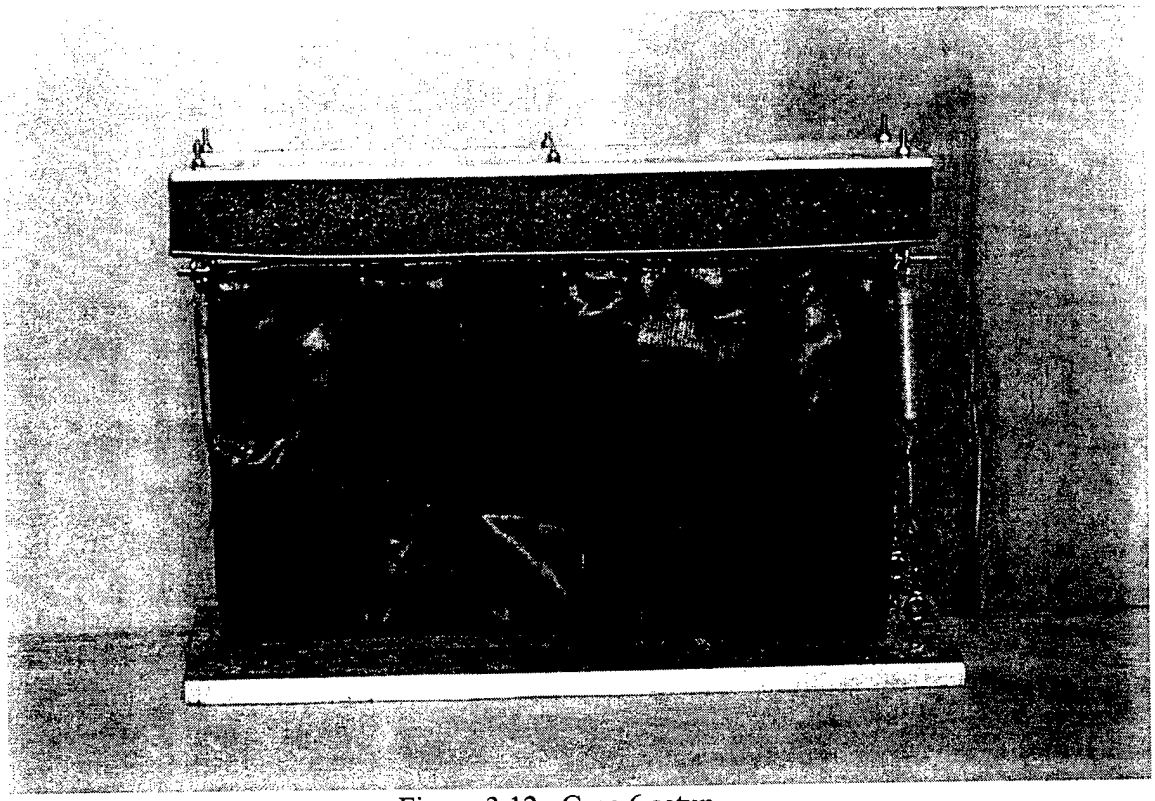

Figure 3.12. Case 6 setup.

Figure 3.13 shows the reflection and transmission coefficients for Case 6. Similar to the previous cases, Cases 6 has a K_e value near 1.0 for most wave periods examined. However, K_e did decreased to 0.8 at $kh \approx 5.6$ (T= 0.5 s). Figure 3.13 also shows that the transmission coefficient varies from approximately 0.44 to approximately 0.81 with the minimum wave transmission occurring at $kh \approx 5.6$ (T= 0.5 s). This seems to be consistent with previous cases by showing strong wave attenuation at the high end of the frequency range.

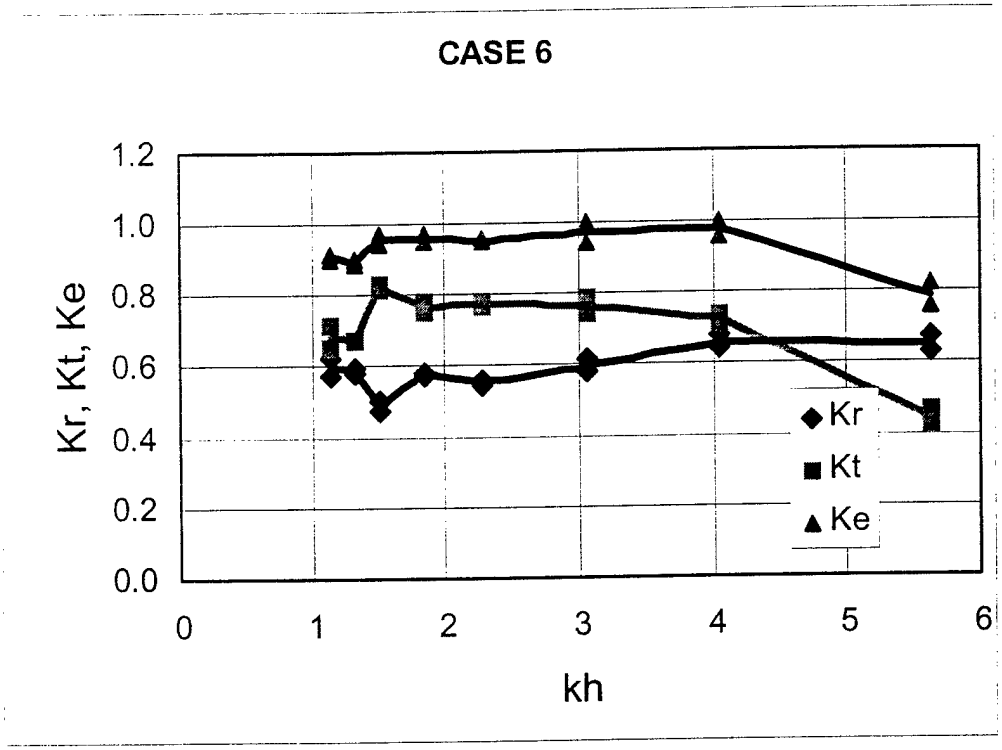

Figure 3.13. Coefficient curves for Case 6.

3.1.7 Case 7

Case 7 had a flexible mooring and a full-depth, impermeable membrane (Fig 3.14). It corresponds to a pontoon breakwater or floating dock section with an attached, full depth, impermeable membrane. This case was used to compare and evaluate the effect of membrane permeability on wave attenuation.

Figure 3.15 shows the reflection and transmission coefficients for Case 7. As with previous cases, Case 7 has a K_e value near 1.0 for all wave periods examined. Figure 3.15 shows that the transmission coefficient varies from approximately 0.7 to approximately 0.85. At high frequencies, $kh \approx 4.0$ (T= 0.6 s) and $kh \approx 5.6$ (T= 0.5 s), the structure appears to have the greatest effect on wave attenuation. Conversely, at mid-rang frequencies, $kh \approx 1.8$ (T= 0.9 s) and $kh \approx 3.1$ (T= 0.7 s), this case seems to provide minimal wave attenuation.

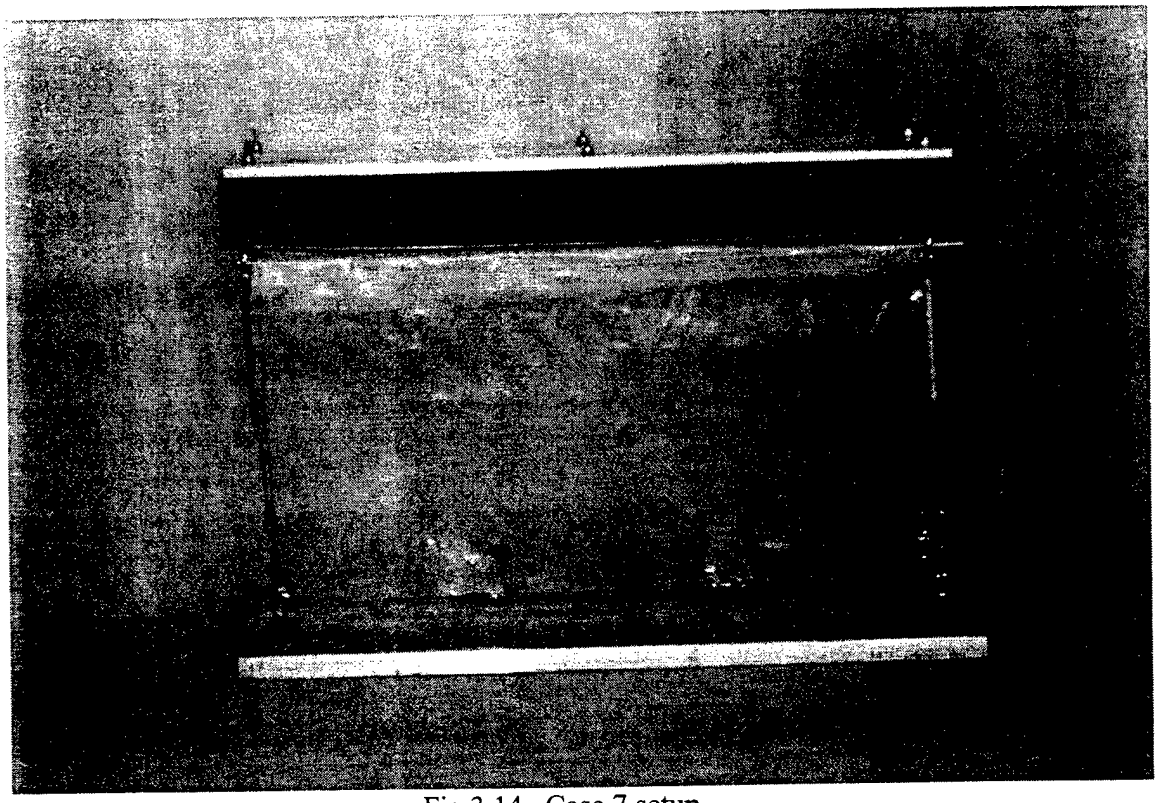

Fig 3.14. Case 7 setup.

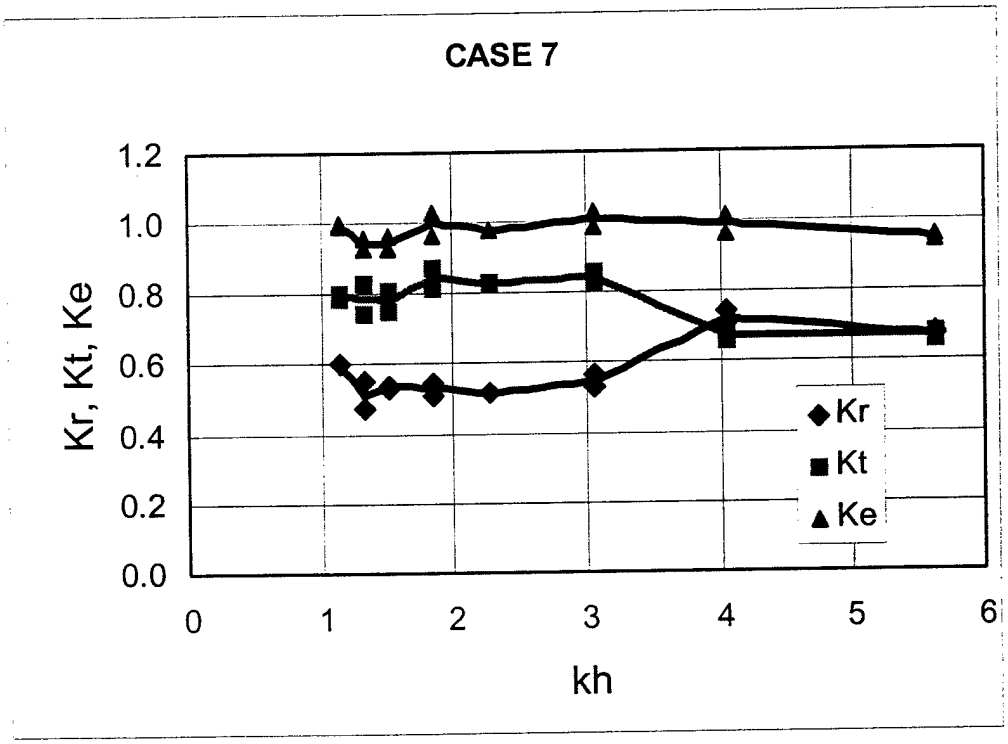

Fig 3.15. Coefficient curves for Case 7.

3.1.8 Case 8

Case 8 had a flexible mooring and a ½ -depth, impermeable membrane (Fig 3.16). It corresponds to a pontoon breakwater or floating dock section with an attached, half depth, impermeable membrane. This case was used to compare and evaluate the effect of membrane permeability and length on wave attenuation.

Figure 3.17 shows the reflection and transmission coefficients for Case 8. Similar to other cases, Case 8 has a K_e value near 1.0 for all wave periods examined. Figure 3.17 shows the transmission coefficient varying from approximately 0.6 to approximately 0.8 with the transmission coefficient increasing at a steady rate from 0.6 at $kh \approx 5.6$ (T= 0.5 s) to 0.78 at $kh \approx 2.3$ (T= 0.8 s).

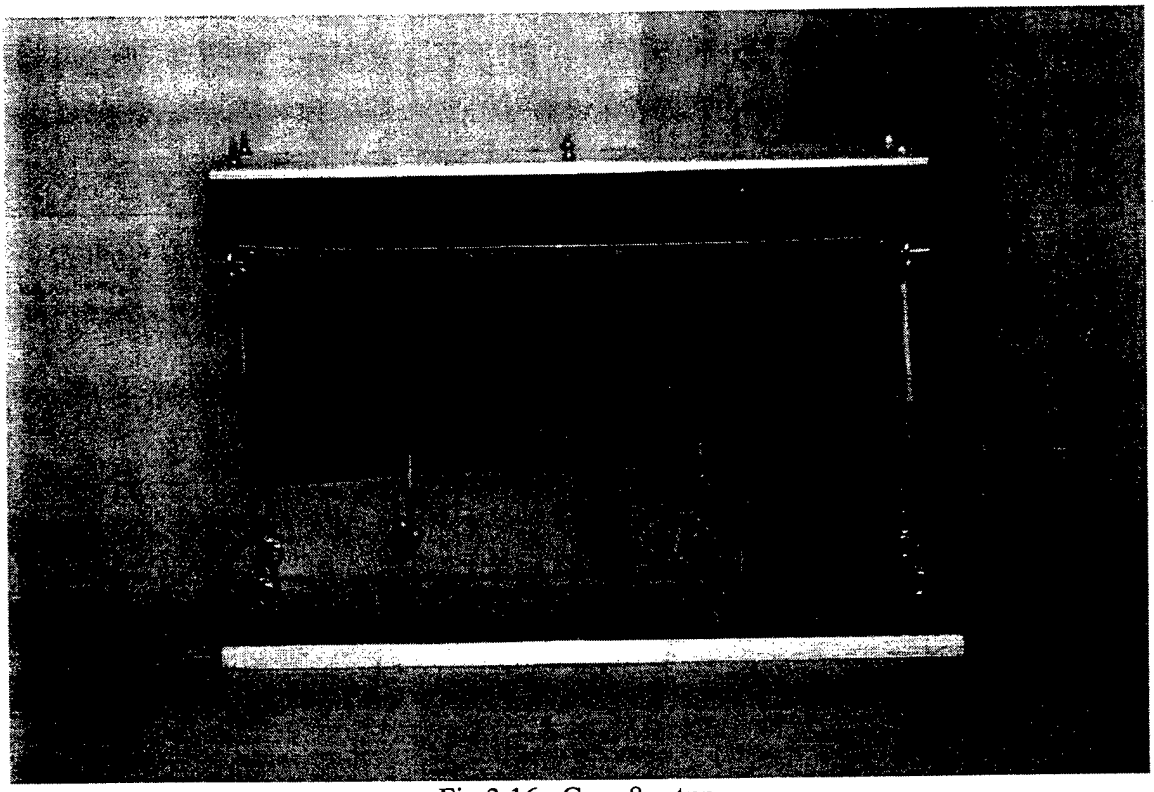

Fig 3.16. Case 8 setup.

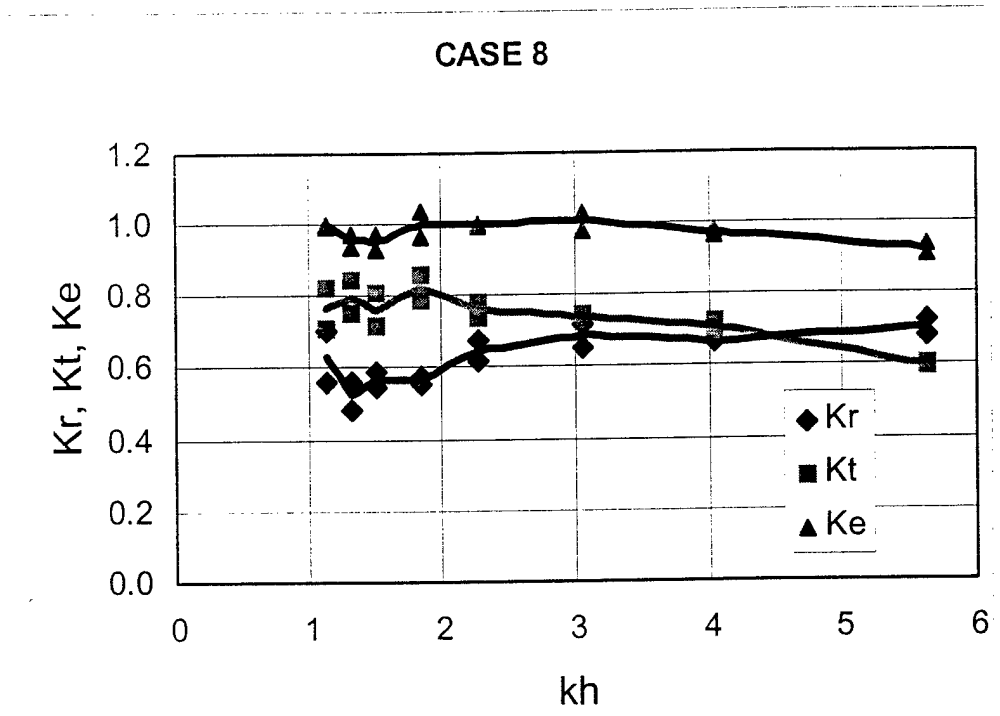

Fig 3.17. Coefficient curves for Case 8.

3.1.9 Case 9

Case 9 had a flexible mooring and a ¼ -depth, impermeable membrane (Fig 3.18). It corresponds to a pontoon breakwater or floating dock section with an attached, quarter depth, impermeable membrane. This case was used to compare and evaluate the effect of membrane permeability and length on wave attenuation.

Figure 3.19 shows the reflection and transmission coefficients for Case 9. Similar to other cases, Case 9 also has a K_e value near 1.0 for all wave periods examined. Figure 3.19 shows that the transmission coefficient remained relatively constant at approximately 0.59 from $kh \approx 4.1$ (T= 0.6 s) to $kh \approx 5.6$ (T= 0.5 s), then increased significantly for the lower frequency range of testing.

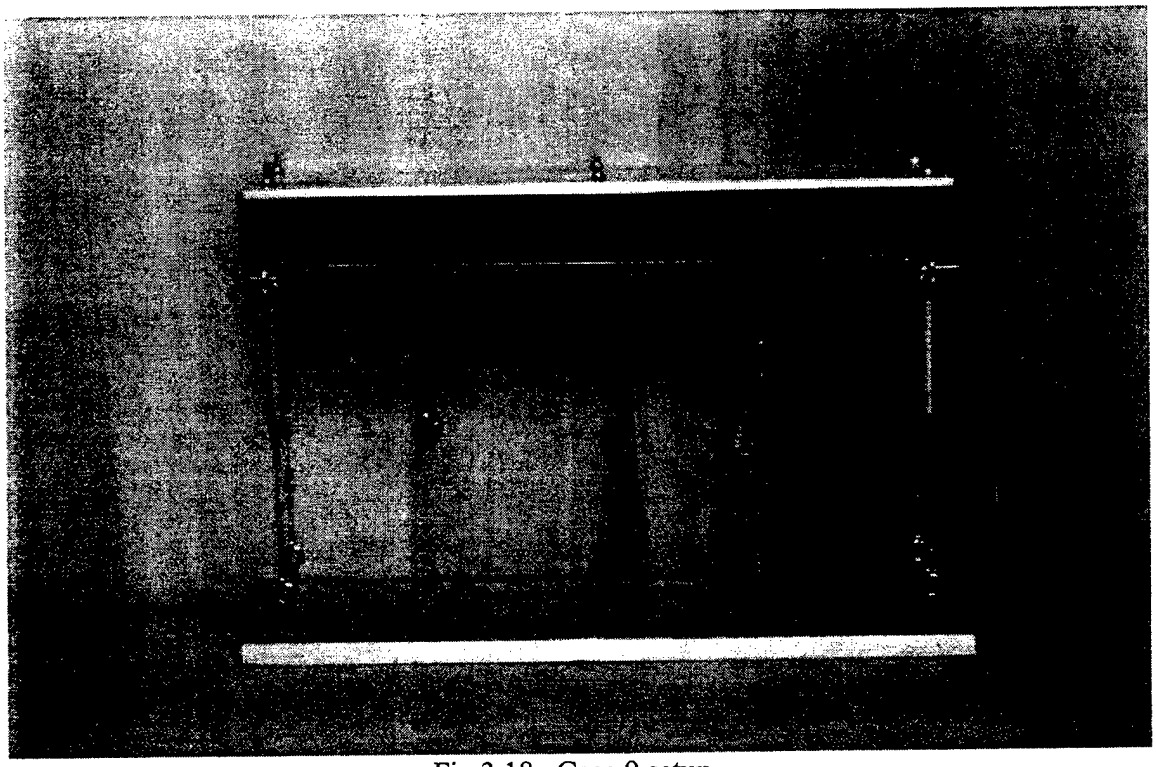

Fig 3.18. Case 9 setup.

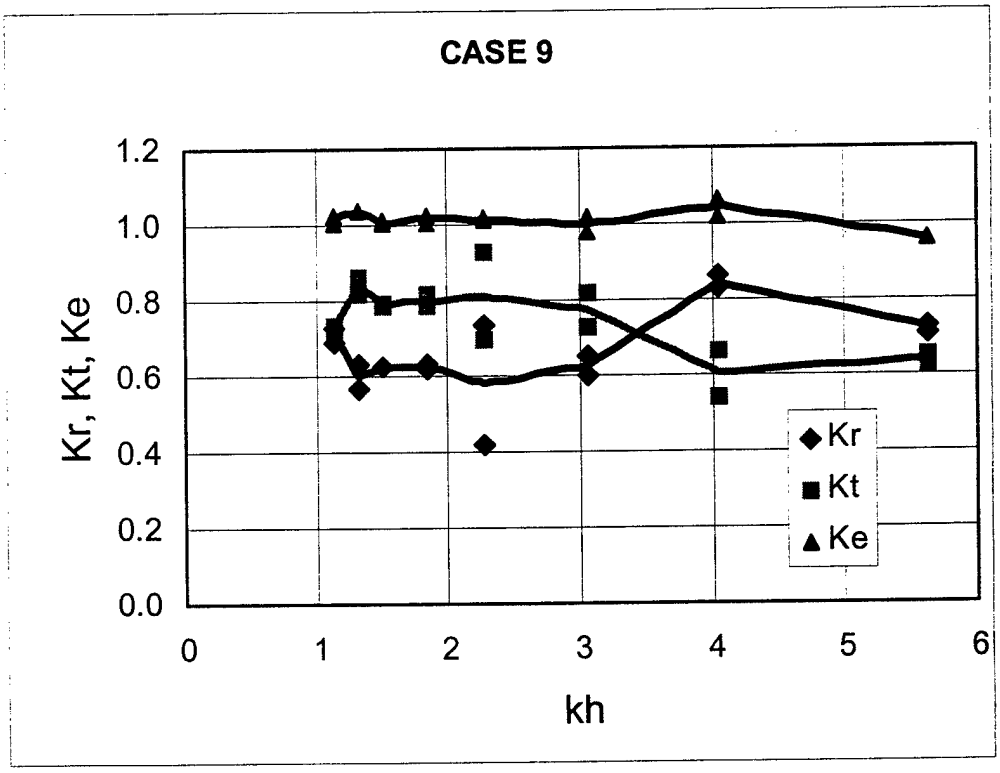

Fig 3.19. Coefficient curves for Case 9.

CHAPTER 4
ANALYSIS AND DISCUSSION

4.1 Data Comparisons

To compare the tests results for the nine case, plots (Fig. 4-1- Fig. 4.9) were generated to compare transmission coefficients of various cases. Each plot includes Case 1 which was used as the base case. Figure 4.1- 4.3 compare only the stiff mooring cases while Figures 4.4- 4.6 compare only the flexible cases. Figures 4.7- 4.9 compare stiff and flexible mooring cases to each other. In Figure 4.1, Cases 2 and 3 were compared to the base case to determine the effects of membrane permeability at full-length. Figure 4.2 compares Cases 4 and 5 to the base case to determine the effects of membrane position while Figure 4.3 compares all stiff mooring, permeable membranes.

For the flexible mooring, Figure 4.4 compared Case 6 and 7 to determine the effects of membrane permeability at full-length with flexible moorings. Figure 4.5 includes Cases 8 and 9 and was used to compare the ½- depth membrane to the ¼ - depth membrane. Figure 4.6 is the similar to Figure 4.5, but also includes Case 7. This allows a comparison of all membrane lengths to be made.

In Figure 4.7, Cases 3 and 6 are compared to determine the effects of mooring compliance on the full-depth permeable membrane. Likewise, Figure 4.8 compares the effects of mooring compliance on the full-depth impermeable membrane. Finally, Figure 4.9 includes Cases 4, 5, and 9 and compares the results of the three positions (back, center and front) of the ¼- length membrane.

4.1.1 Stiff Mooring Results

The stiffly moored breakwater was tested in five configurations by using two types of membrane material, three membrane lengths, and three membrane positions. The five configurations considered are tabulated in Table 4.1

Table 4.1 Configurations for stiff moorings.

Case #	Membrane Type	Membrane Length	Position
1	none	none	none
2	impermeable	full	front
3	permeable	full	front
4	permeable	1/4	back
5	permeable	1/4	center

Figure 4.1 shows a comparison of polynomial fit curves of the transmission coefficients, K_t, for the full-length permeable membrane, full-length impermeable membrane and the no-membrane case (Case 1). In the figures, the lines are polynomial approximations to the data. The permeable membrane (Case 3) has the lowest transmission coefficient for most of frequencies tested; however, Case 2 has lower K_t values at each end frequency test range. Case 2 results in an average decrease in the transmission coefficient of 4 %. Case 3 results in an average decrease in the transmission coefficient of 11%. Case 3 provides the highest wave attenuation for most, but not all, of the wave periods for the three cases.

Figure 4.2 shows a comparison of the transmission coefficients for the ¼ -length permeable membrane positioned on the back on the model (Case 4), ¼ -length permeable membrane positioned in the center of the model (Case 5), and the no-membrane case (Case 1).

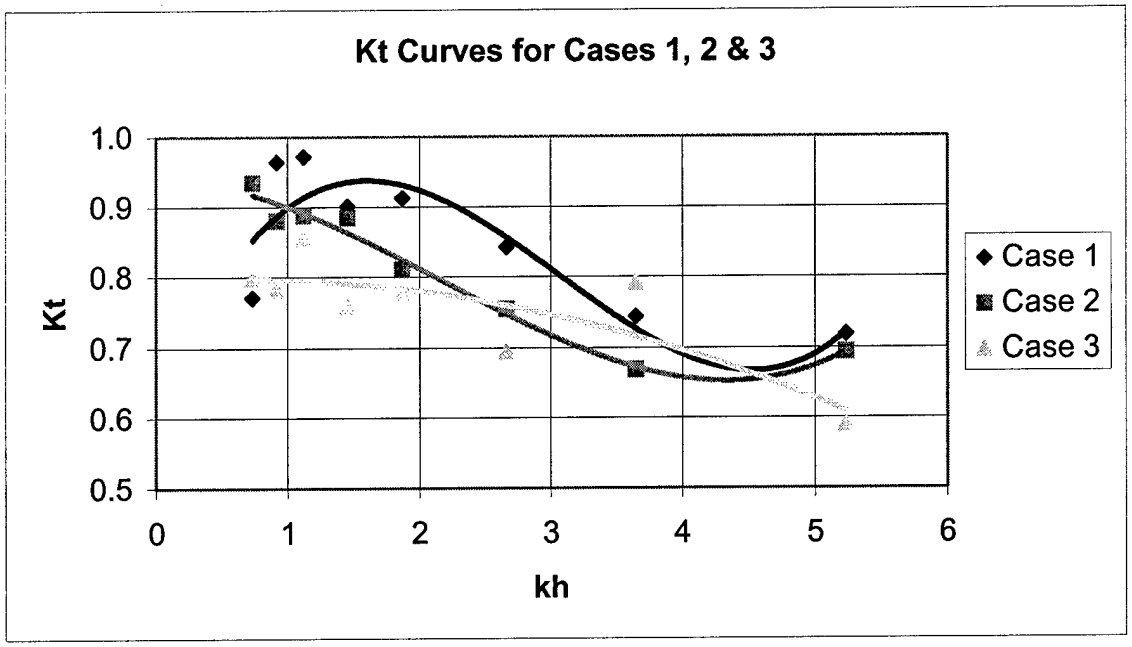

Figure 4.1 Comparison of transmission coefficients for case 1,2, and 3.

It is apparent in Figure 4.2 that the 1/4-length permeable membrane placed on the back on the model (Case 4) has the lowest transmission coefficient throughout most of the range of periods. Thus, Case 4 appears to provide the highest wave attenuation of these three cases. Case 4 results in an average decrease in the transmission coefficient of 17%.

Figure 4.3 shows a comparison of the transmission coefficients for the ¼ -length permeable membrane placed on the back on the model (Case 4), 1/4-length permeable membrane places in the center of the model (Case 5), the full-length permeable membrane (Case 3) and the no-membrane case (Case 1). It is apparent in Figure 4.3 that the ¼ -length permeable membrane placed on the back on the model (Case 4) has the lowest transmission coefficient throughout most of the range of periods. Thus, Case 4 appears to provide the highest wave attenuation of these four cases. While Case 4 results

in an average decrease in the transmission coefficient of 17 %, Cases 3 and 5 result in lower average decreases of 11 % and 15 %, respectfully.

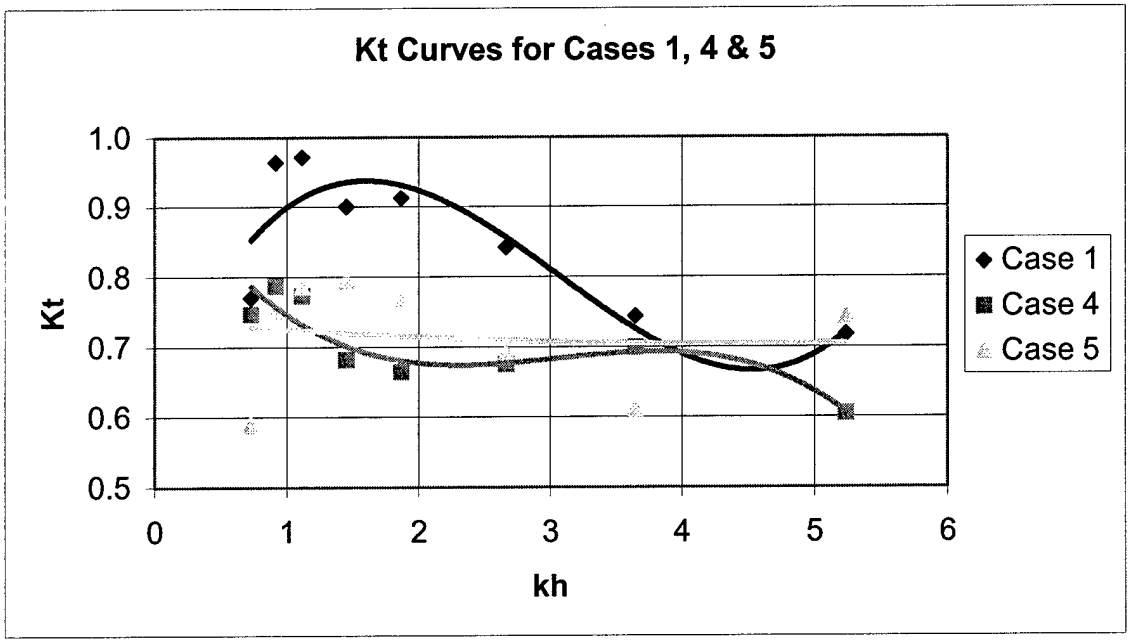

Figure 4.2 Comparison of transmission coefficients for cases 1, 4, and 5.

As expected, all cases with a membrane provided lower transmission coefficients than the no-membrane case throughout the range of periods tested. Conversely, other results were not as intuitive. The ¼-length fabric, when placed in the center or front, provided lower average transmission coefficients than the full membrane at the front. Furthermore, the ¼- length membrane placed in the back (Case 4) provided the a slightly lower average transmission coefficient then the ¼- length membrane placed in the center (Case 5).

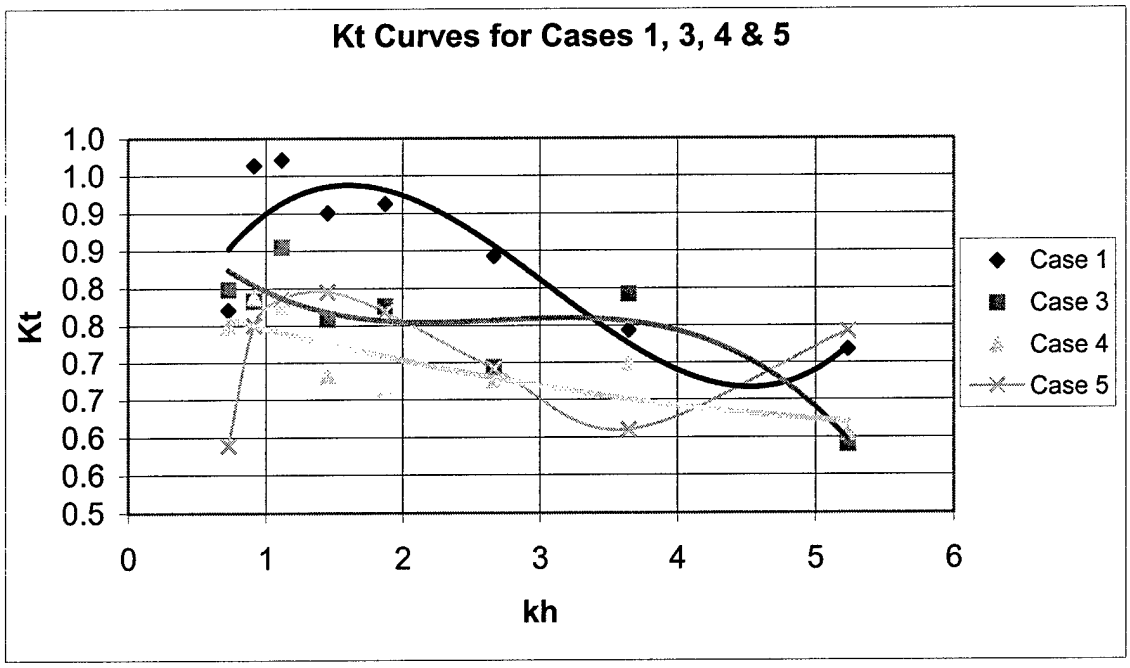

Figure 4.3 Comparison of transmission coefficients for cases 1, 3, 4, and 5.

4.1.2 Flexible Mooring Results

Four cases (Cases 6-9) were configured by using combinations of two types of membrane material and three membrane lengths. Only one membrane position (front) was used in each of these four cases. The four flexible-mooring configurations considered are summarized in Table 4.2.

Table 4.2 Configurations for flexible moorings.

Case #	Membrane Type	Membrane Length	Position
6	Permeable	full	none
7	Impermeable	full	front
8	Permeable	1/2	front
9	Permeable	1/4	front

Figure 4.4 shows a comparison of polynomial fit curves of the transmission coefficients for the full-length permeable membrane (Case 6), full-length non-permeable

membrane (Case 7) and the no-membrane case (Case 1). The permeable membrane (Case 6) has a lowest transmission coefficient providing the most wave attenuation. This is consistent with the stiff mooring results shown in Figure 4.1. Case 6 results in an average decrease in the transmission coefficient of 14 %, while Case 7 results in a lower average decrease of 8 %.

Figure 4.5 shows a comparison of the transmission coefficients for the ½ -length permeable membrane (Case 8), ¼ -length permeable membrane (Case 9), and no-membrane (Case 1). Figure 4.5 shows that the 1/4-length permeable membrane (Case 9) and the 1/2-length permeable membrane (Case 8) have very similar transmission coefficient values. The ¼- length membrane virtually parallels the performance of the longer ½-length membrane. This suggests there is little benefit, in terms of wave protection; saved by using a longer membrane.

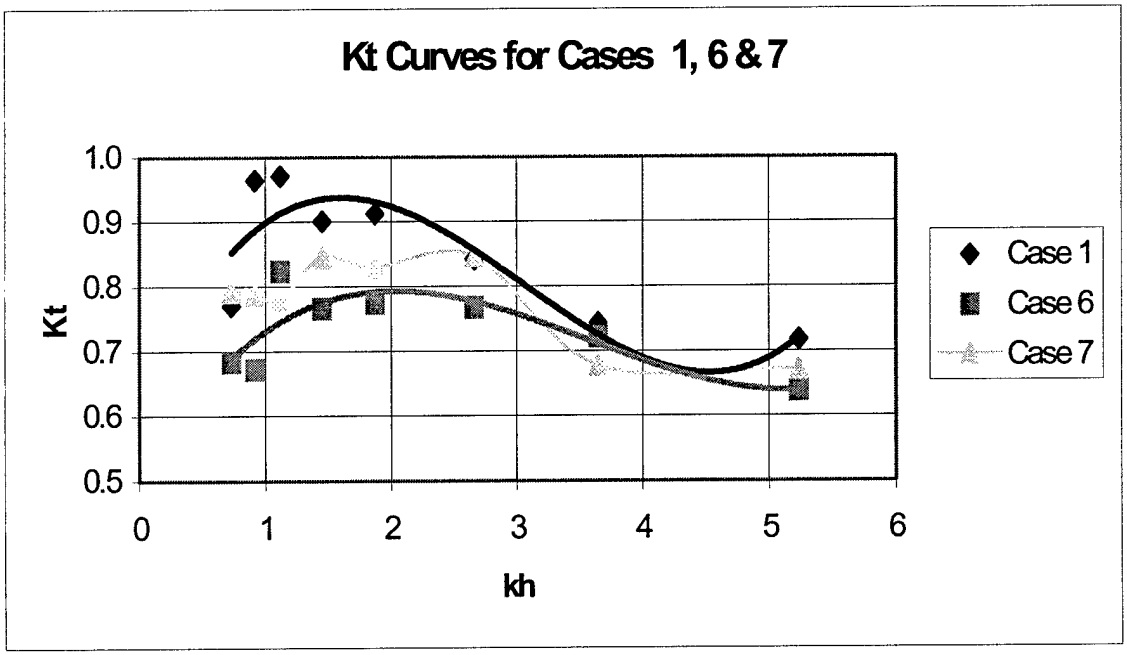

Figure 4.4 Comparison of transmission coefficients for cases 1, 6, and 7.

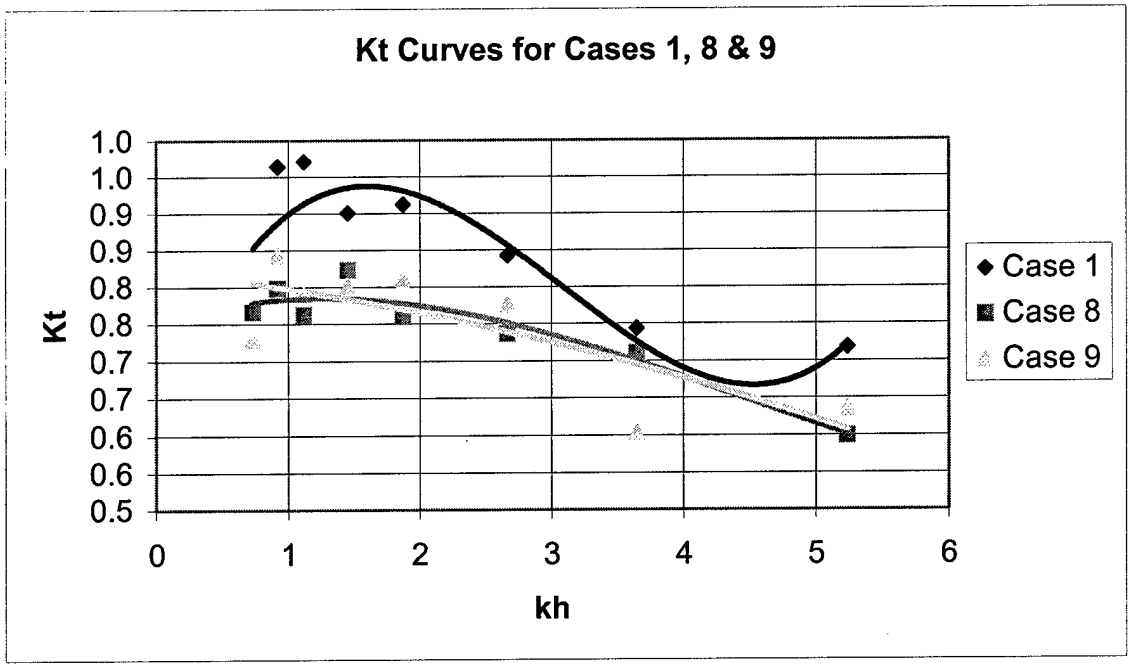

Figure 4.5. Comparison of transmission coefficients for cases 1, 8, and 9.

Figure 4.6 shows a of the transmission coefficients for the ¼ -length permeable membrane (Case 9), ½ -length permeable membrane (Case 8), the full-length permeable membrane (Case 7) and no-membrane (Case 1). The three cases with membranes all have lower transmission coefficients than Case 1. Also, both the 1/4-length permeable membrane and the ½ -length permeable membrane appear to have lower transmission coefficients than the full-length permeable membrane throughout range of periods. Thus, Cases 8 and 9 appear to provide the highest wave attenuation of these four cases. Cases 8 and 9 each result in average decreases in the transmission coefficient of 12 %.

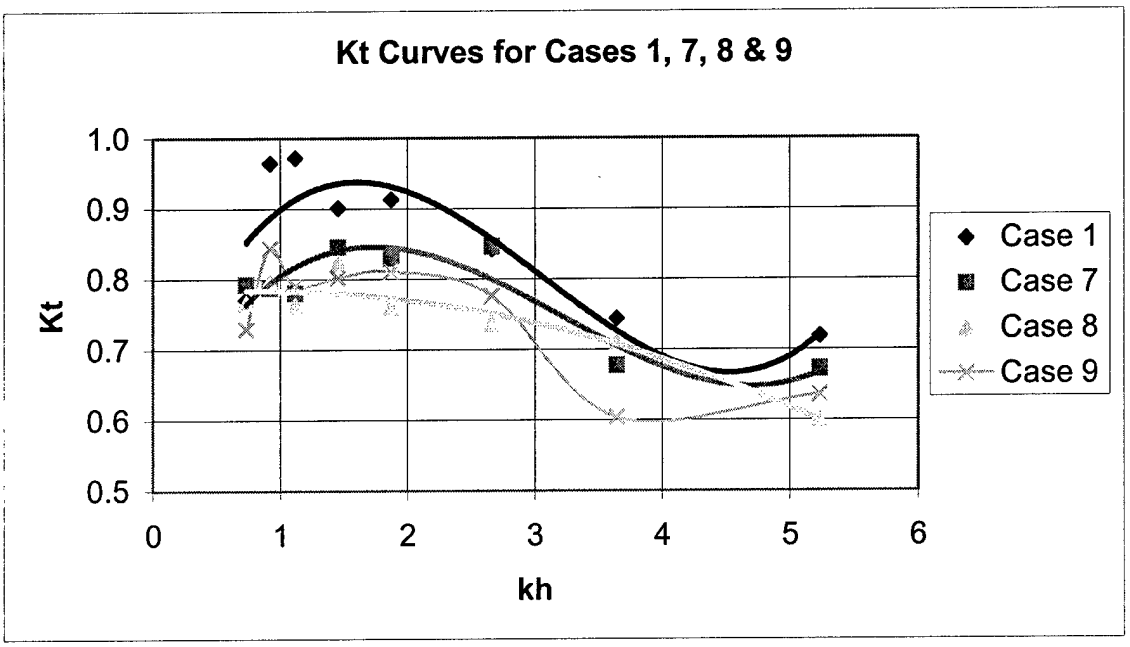

Figure 4.6. Comparison of transmission coefficients for cases 1, 7, 8, and 9.

Like the stiff mooring results, all flexible mooring cases including a membrane provided lower transmission coefficients throughout the range of periods tested than the no-membrane base case. A full- length, the permeable membrane gave a lower transmission coefficient then the impermeable membrane over the entire range of periods. The ¼- length and ½- length permeable membranes provided similar results with the ½ - length membrane providing lower values through the mid-range of wave periods and ¼ - length membrane showing lower values on each end of the wave period range. Both the ¼- length and ½- length permeable membranes provided lower transmission coefficients than the full-length permeable membrane.

4.1.3 Mooring Compliance Comparisons

Figure 4.7 shows a comparison of polynomial fit curves of the transmission coefficients for the stiff mooring full-length, permeable membrane (Case3), the flexible mooring full-length, permeable membrane (Case 6), and the no-membrane case (Case 1).

From Figure 4.7, it is seen that the flexible mooring case (Case 6) has the lowest transmission coefficient throughout the range of frequencies tested. This suggests that the flexible mooring case provides more wave attenuation when the full-length, permeable membranes are compared.

Figure 4.8 shows a comparison of the transmission coefficients for the stiff mooring full-length non-permeable membrane (Case 2), the flexible mooring full-length non-permeable membrane (Case 7), and the no-membrane case (Case 1). Figure 4.8 shows how the stiff mooring case (Case 2.) has the lowest transmission coefficient throughout high the frequency range. This suggests that for smaller wave periods, the stiff moorings provide more wave attenuation then the flexible moorings when full-length, non-permeable membrane is used.

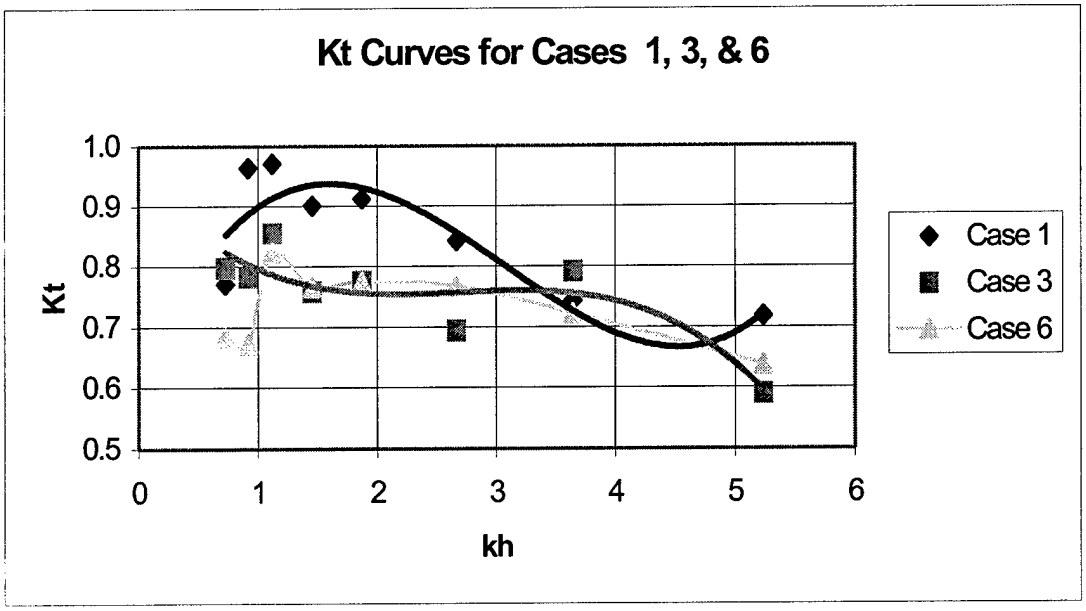

Fig 4.7 Comparison of transmission coefficients for cases 1, 3, and 6.

Figure 4.9 shows a comparison of the transmission coefficients of the ¼- length membrane in the back (Case 4), center (Case 5), and front (Case 9) positions. Case 9 had flexible moorings while Cases 4 and 5 had stiff moorings. Case 9 (flexible moorings with membrane in front) has the lowest transmission coefficient in the higher frequency ranges ($kh \geq 3.6$) while Case 4 (stiff moorings with membrane in back) provided lower K_t values in the lower frequency range ($kh \leq 2.8$). While Case 9 provided an 11 % reduction in the average transmission coefficient when compared to Case 1, Case 4 and 5 provided even higher reductions at 17 % and 16 %, respectively.

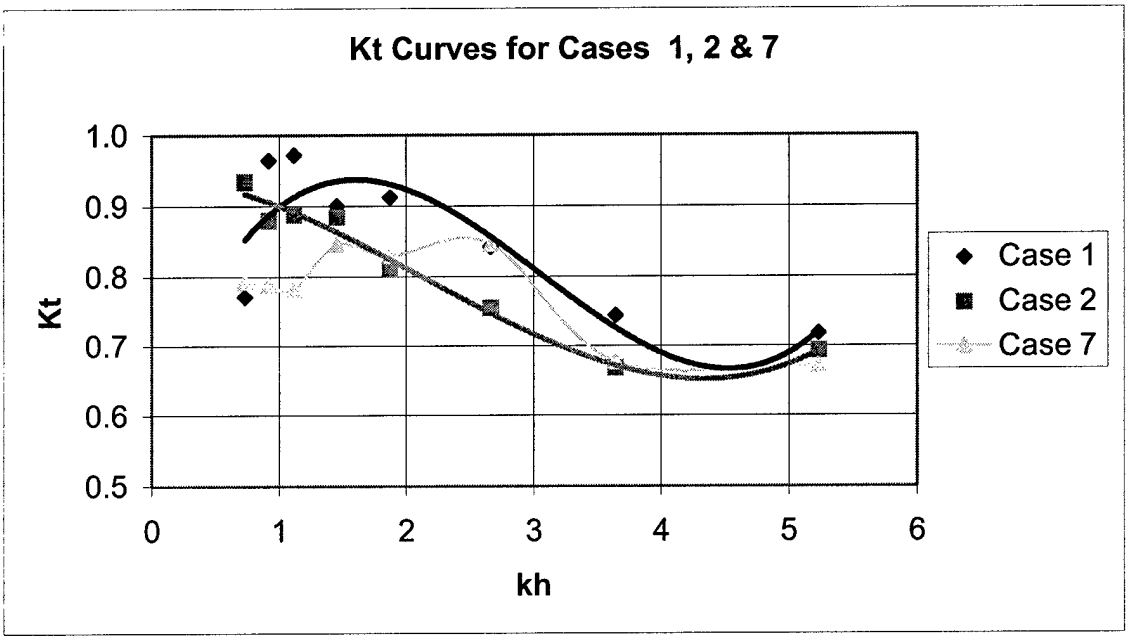

Fig 4.8. Comparison of transmission coefficients for cases 1, 2, and 7.

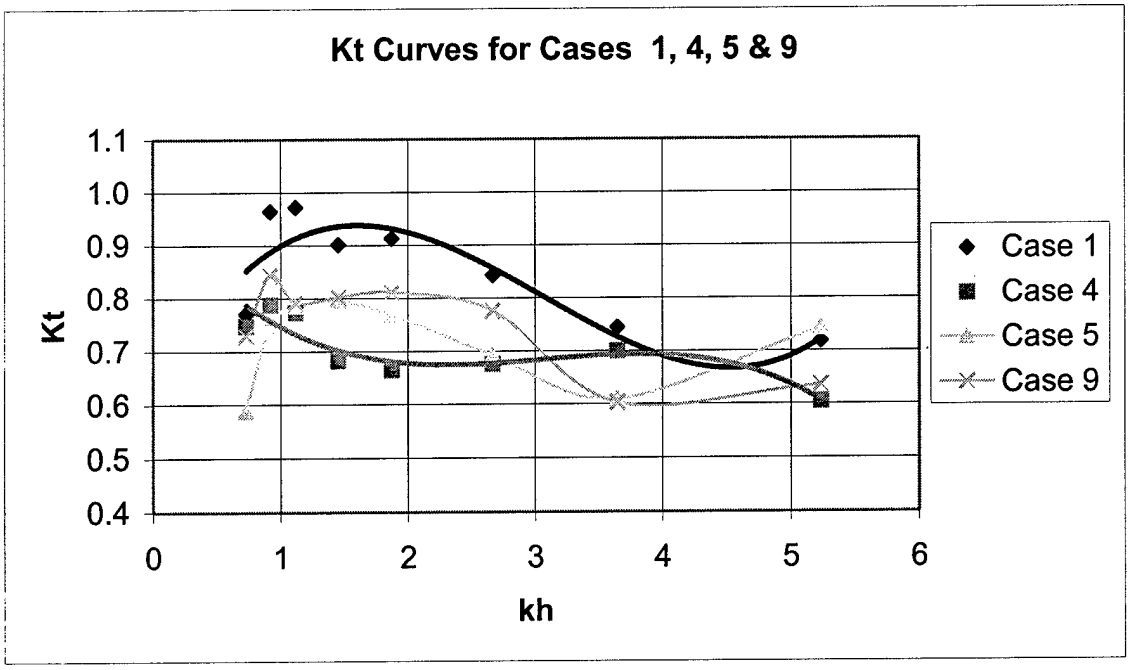

Fig 4.9. Comparison of transmission coefficients for cases 1, 4, 5, and 9.

CHAPTER 5
CONCLUSIONS

5.1 Summary

A physical model study of a floating breakwater with an attached vertical membrane was conducted with the intent of determining the effects of vertical membranes on wave attenuation. The wave characteristics were analyzed with an emphasis on transmission coefficients. The nine different configurations were chosen to provide comparisons of various moorings, membrane permeability, membrane position, and membrane length. Eight wave periods ranging from 0.54 seconds to 1.29 seconds were used and each test was duplicated. Therefore, 72 combinations were examined requiring approximately 150 flume runs to be performed. All data collection was completed at the University of Florida's Coastal Engineering Laboratory located in Gainesville, Florida.

5.2 Conclusions

Each configuration provided partial reduction of the transmission coefficients when compared the no-membrane case, Case 1. The average transmission coefficient for each of the nine cases ranged from 0.705 to 0.853 with an average value of 0.761. Case 4, the ¼- length permeable membrane with stiff moorings provided the lowest average transmission coefficient of 0.705. However, other cases provided lower transmission coefficients at specific wave periods. For example, at T= 0.54 s, Case 3 provided the lowest transmission coefficient at 0.591. Likewise, at T= 1.16 s, Case 6 provided the lowest transmission coefficient with a value of 0.672. Neglecting the base case, the full-length impermeable membrane with stiff moorings (Case 2) permitted the most wave

transmission with a transmission coefficient of 0.814. The transmission coefficients for each configuration are provided in Table 5.1 below.

Table 5.1 Summary of Transmission Coefficients

T (s)	Transmission Coefficient, K_t								
	Case 1	Case 2	Case 3	Case 4	Case 5	Case 6	Case 7	Case 8	Case 9
0.54	0.718	0.694	0.591	0.606	0.743	0.639	0.673	0.600	0.636
0.62	0.744	0.668	0.792	0.700	0.610	0.723	0.678	0.711	0.604
0.71	0.842	0.755	0.694	0.676	0.693	0.768	0.847	0.737	0.776
0.83	0.913	0.811	0.776	0.665	0.769	0.775	0.830	0.760	0.811
0.93	0.901	0.885	0.759	0.682	0.795	0.767	0.846	0.823	0.802
1.06	0.972	0.888	0.855	0.773	0.786	0.824	0.781	0.763	0.791
1.16	0.964	0.880	0.783	0.788	0.751	0.672	0.788	0.798	0.843
1.29	0.771	0.935	0.798	0.748	0.589	0.684	0.793	0.767	0.729
K_t (AVG)	0.853	0.814	0.756	**0.705**	0.717	0.732	0.779	0.745	0.749

The test results were somewhat counterintuitive. The ¼- length membrane with stiff moorings provided less wave transmission than both the ½- length and full- length membranes. Furthermore, the wave transmission was minimized with the ¼- length membrane positioned in the back of the breakwater. These results provide two important preliminary conclusions: 1) Longer membranes do not necessarily provide decreased wave transmission, 2) Membrane position has an impact on wave transmission, and 3) A permeable membrane is more effective than an impermeable one.

APPENDIX A
OBSERVED MODEL DISPLACEMENTS

	T	Oserved Displacements (mm)			
		Forward	Backward	Upward	Downward
CASE 1	0.539	8	25	0	0
	0.622	3	29	0	0
	0.711	4	39	0	6
	0.831	5	48	0	8
	0.933	11	52	0	10
	1.055	16	56	0	15
	1.16	36	56	0	20
	1.294	47	47	0	23

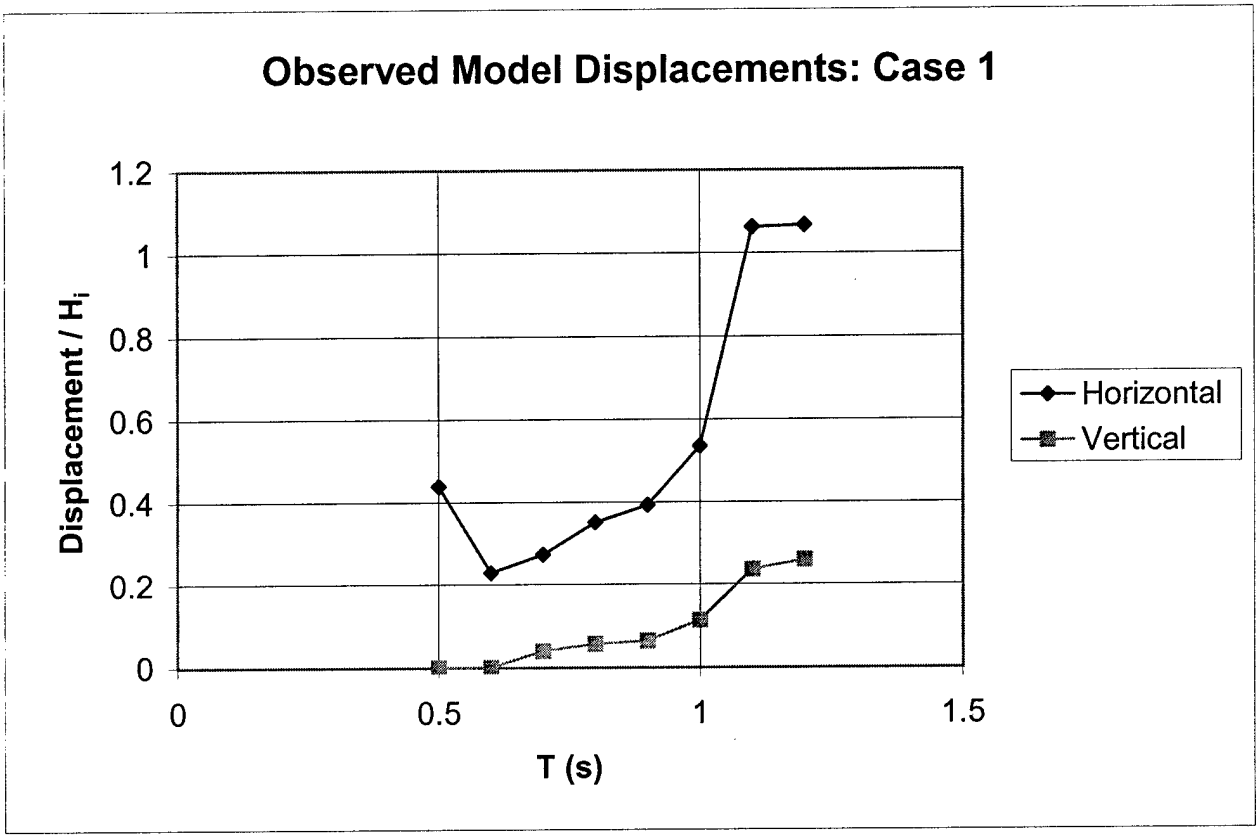

	T	Oserved Displacements (mm)			
		Forward	Backward	Upward	Downward
CASE 2	0.539	8	34	0	3
	0.622	4	77	0	15
	0.711	17	42	0	4
	0.831	18	46	0	4
	0.933	25	44	0	5
	1.055	27	41	0	5
	1.16	24	37	0	5
	1.294	20	30	0	4

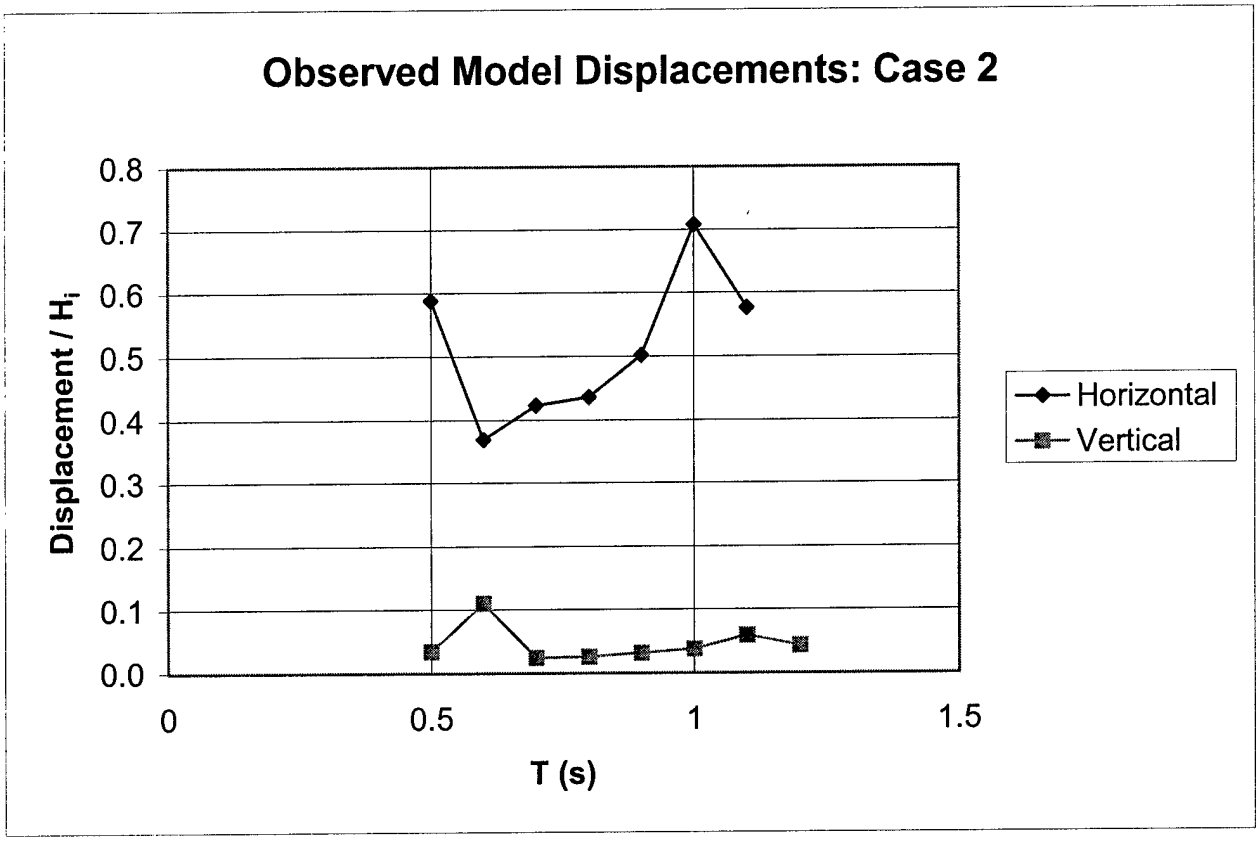

	T	Oserved Displacements (mm)			
		Forward	Backward	Upward	Downward
CASE 3	0.539	17	41	0	0
	0.622	6	144	0	6
	0.711	0	119	0	19
	0.831	15	121	0	15
	0.933	23	137	0	13
	1.055	64	123	0	9
	1.16	69	91	0	5
	1.294	53	76	0	8

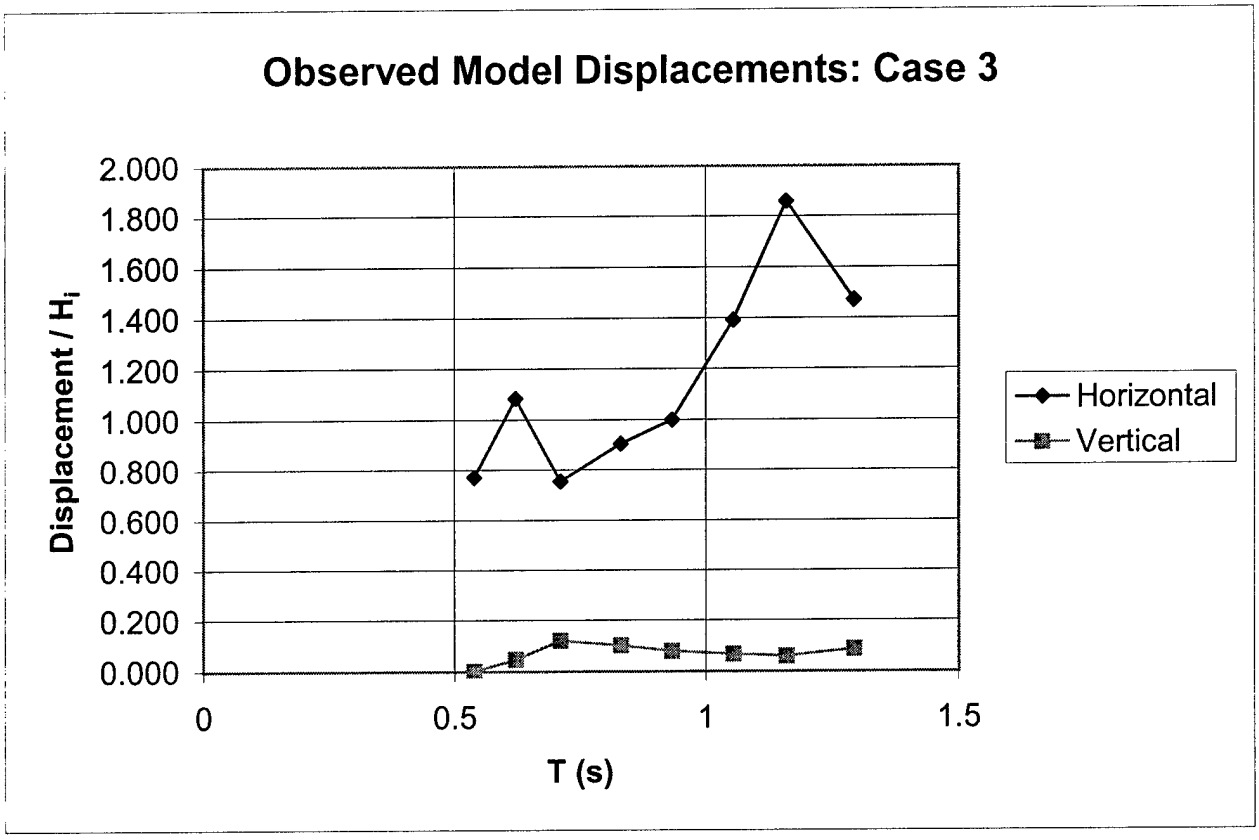

	T	Oserved Displacements (mm)			
		Forward	Backward	Upward	Downward
CASE 4	0.539	5	23	0	0
	0.622	6	43	0	6
	0.711	0	58	0	10
	0.831	10	61	0	8
	0.933	10	51	0	6
	1.055	15	48	0	6
	1.16	23	36	0	3
	1.294	25	33	0	0

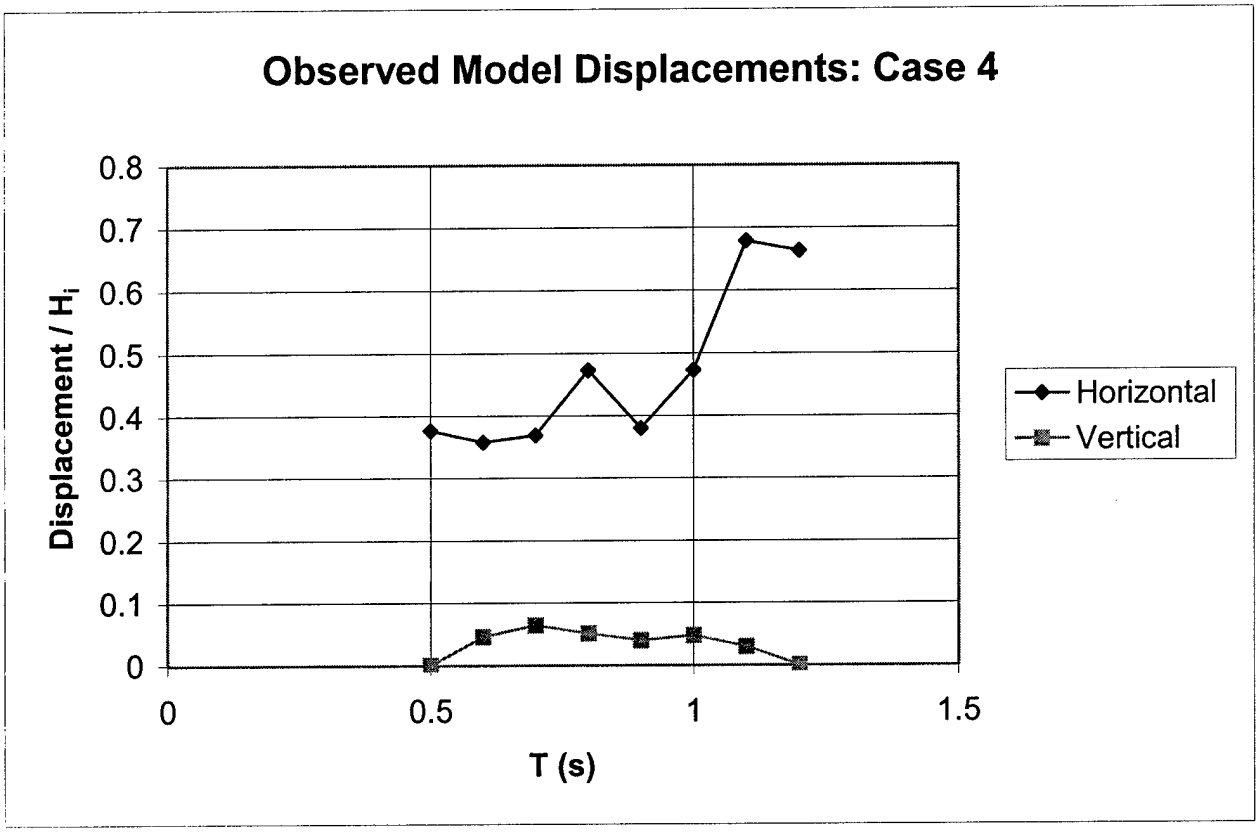

	T	Oserved Displacements (mm)			
		Forward	Backward	Upward	Downward
CASE 5	0.539	4	17	0	0
	0.622	4	29	0	4
	0.711	6	37	0	10
	0.831	8	48	0	13
	0.933	15	52	0	5
	1.055	19	43	0	4
	1.16	24	39	0	0
	1.294	29	32	0	1

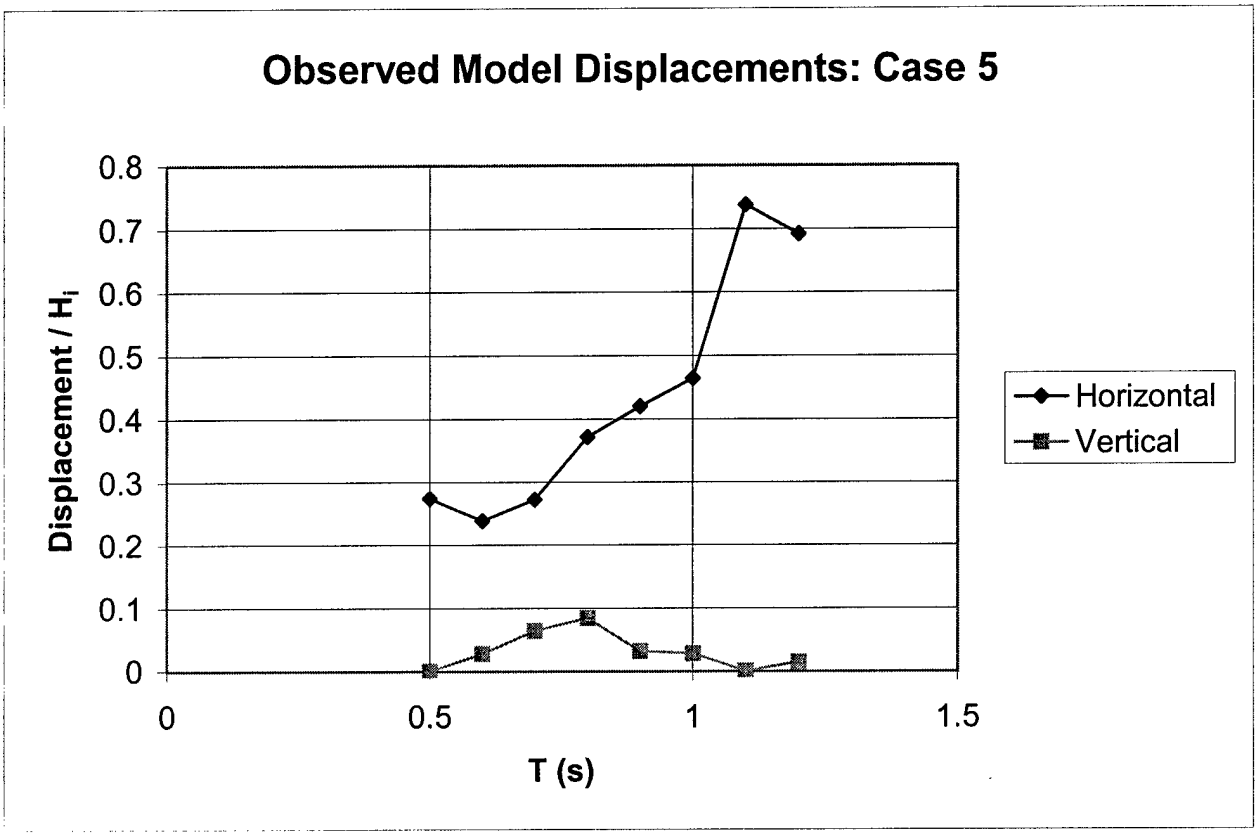

	T	Oserved Displacements (mm)			
		Forward	Backward	Upward	Downward
CASE 6	0.539	6	25	13	10
	0.622	15	47	25	20
	0.711	20	37	23	20
	0.831	19	41	28	24
	0.933	27	42	23	19
	1.055	24	39	19	20
	1.16	29	32	20	19
	1.294	29	32	15	17

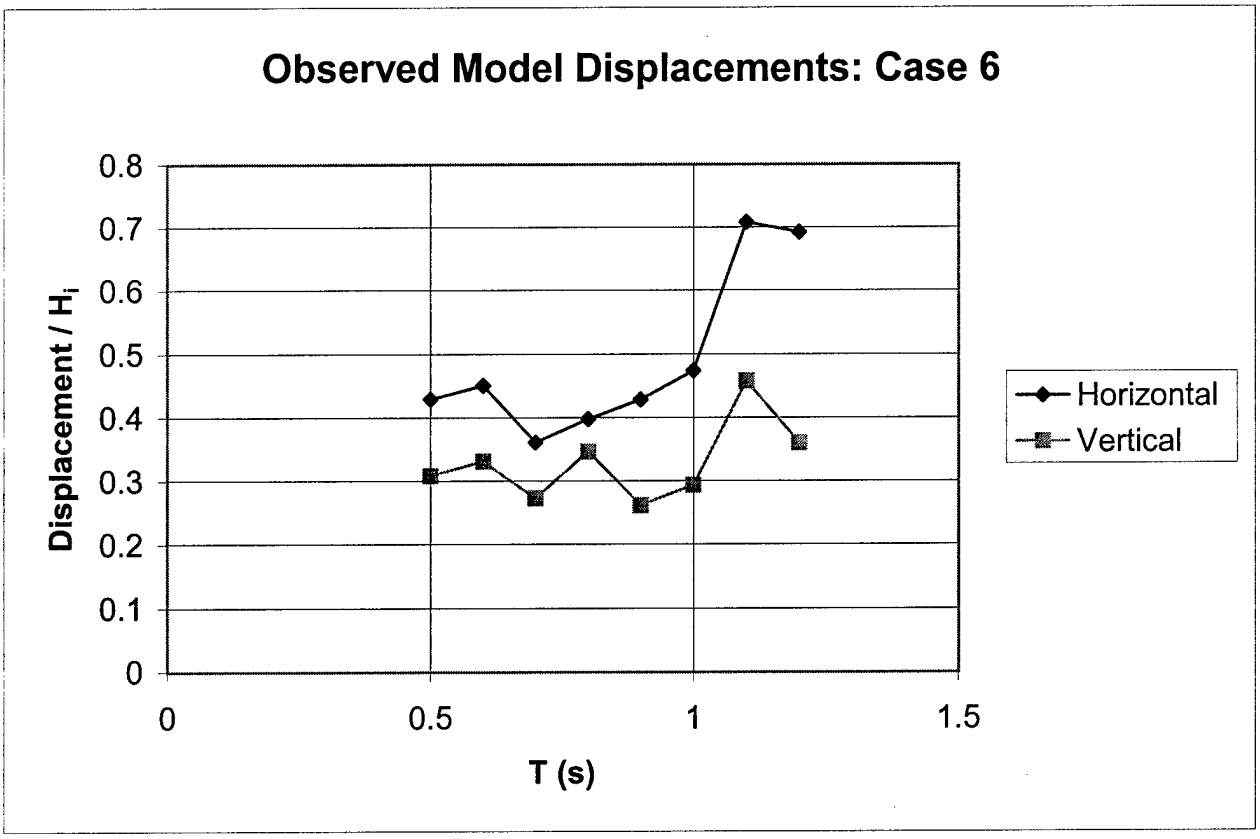

	T	Oserved Displacements (mm)			
		Forward	Backward	Upward	Downward
CASE 7	0.539	9	30	17	9
	0.622	17	38	27	18
	0.711	24	34	29	18
	0.831	30	34	30	22
	0.933	33	39	24	20
	1.055	28	36	20	19
	1.16	34	34	18	18
	1.294	34	34	15	15

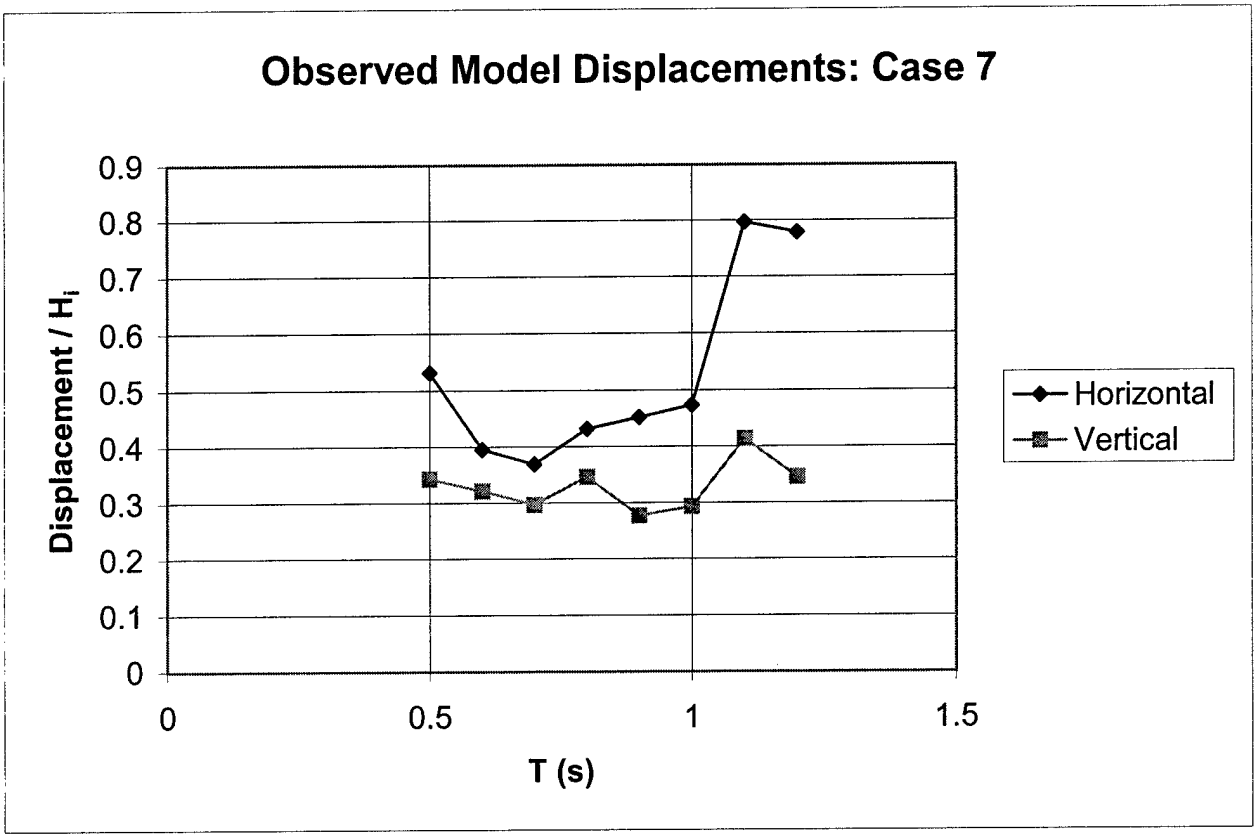

	T	Oserved Displacements (mm)			
		Forward	Backward	Upward	Downward
CASE 8	0.539	8	27	17	10
	0.622	17	52	34	20
	0.711	18	48	32	20
	0.831	32	41	32	24
	0.933	42	34	24	19
	1.055	38	33	20	20
	1.16	30	28	15	19
	1.294	34	29	15	17

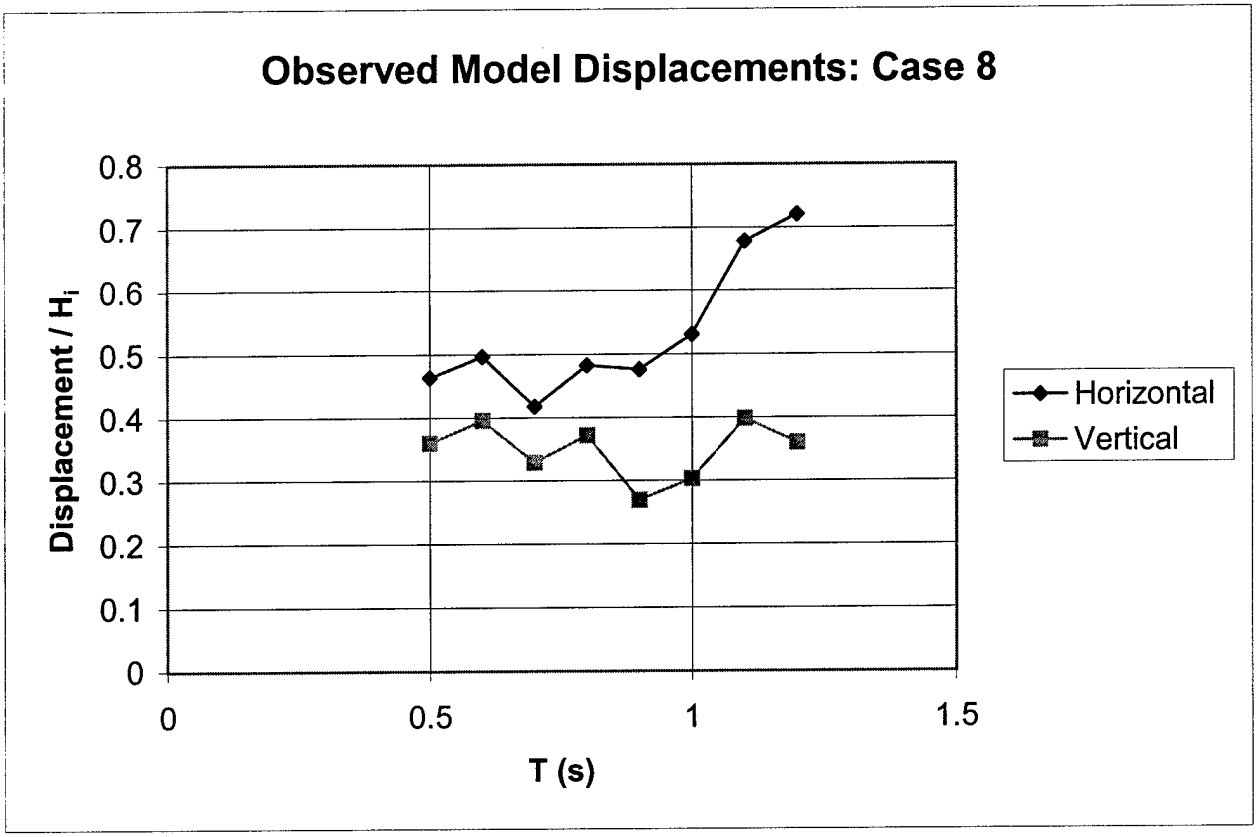

	T	Oserved Displacements (mm)			
		Forward	Backward	Upward	Downward
CASE 9	0.539	9	30	19	5
	0.622	10	34	28	6
	0.711	15	34	20	14
	0.831	32	37	23	19
	0.933	34	39	17	19
	1.055	30	25	9	28
	1.16	28	30	13	15
	1.294	25	25	13	17

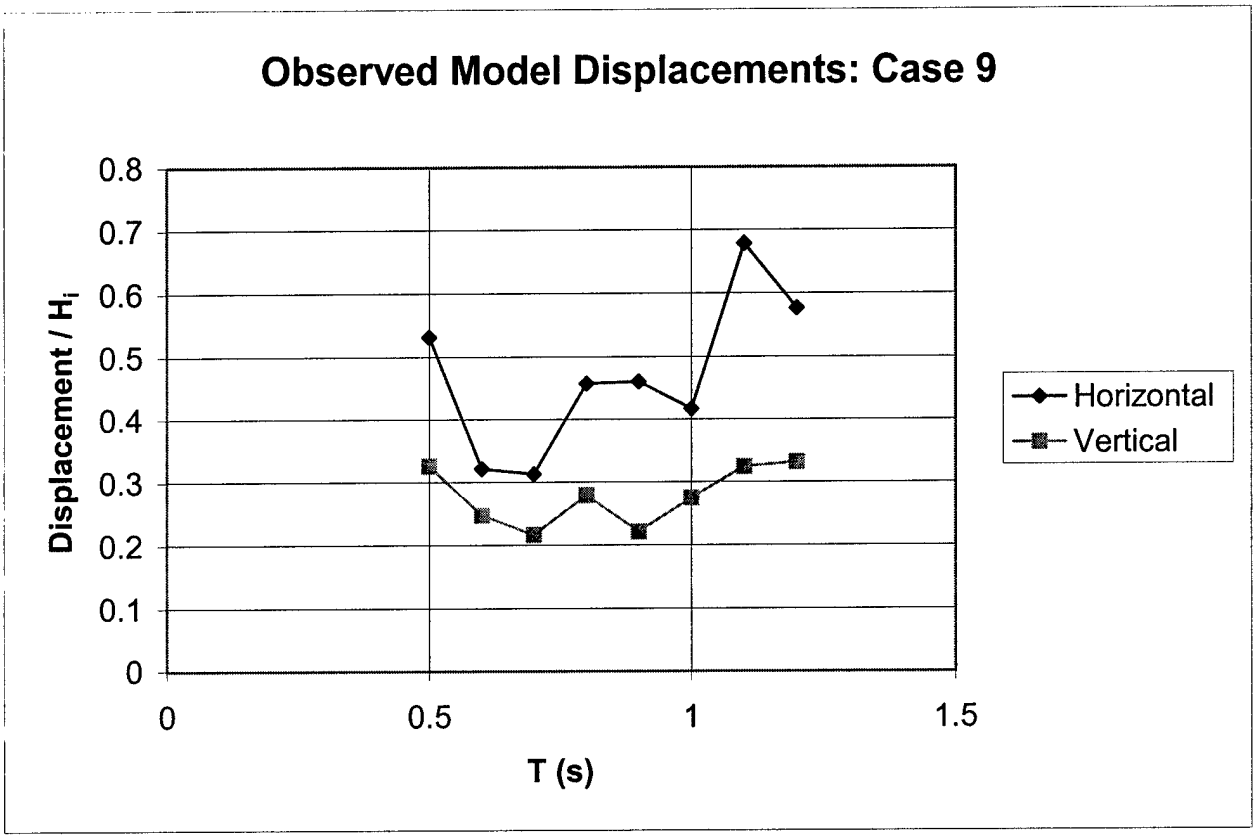

APPENDIX B
WAVE HEIGHT MEASUREMENTS

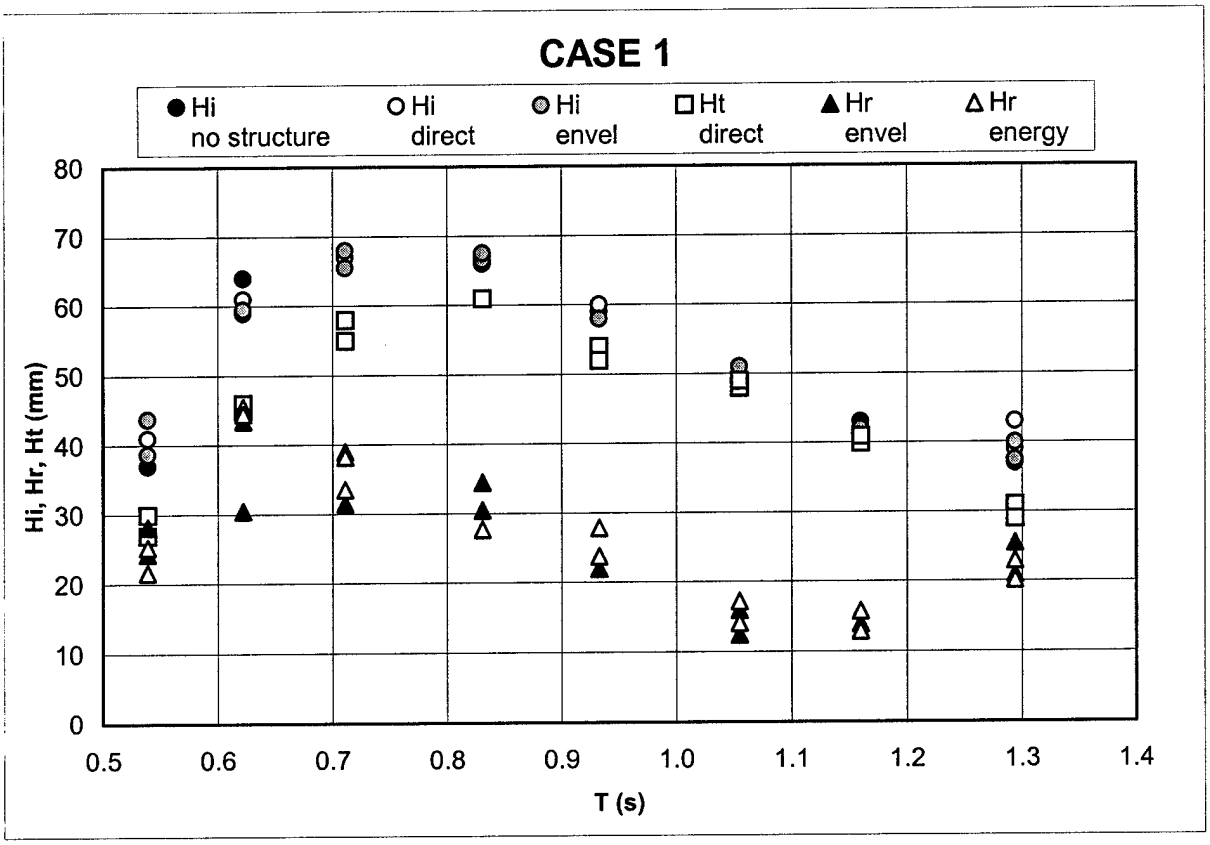
CASE 1
Hi no structure
Hi direct
Hi envel
Ht direct
Hr envel
Hr energy
Hi, Hr, Ht (mm)
0
10
20
30
40
50
60
70
80
0.5
0.6
0.7
0.8
0.9
1.0
1.1
1.2
1.3
1.4
T (s)

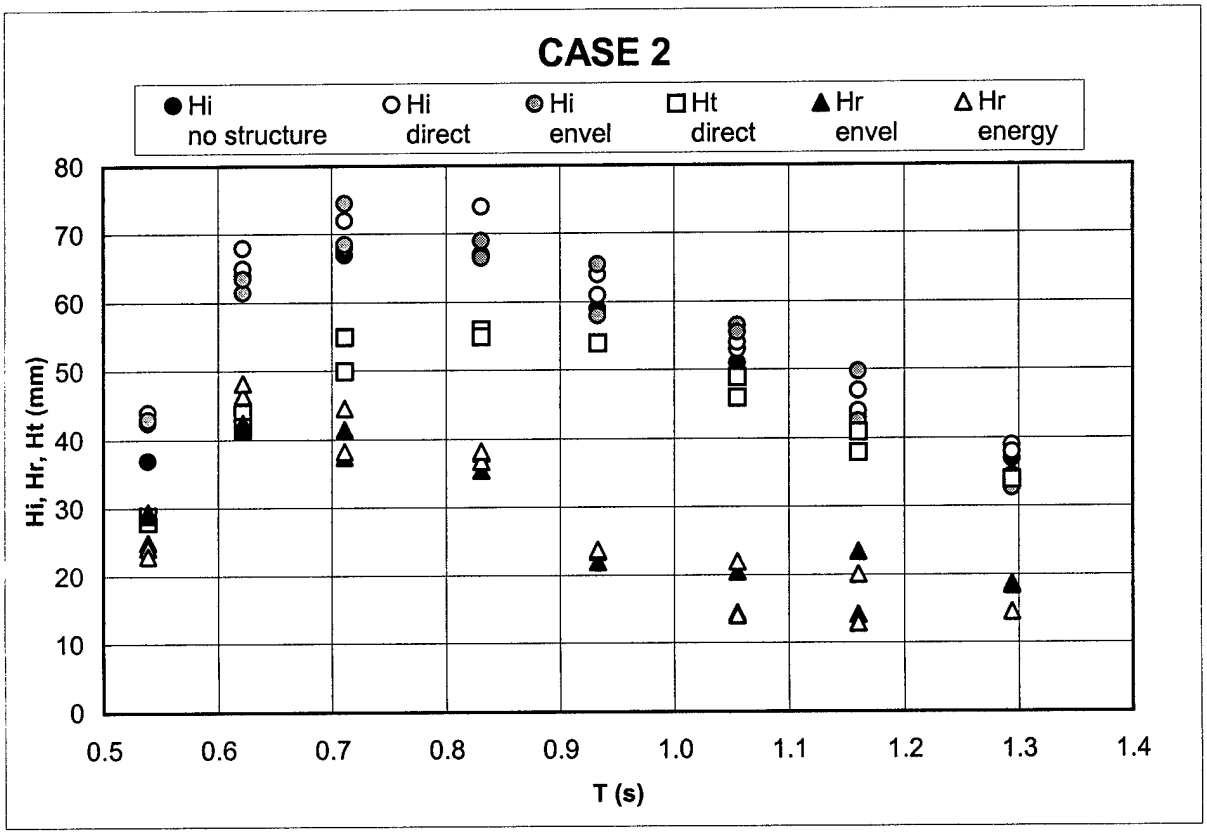
CASE 2
Hi no structure
Hi direct
Hi envel
Ht direct
Hr envel
Hr energy
Hi, Hr, Ht (mm)
0
10
20
30
40
50
60
70
80
0.5
0.6
0.7
0.8
0.9
1.0
1.1
1.2
1.3
1.4
T (s)

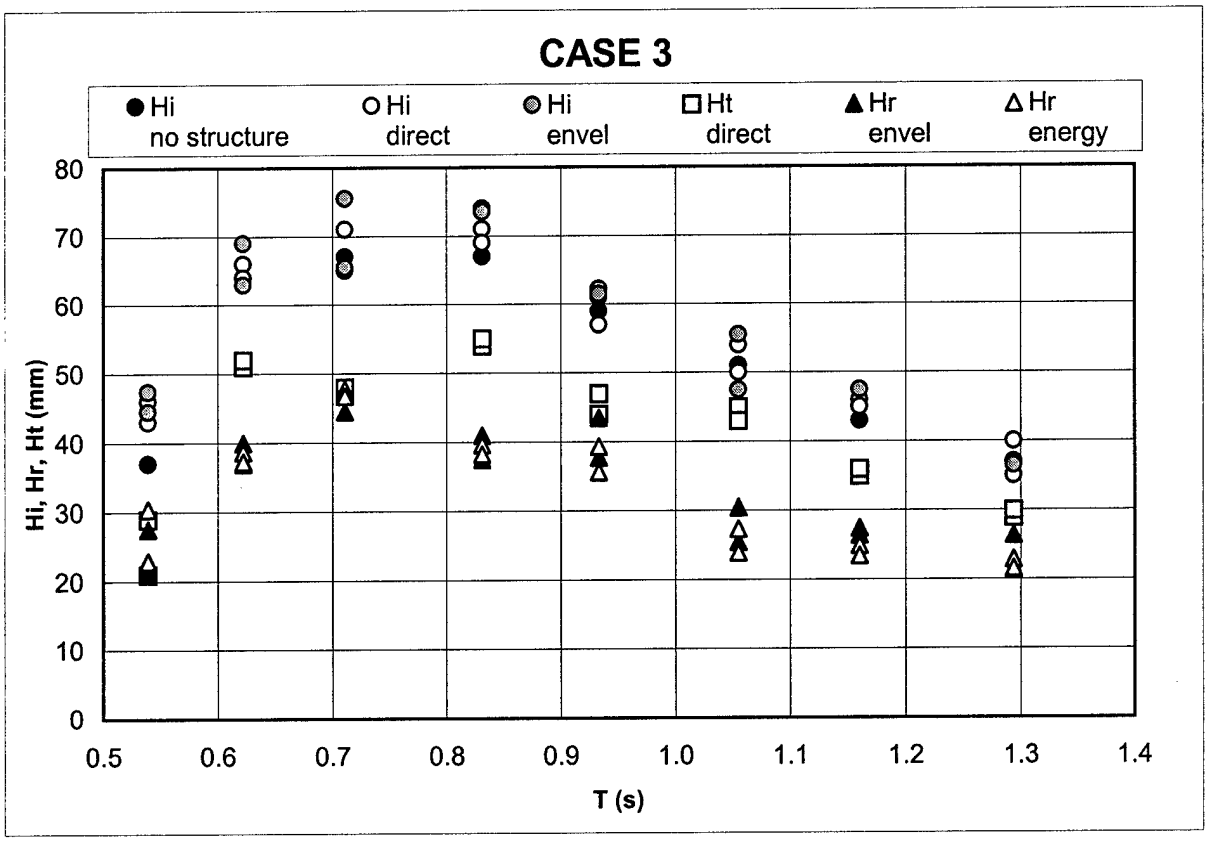
CASE 3
Hi no structure
Hi direct
Hi envel
Ht direct
Hr envel
Hr energy
Hi, Hr, Ht (mm)
0
10
20
30
40
50
60
70
80
0.5
0.6
0.7
0.8
0.9
1.0
1.1
1.2
1.3
1.4
T (s)

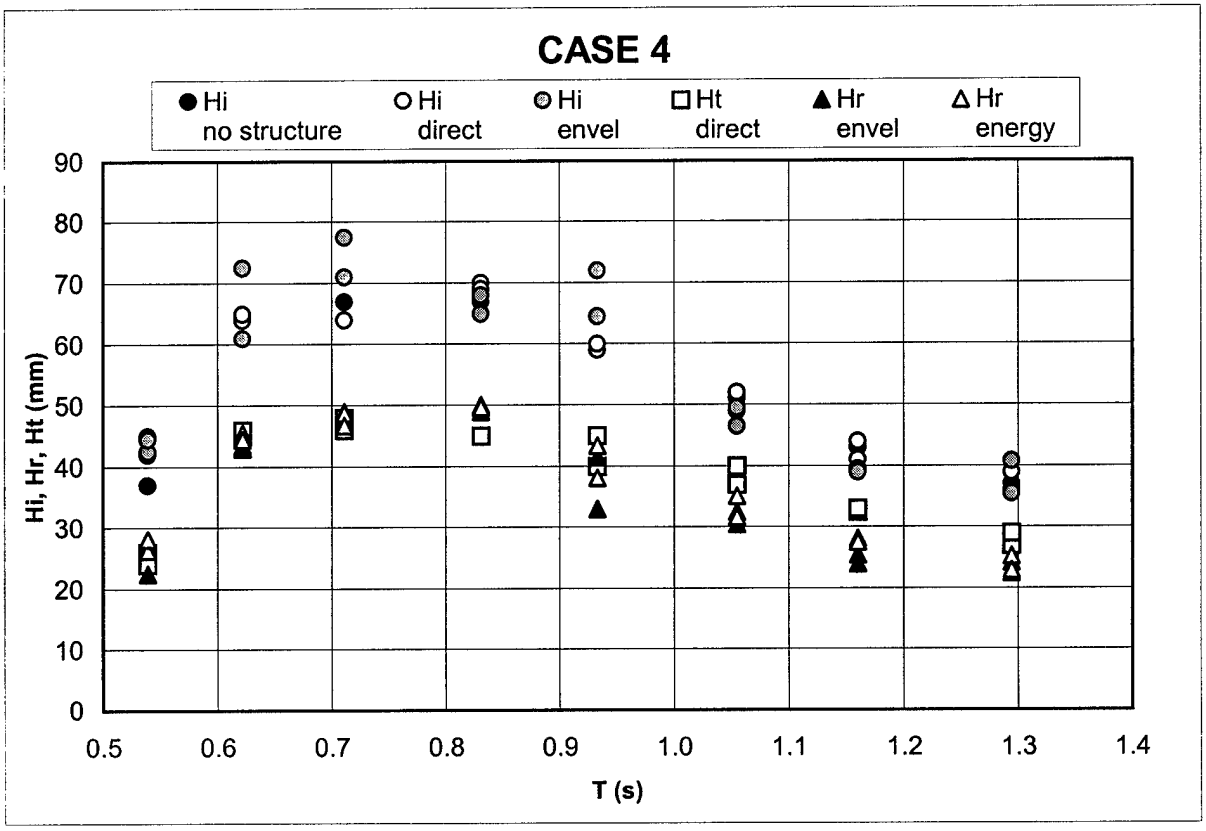
CASE 4
Hi no structure
Hi direct
Hi envel
Ht direct
Hr envel
Hr energy
Hi, Hr, Ht (mm)
0
10
20
30
40
50
60
70
80
90
0.5
0.6
0.7
0.8
0.9
1.0
1.1
1.2
1.3
1.4
T (s)

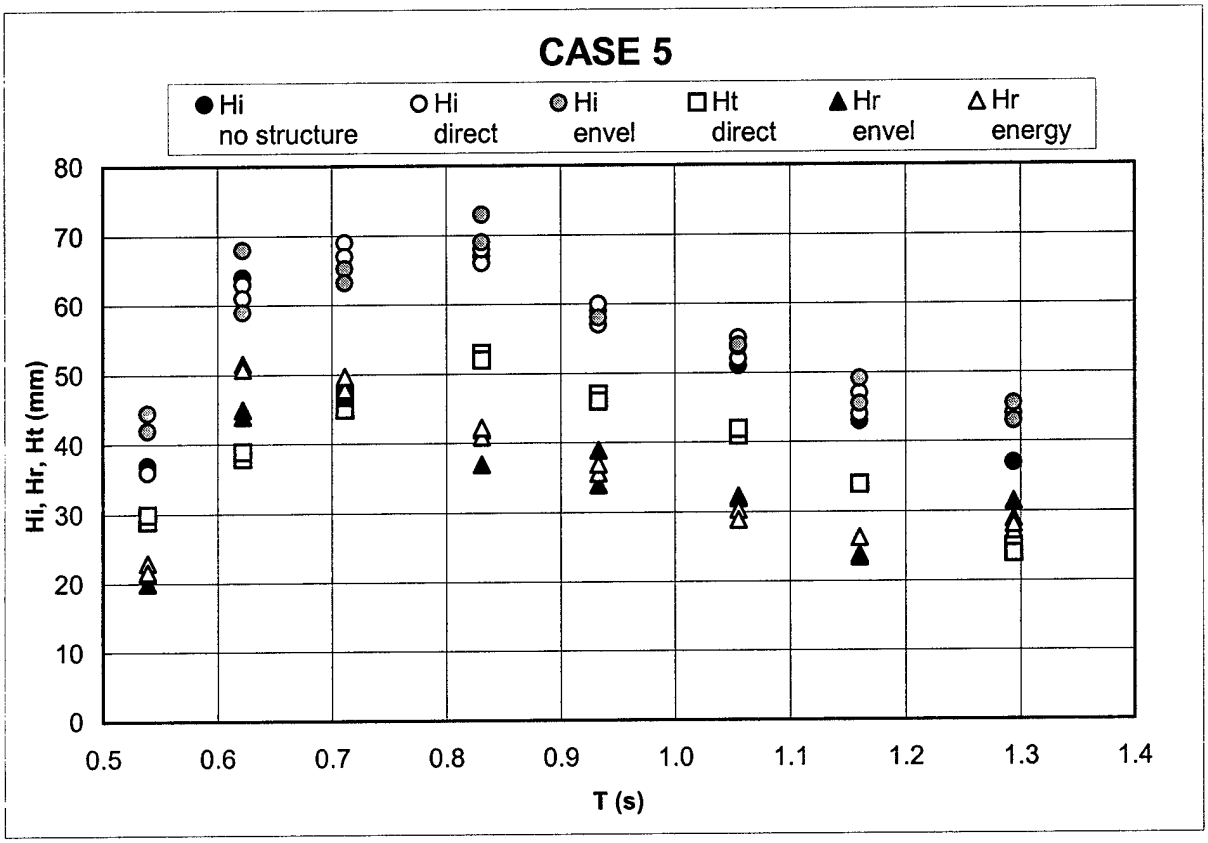
CASE 5
Hi no structure
Hi direct
Hi envel
Ht direct
Hr envel
Hr energy
Hi, Hr, Ht (mm)
0
10
20
30
40
50
60
70
80
0.5
0.6
0.7
0.8
0.9
1.0
1.1
1.2
1.3
1.4
T (s)

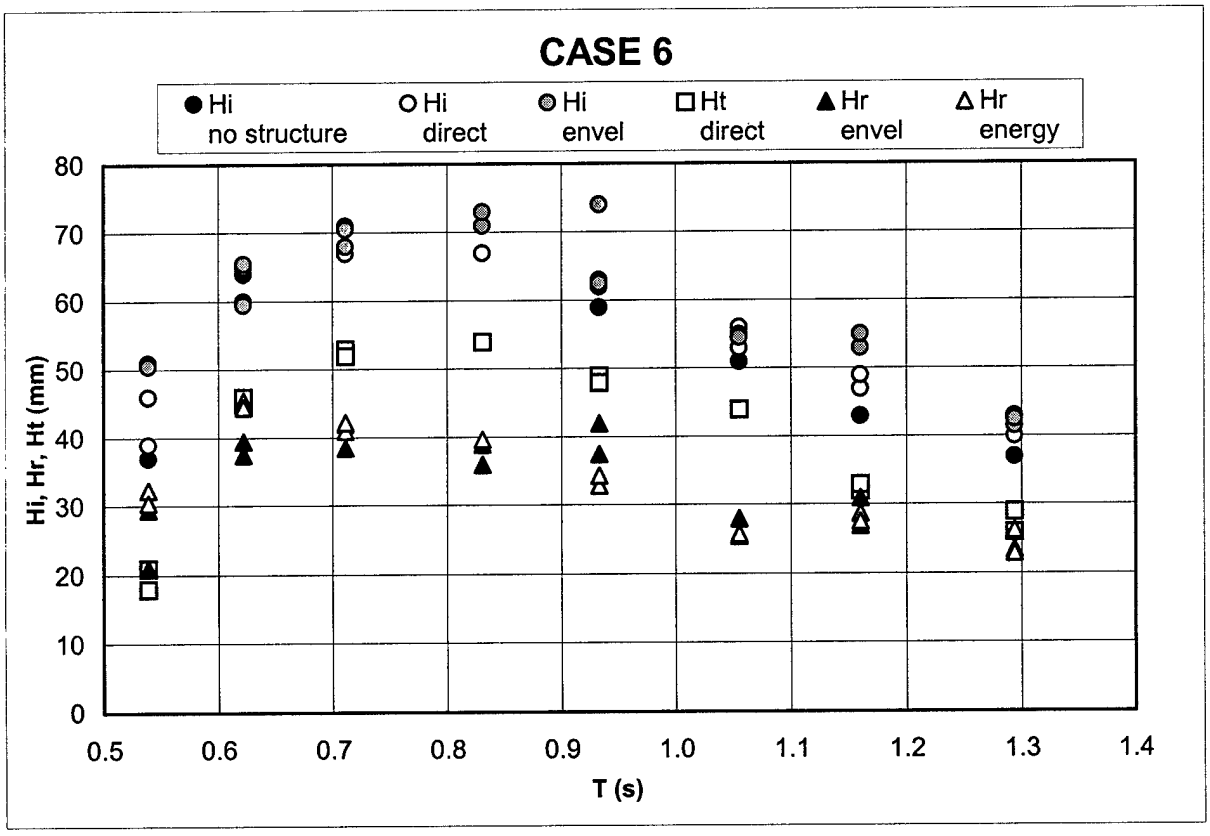
CASE 6
Hi no structure
Hi direct
Hi envel
Ht direct
Hr envel
Hr energy
Hi, Hr, Ht (mm)
0
10
20
30
40
50
60
70
80
0.5
0.6
0.7
0.8
0.9
1.0
1.1
1.2
1.3
1.4
T (s)

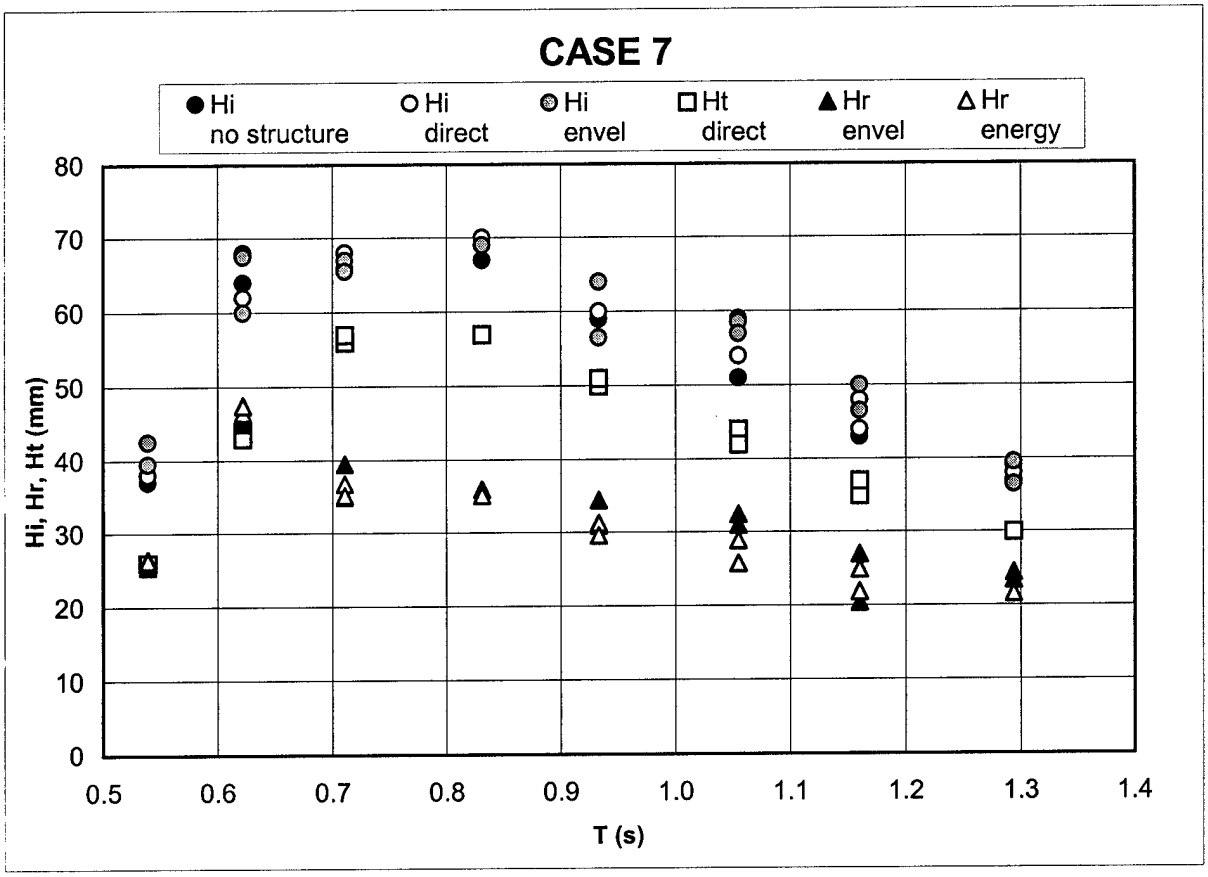
CASE 7
Hi no structure
Hi direct
Hi envel
Ht direct
Hr envel
Hr energy
Hi, Hr, Ht (mm)
T (s)
0
10
20
30
40
50
60
70
80
0.5
0.6
0.7
0.8
0.9
1.0
1.1
1.2
1.3
1.4

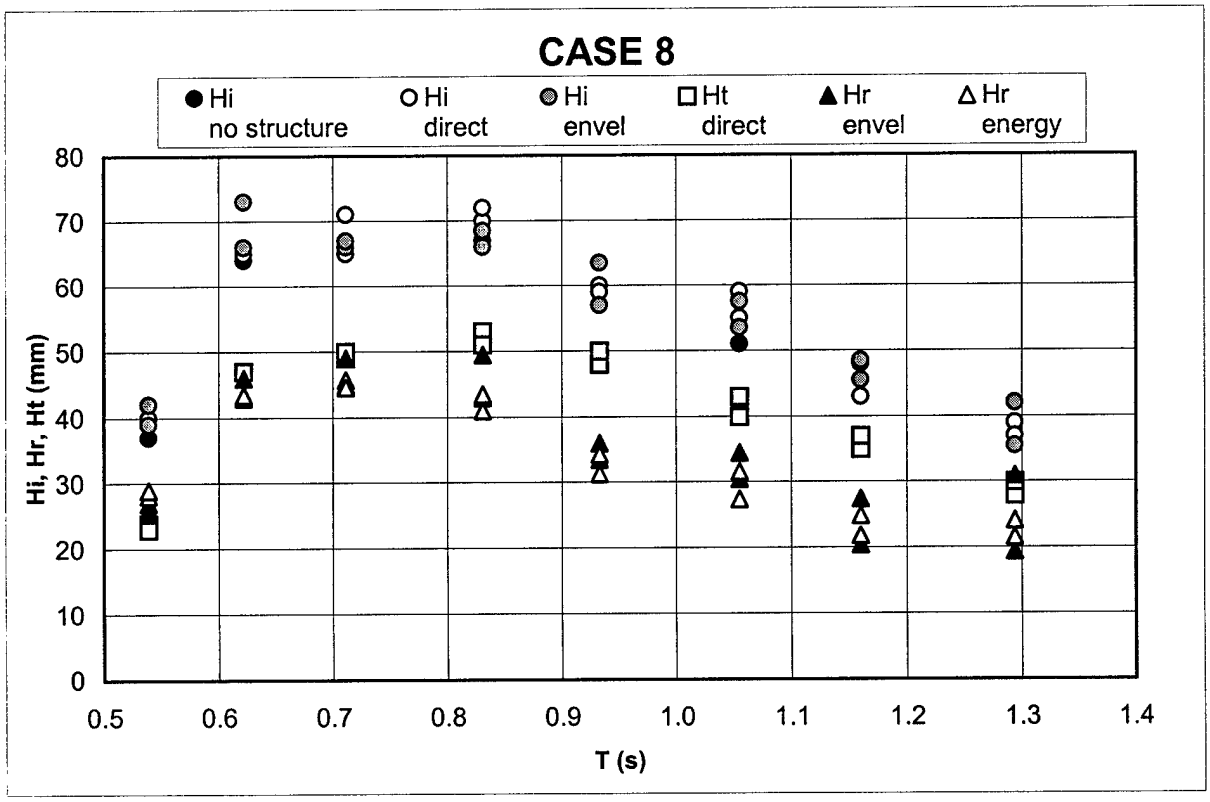
CASE 8
Hi no structure
Hi direct
Hi envel
Ht direct
Hr envel
Hr energy
Hi, Hr, Ht (mm)
T (s)
0
10
20
30
40
50
60
70
80
0.5
0.6
0.7
0.8
0.9
1.0
1.1
1.2
1.3
1.4

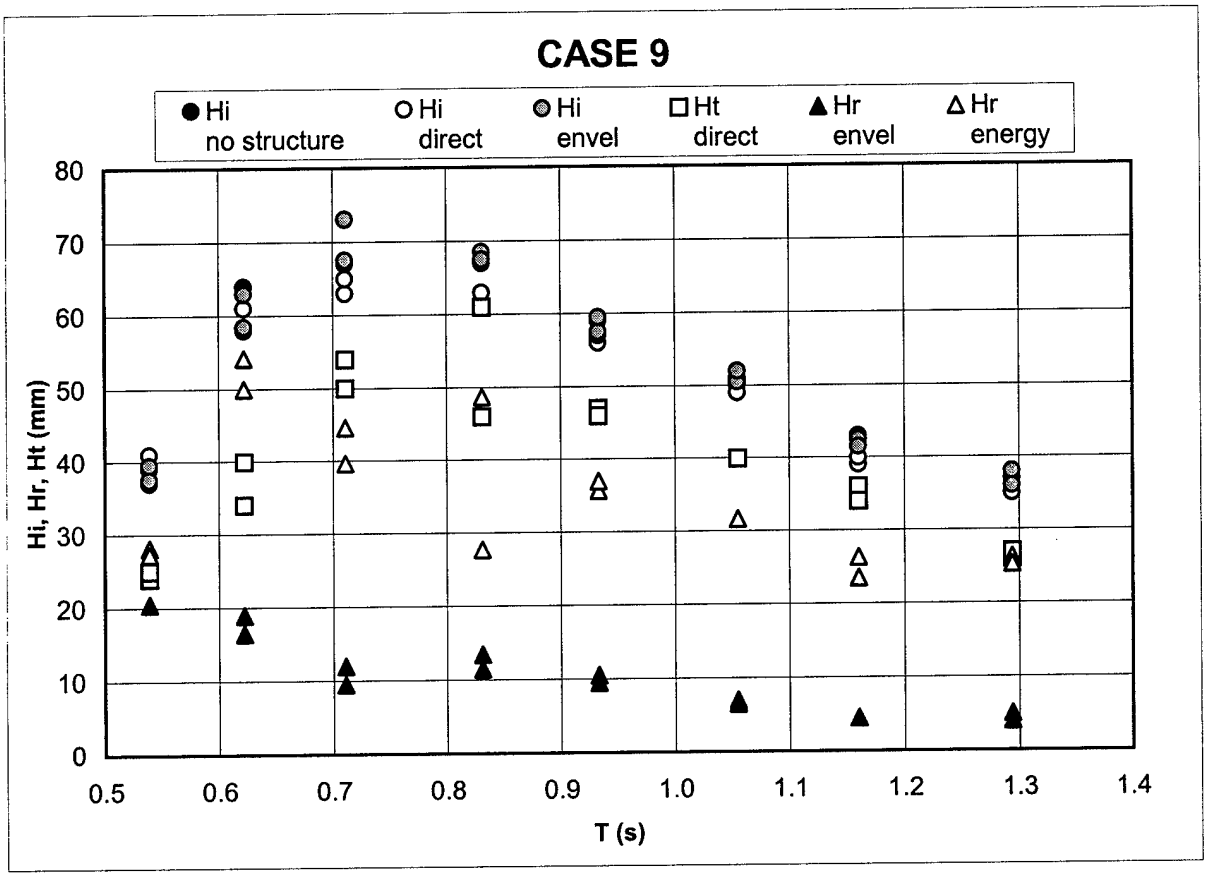
CASE 9
Hi no structure
Hi direct
Hi envel
Ht direct
Hr envel
Hr energy
Hi, Hr, Ht (mm)
0
10
20
30
40
50
60
70
80
0.5
0.6
0.7
0.8
0.9
1.0
1.1
1.2
1.3
1.4
T (s)

APPENDIX C
PROJECT PHOTOS

Coastal Engineering Laboratory sign.

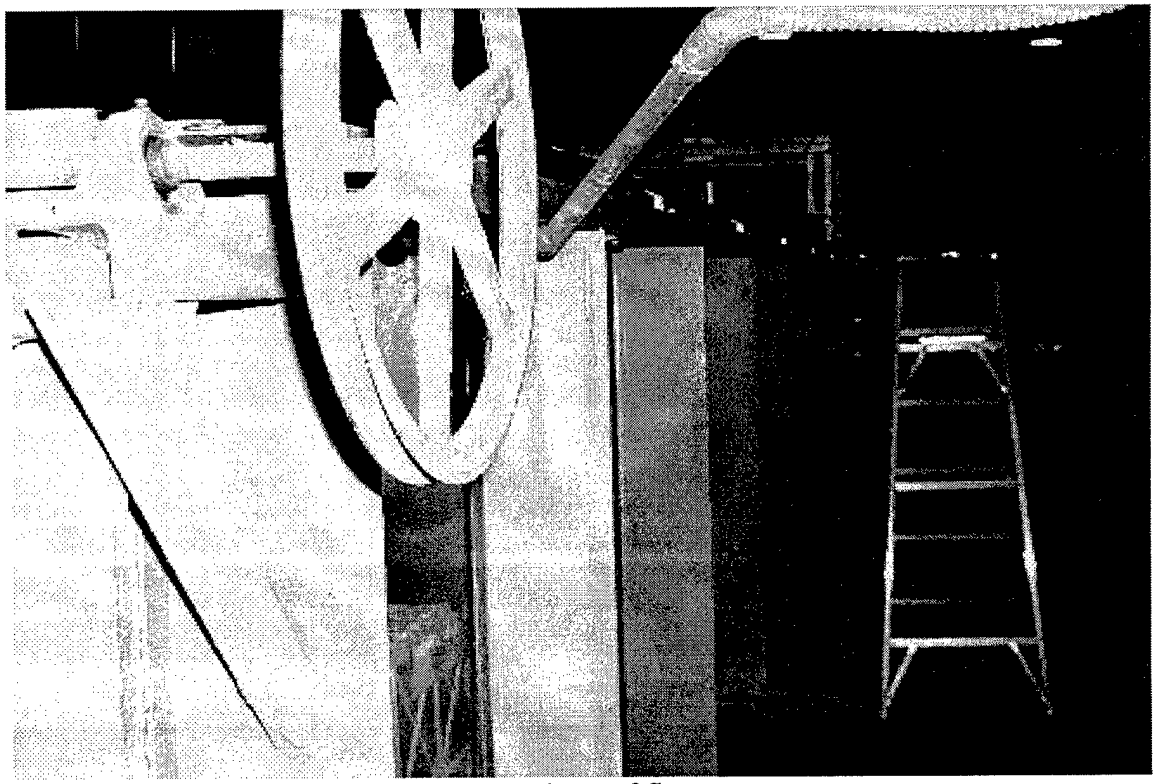
Close up photo of flume.

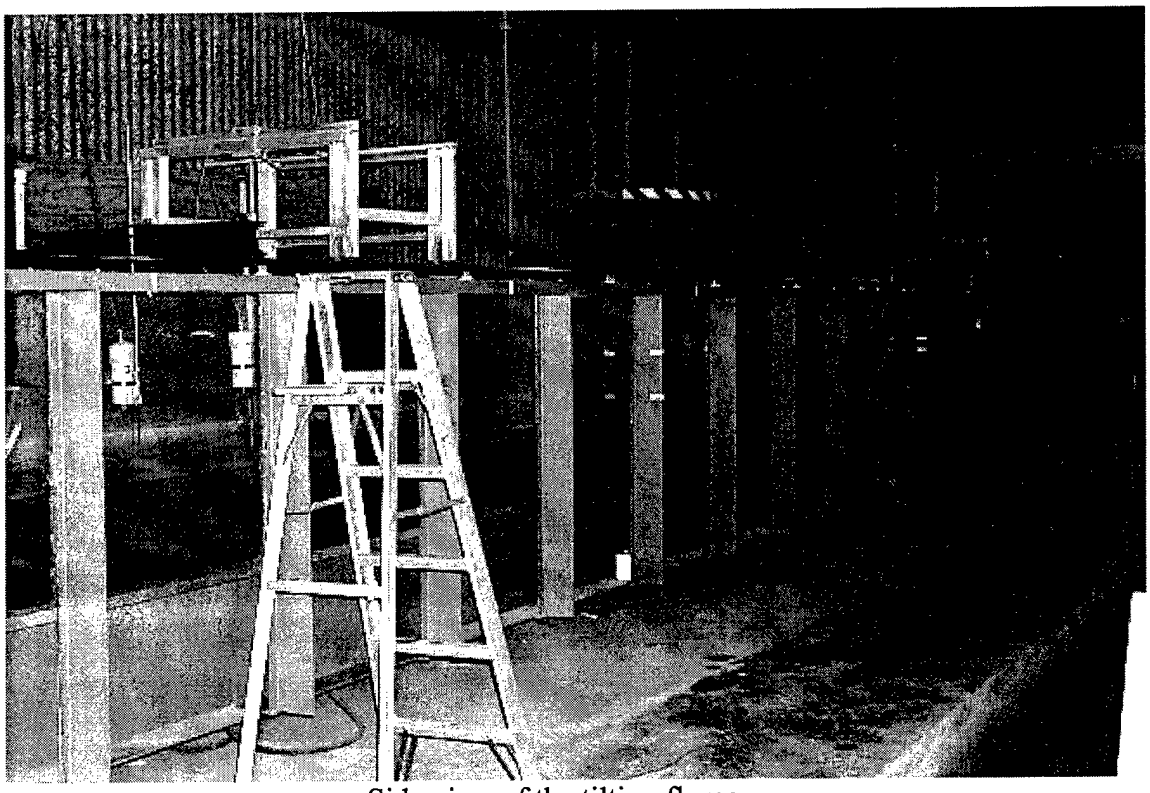

Side view of the tilting flume.

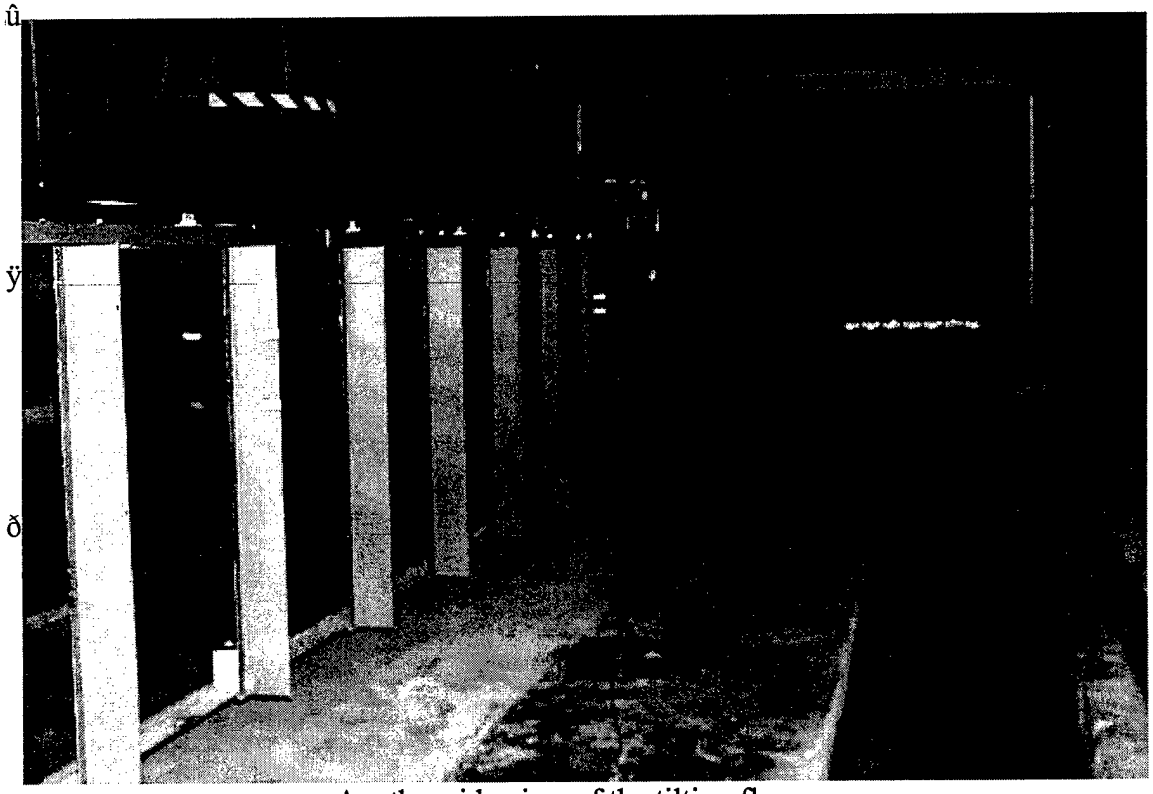

Another side view of the tilting flume.

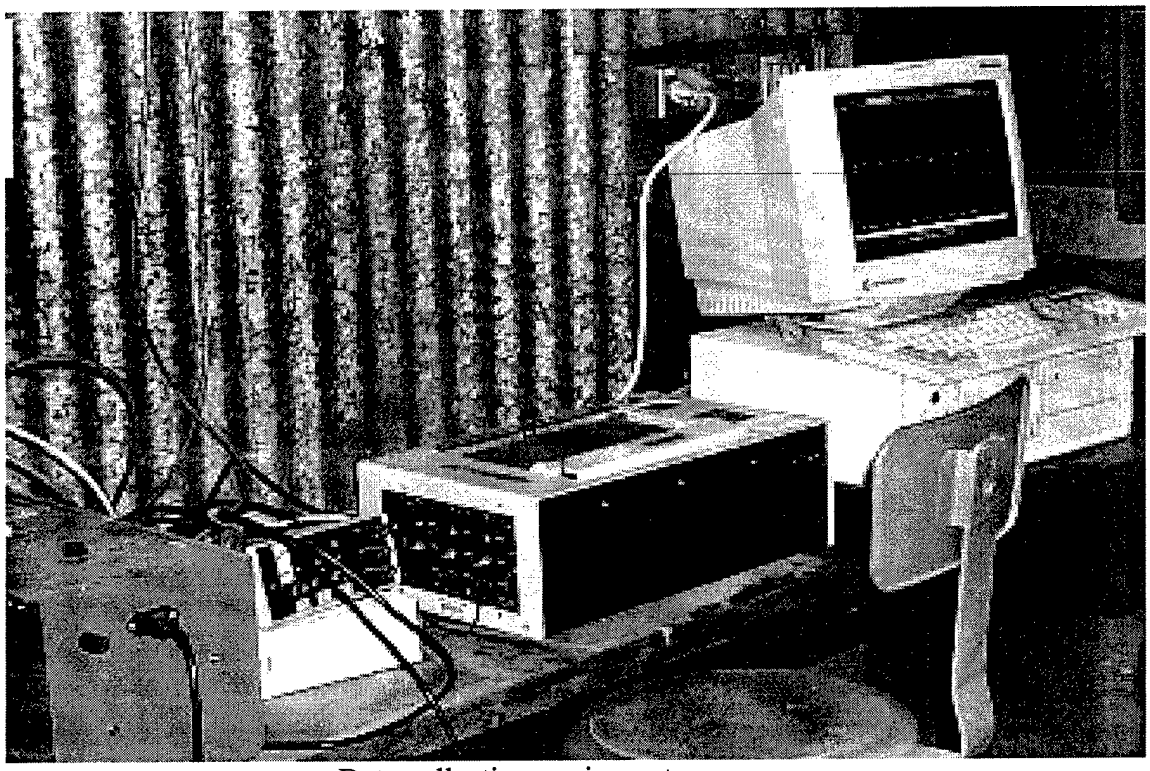

Data collection equipment.

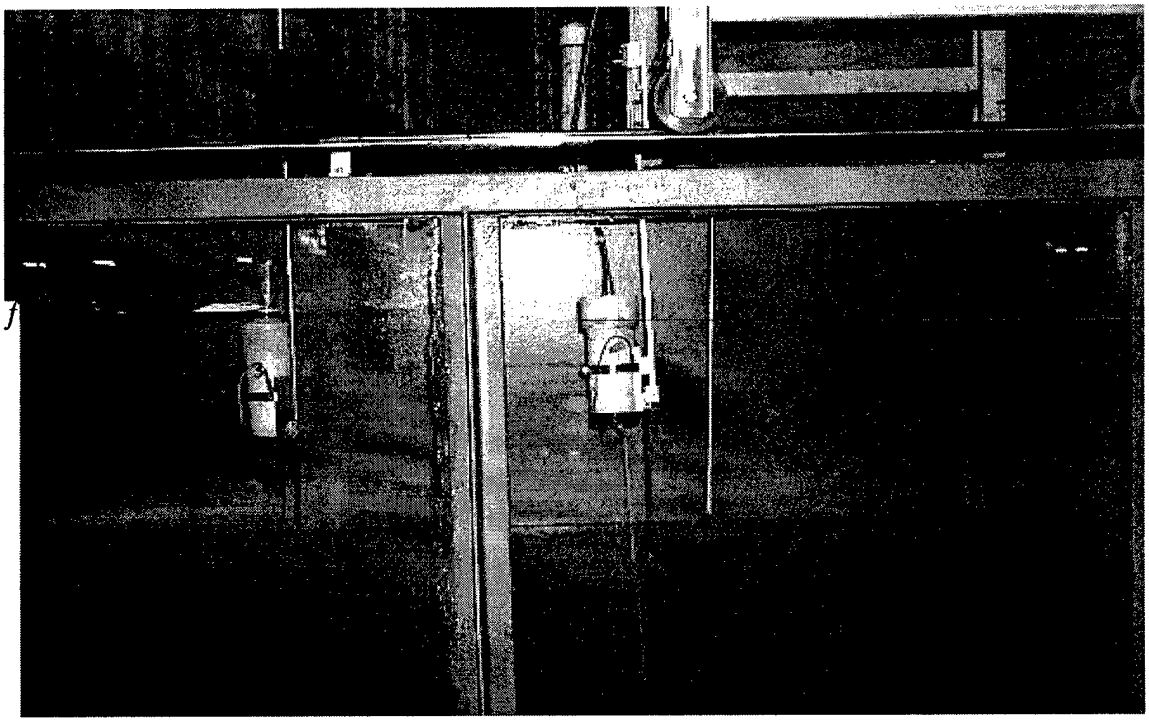

Resistance wave guages.

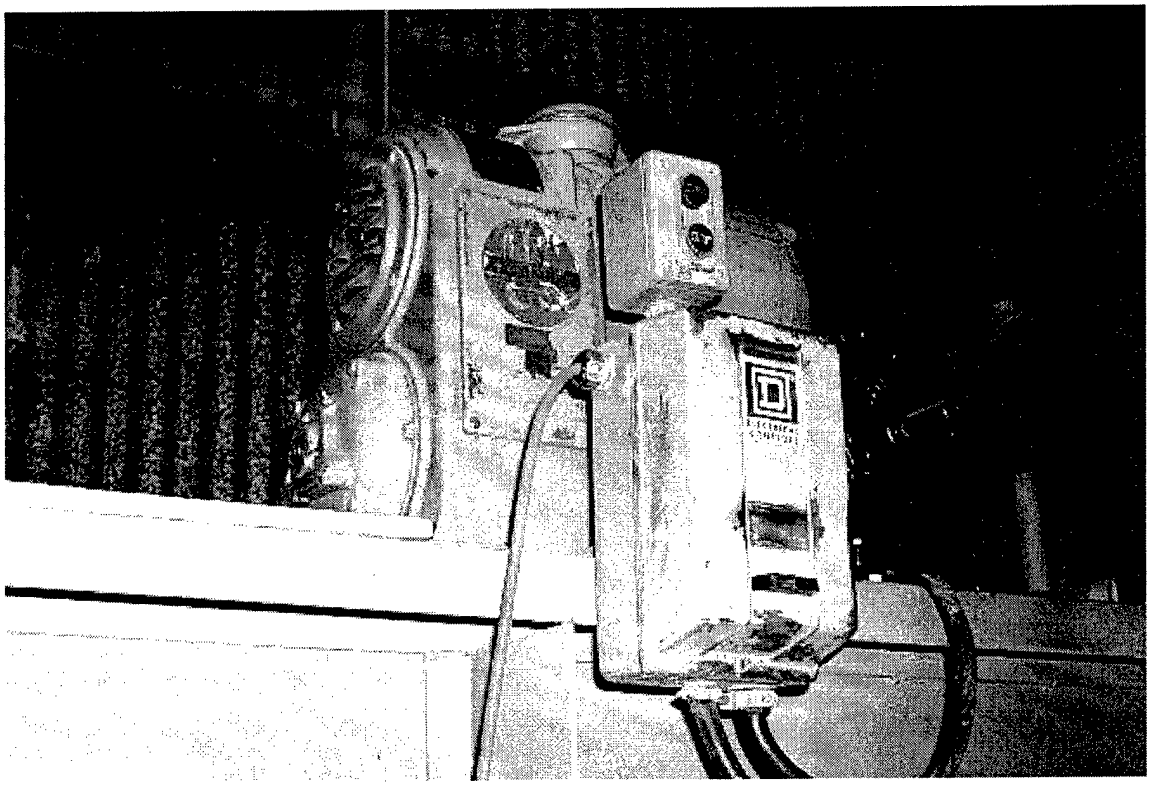

Wave maker motor.

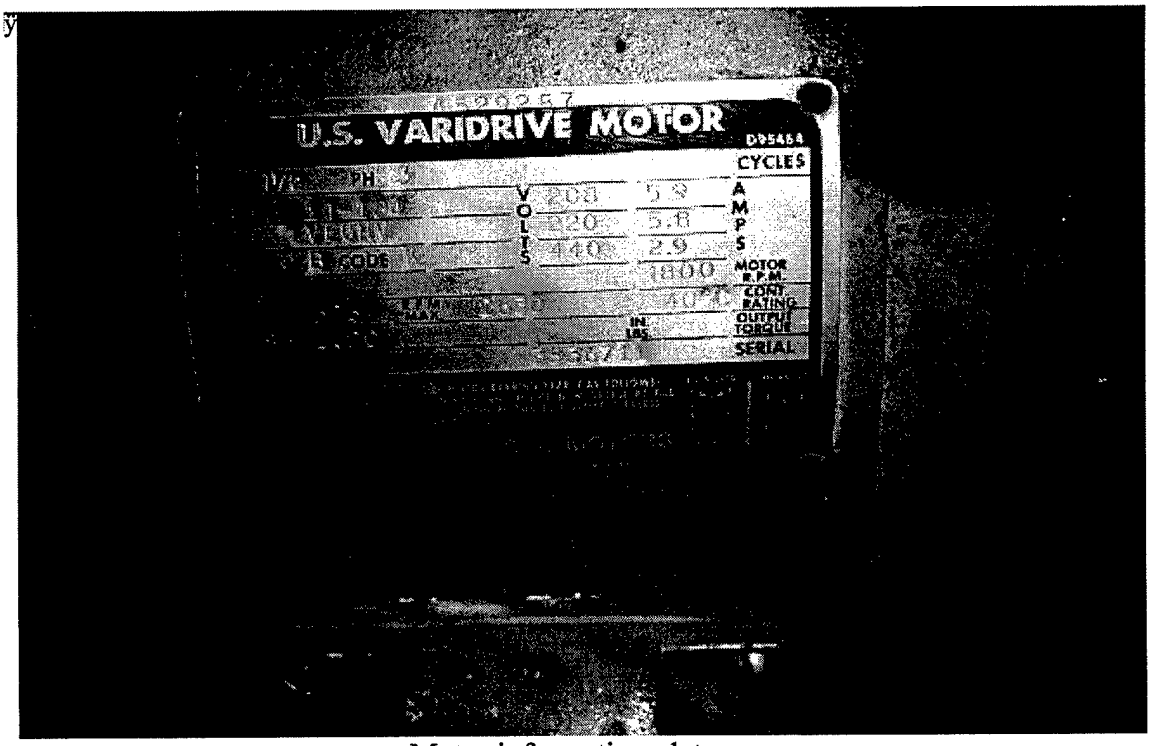

Motor information plate.

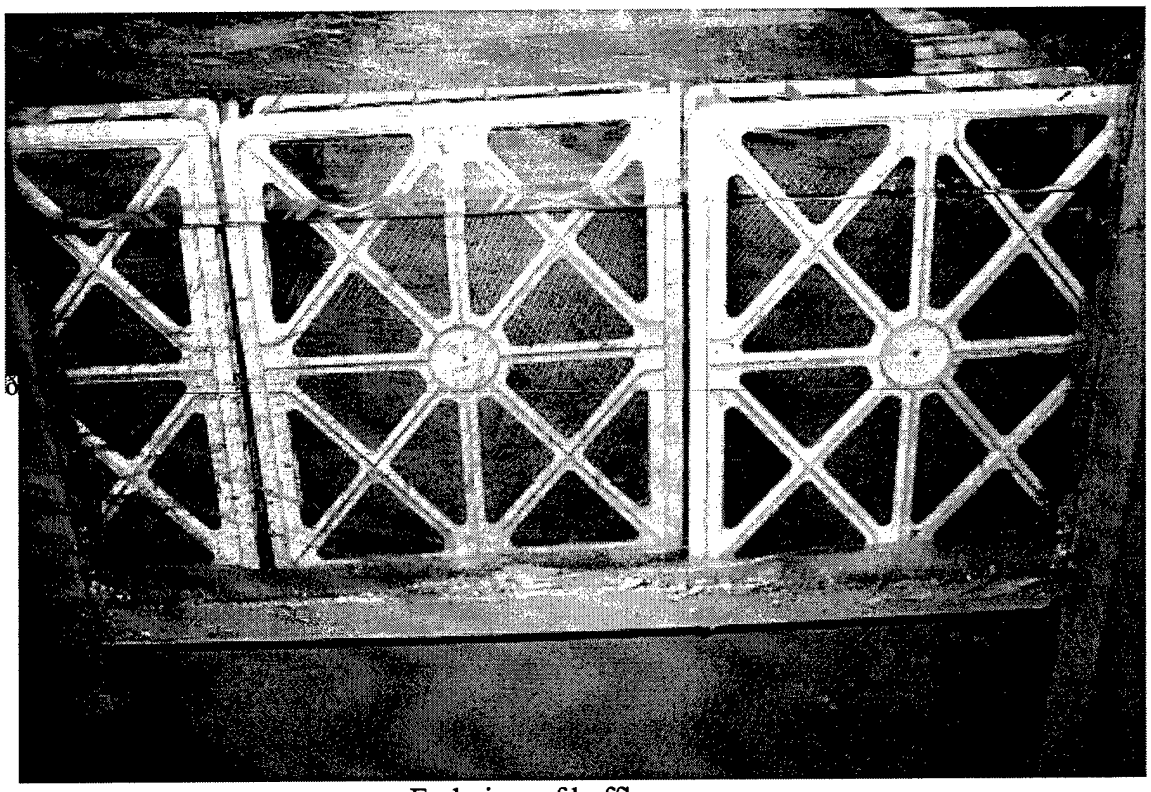

End view of baffles.

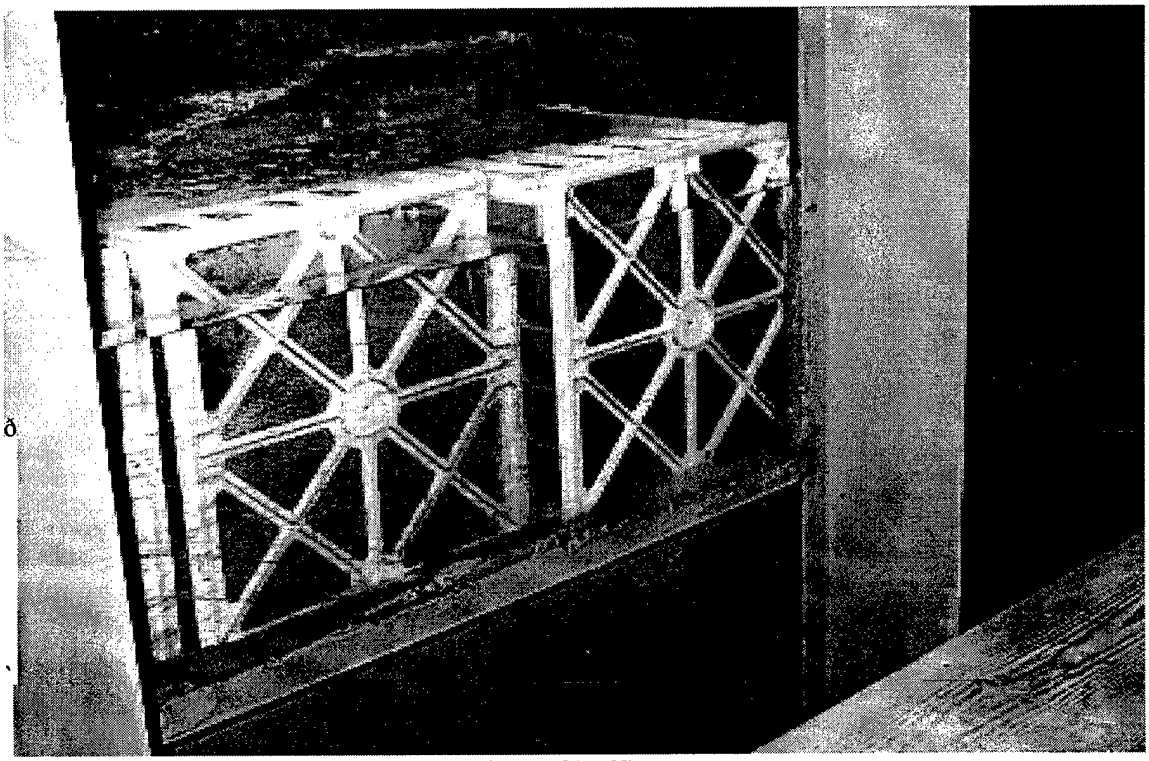

Side view of baffles.

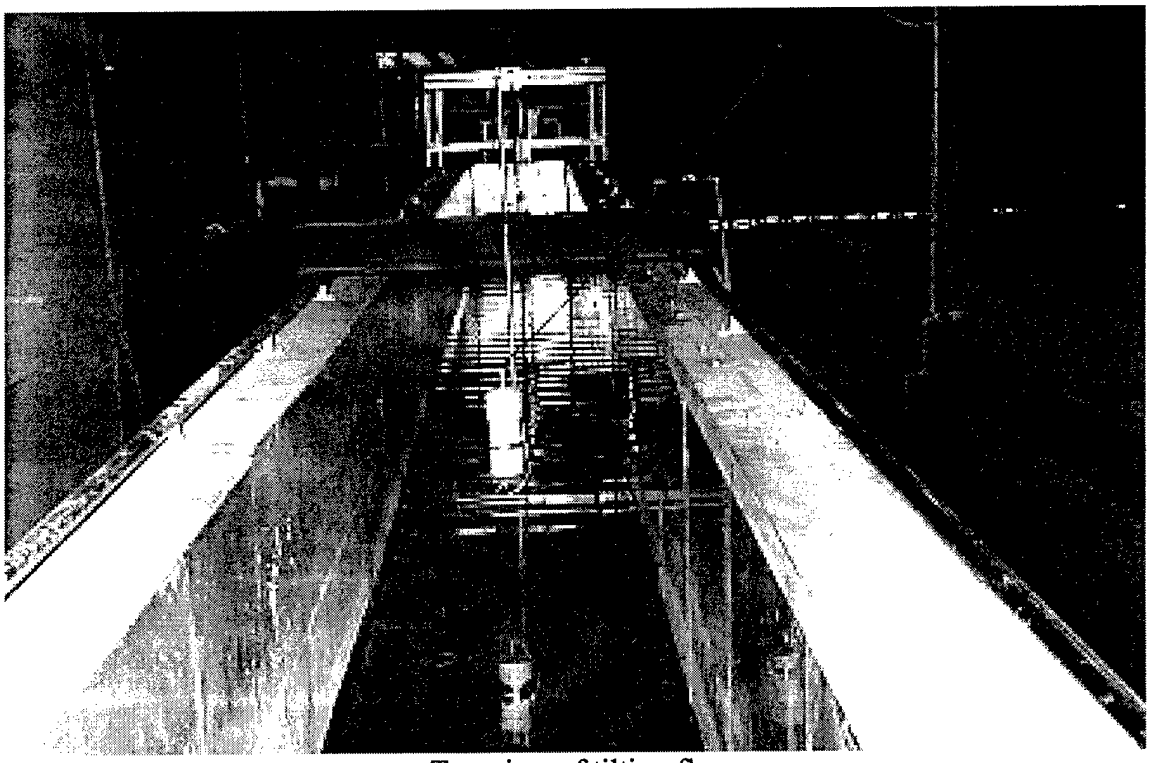

Top view of tilting flume.

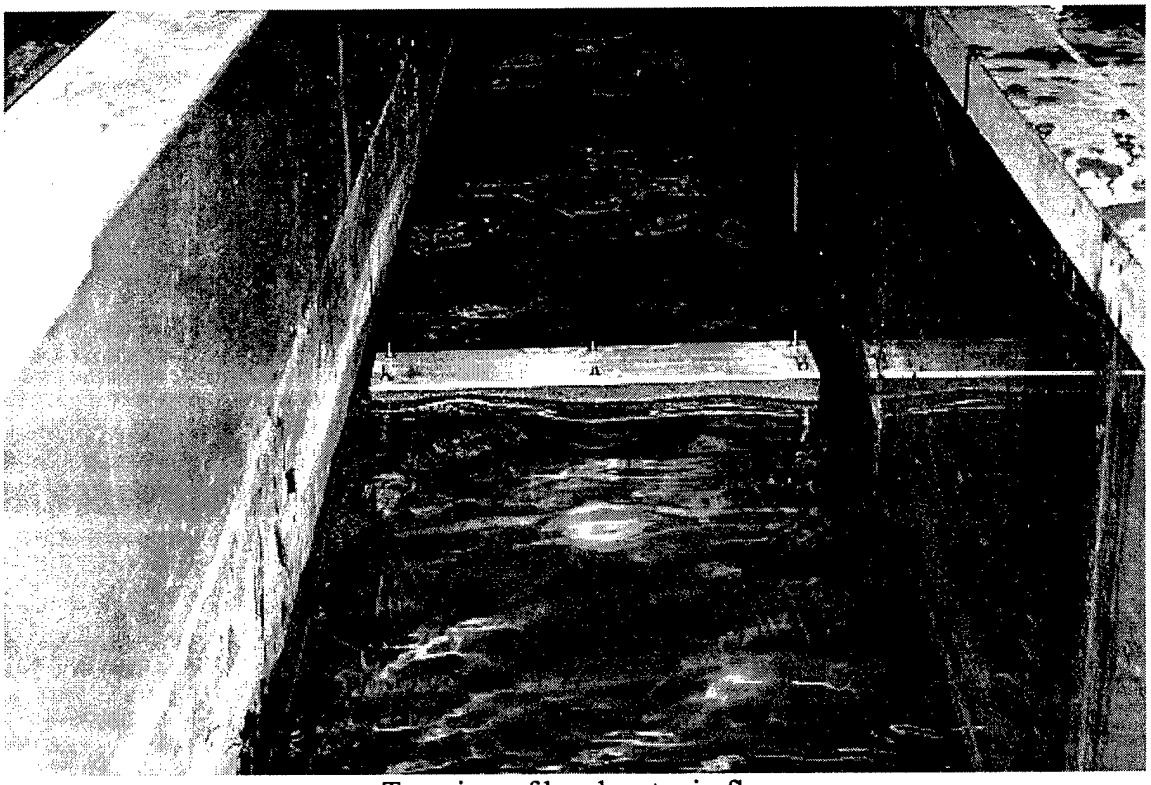

Top view of breakwater in flume.

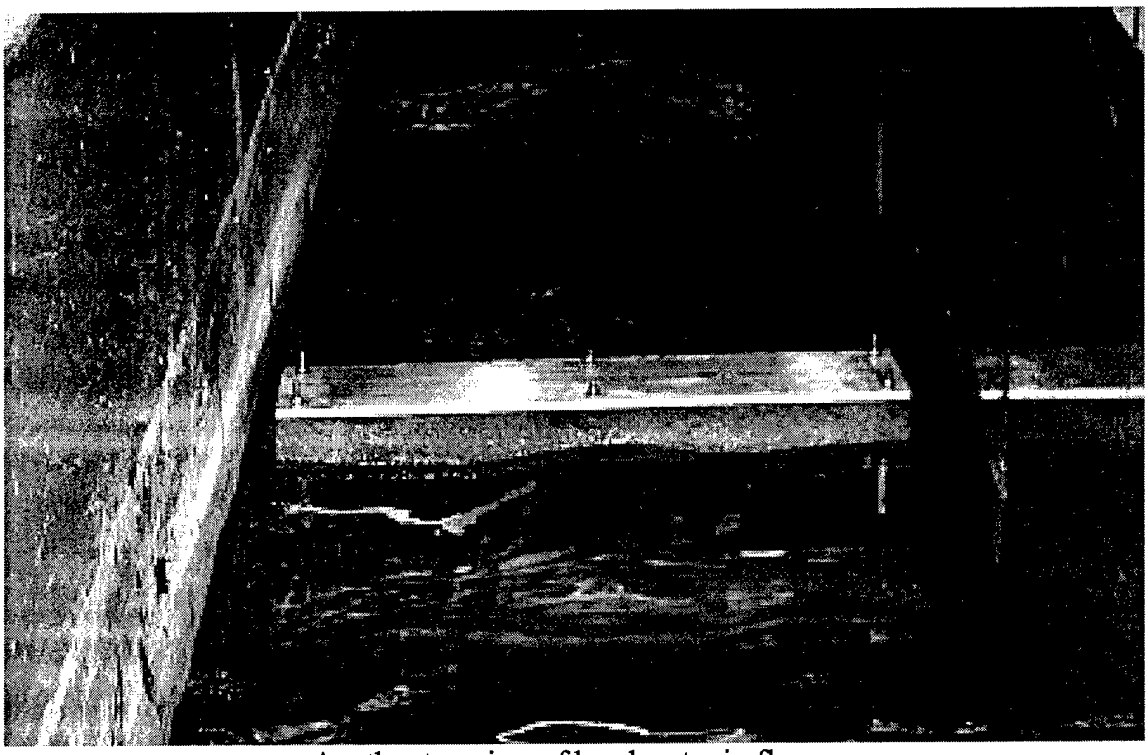

Another top view of breakwater in flume.

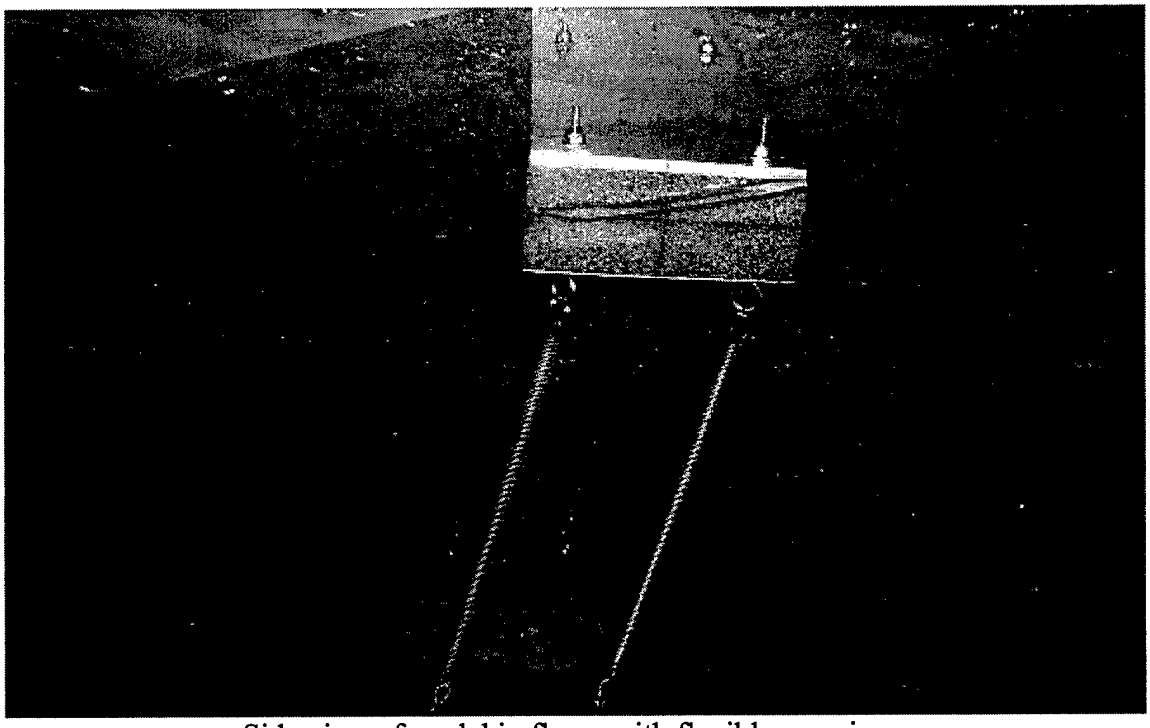

Side view of model in flume with flexible moorings.

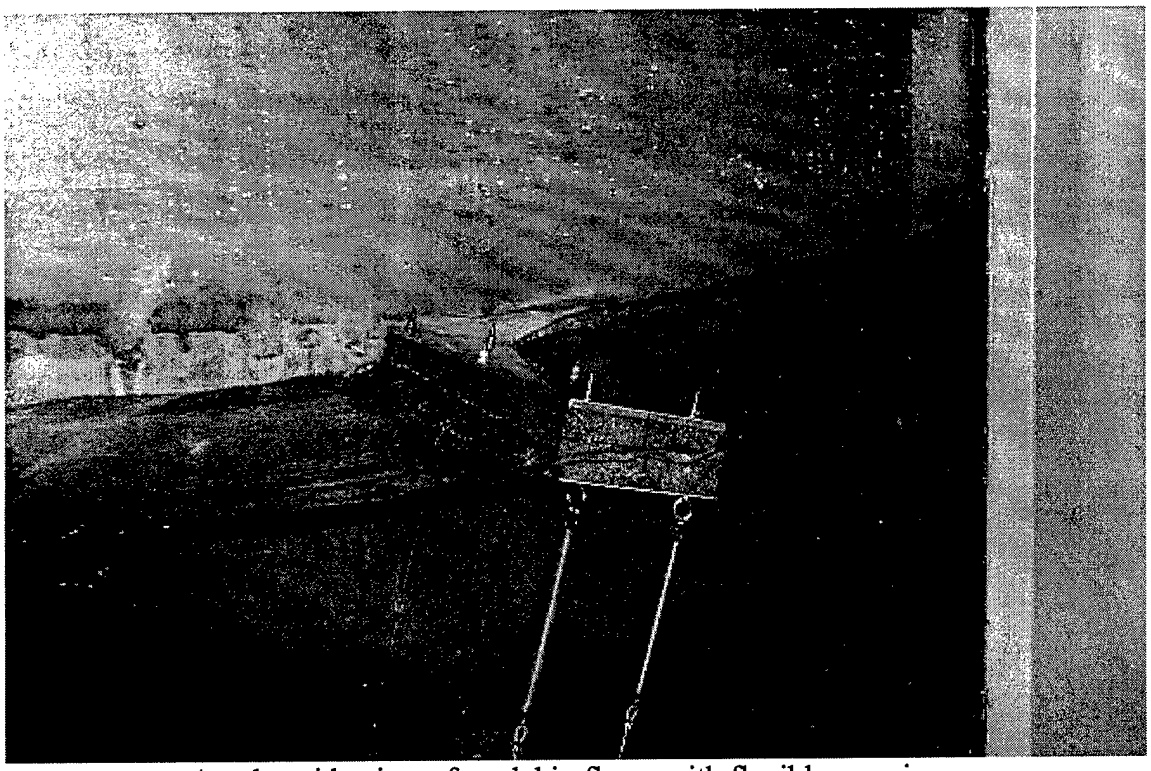

Another side view of model in flume with flexible moorings.

Side view of model in flume with flexible moorings and ¼- length membrane.

Another view of model in flume with flexible moorings and ¼- length membrane.

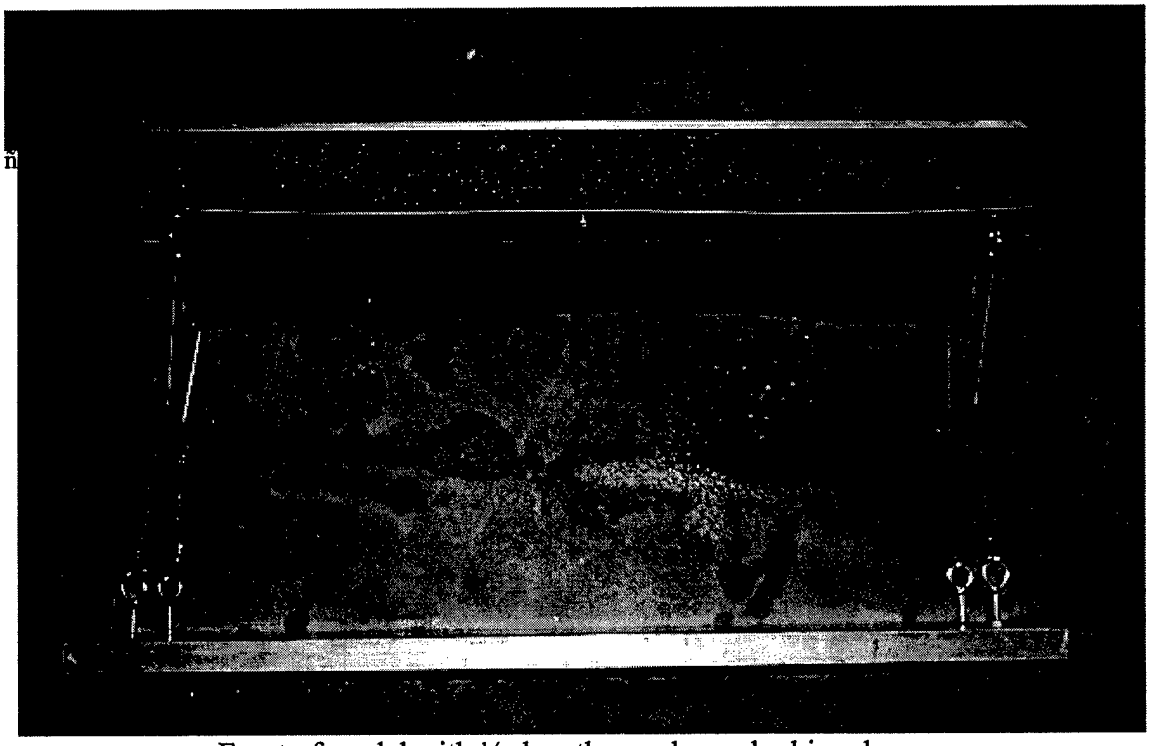

Front of model with ¼- length membrane looking down.

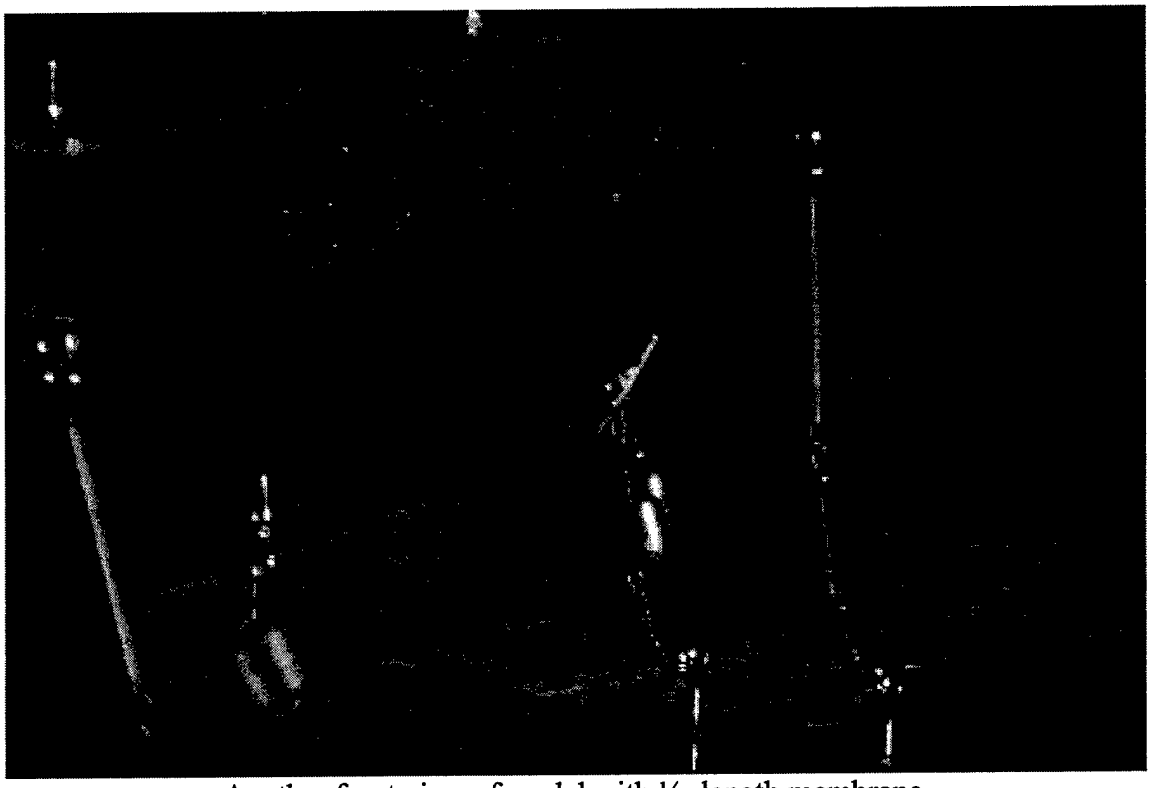

Another front view of model with ¼- length membrane.

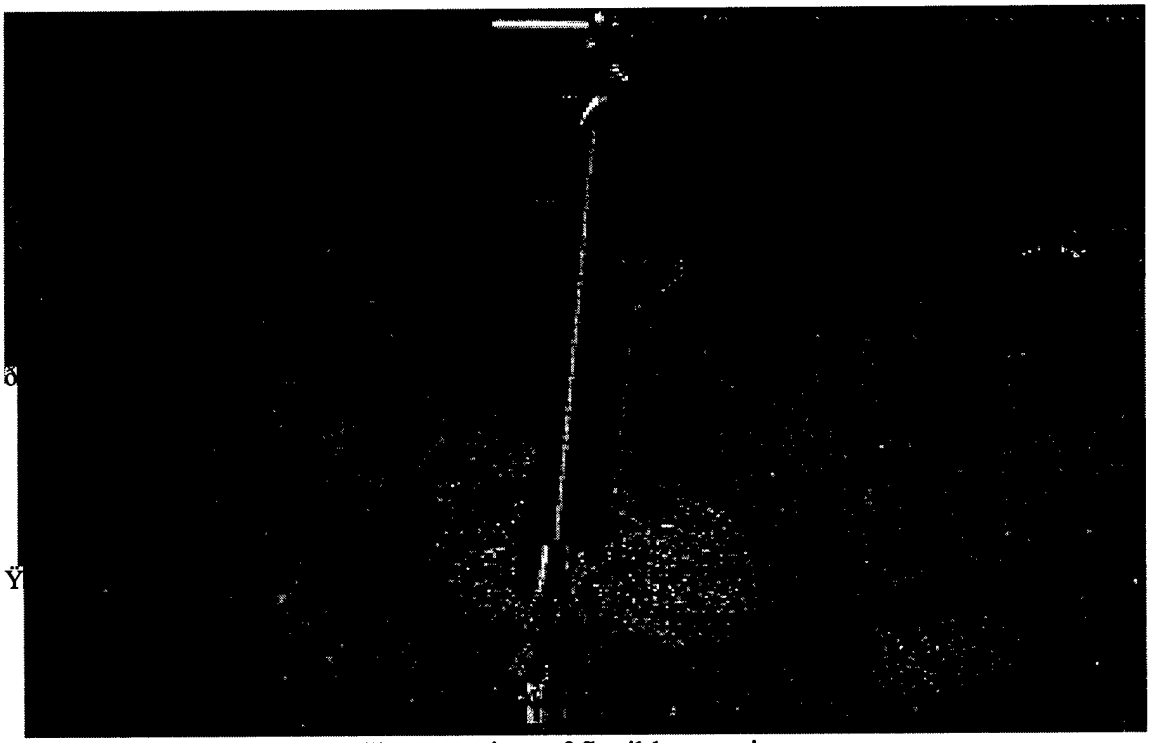

Close up view of flexible mooring.

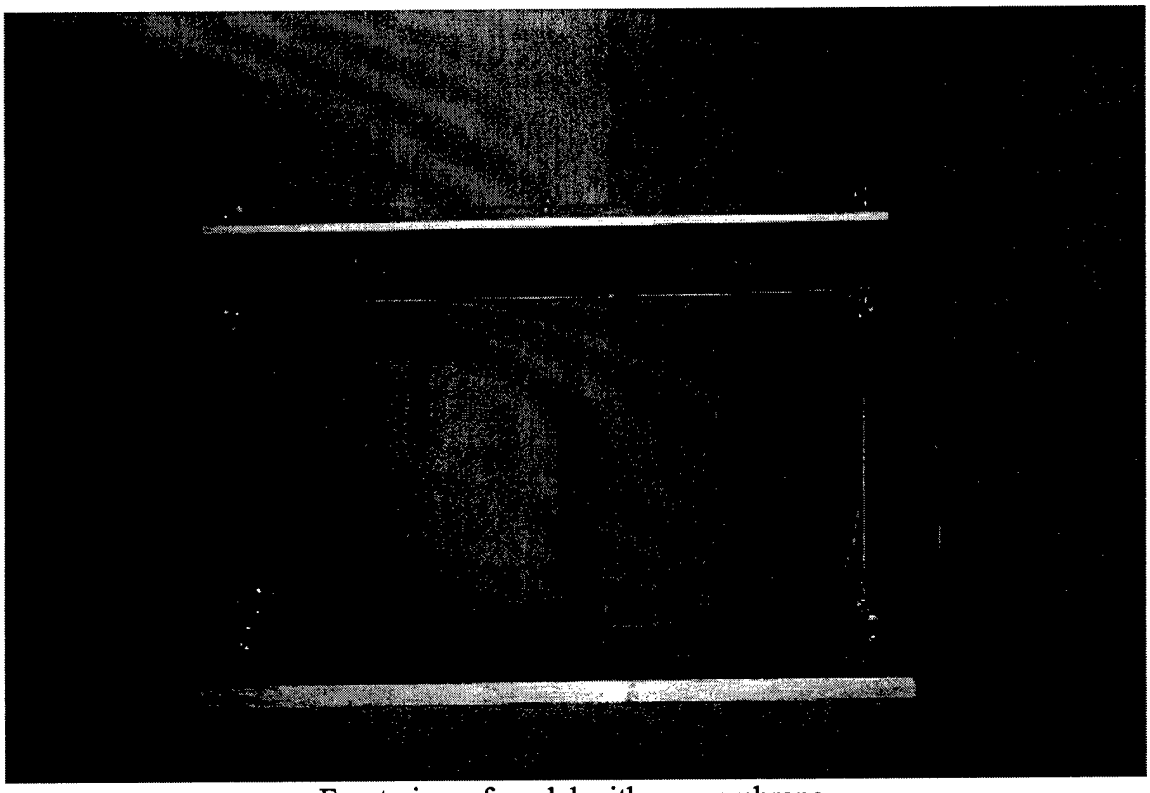

Front view of model with no membrane.

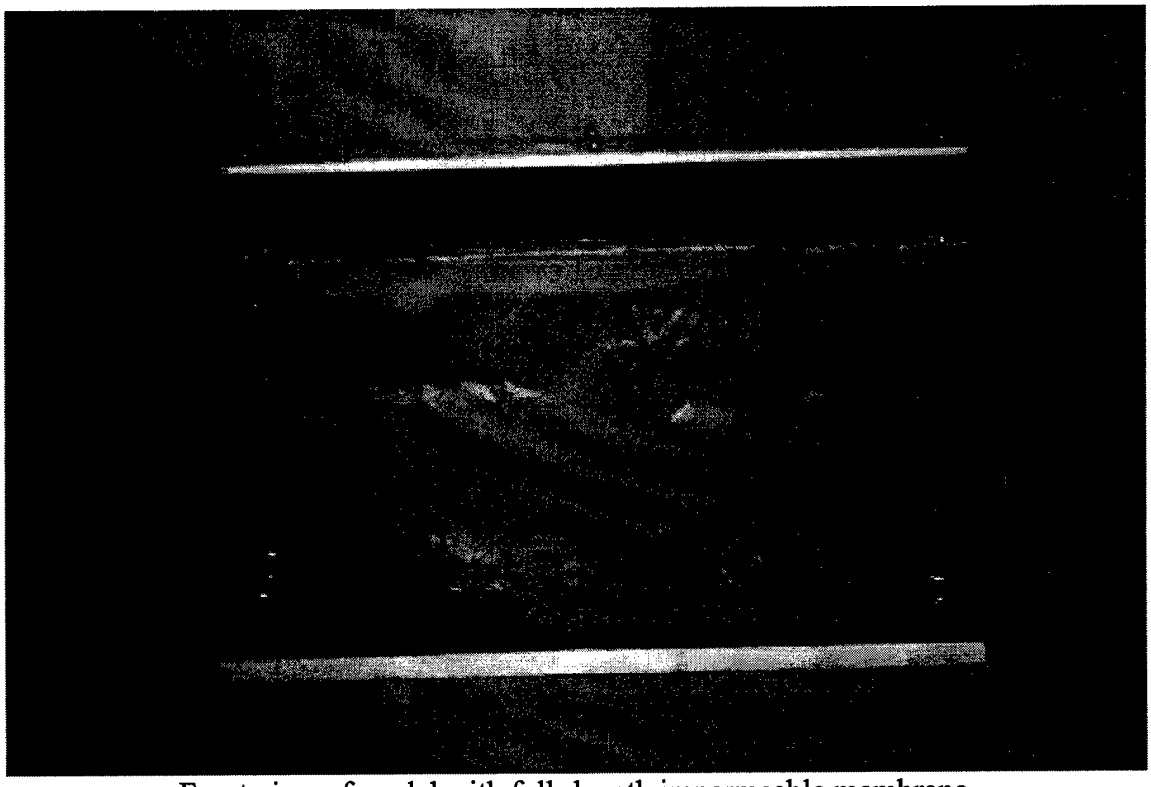

Front view of model with full- length impermeable membrane.

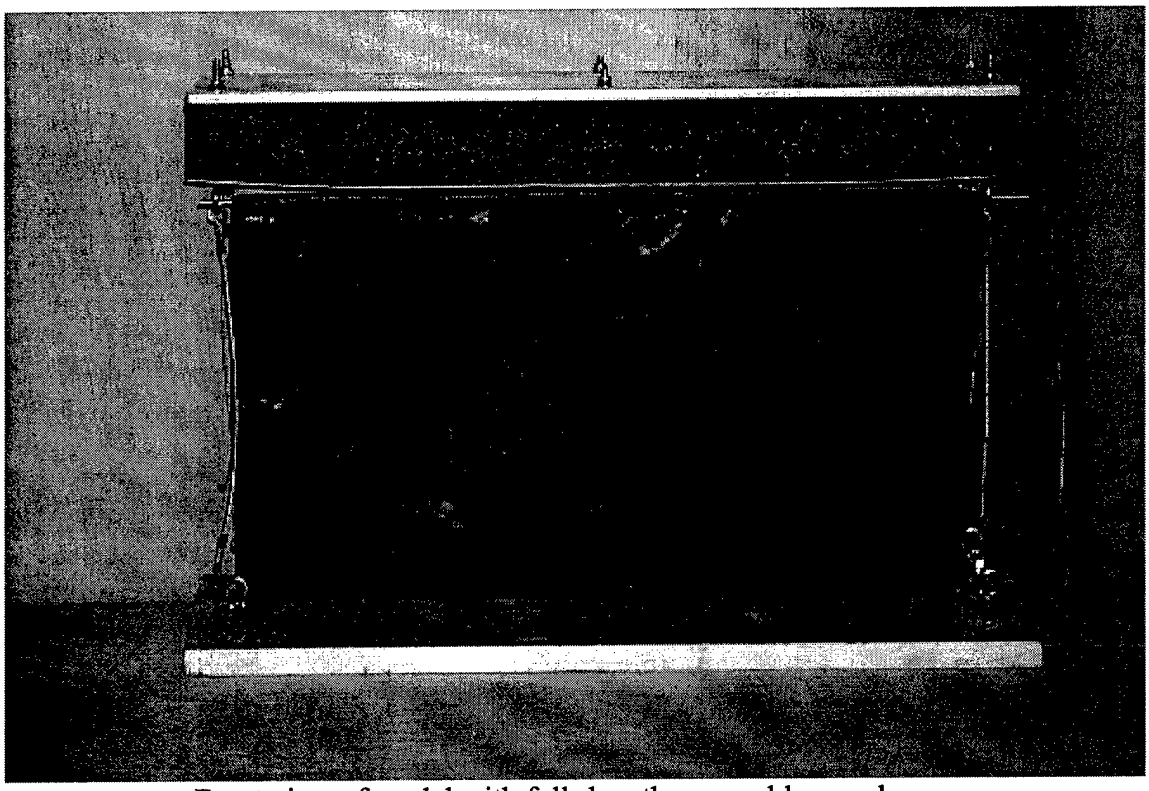

Front view of model with full- length permeable membrane.

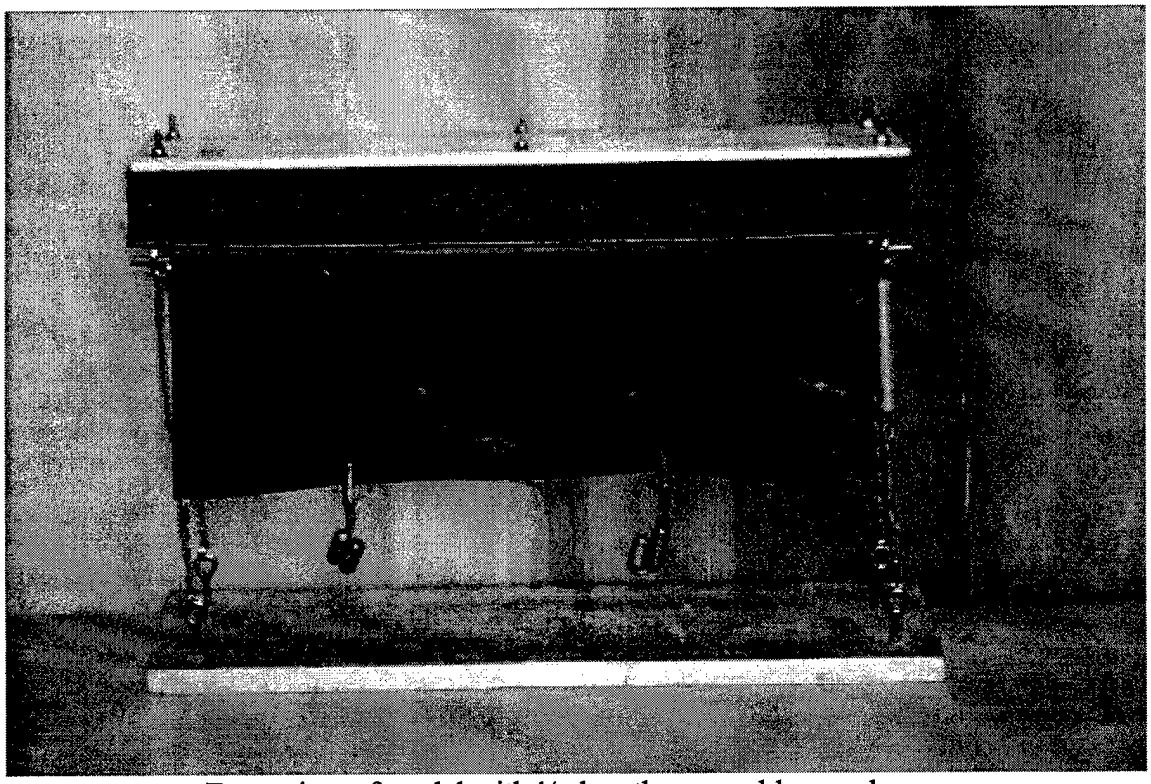

Front view of model with ½- length permeable membrane.

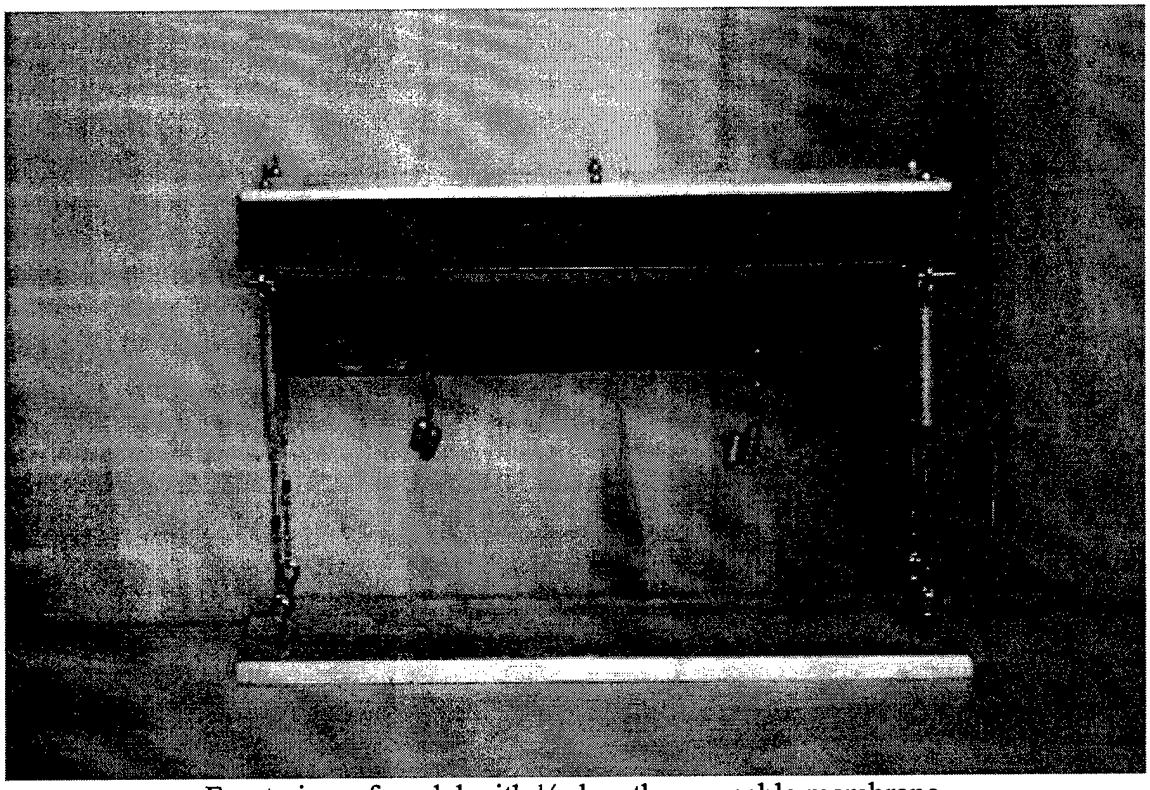

Front view of model with ¼- length permeable membrane.

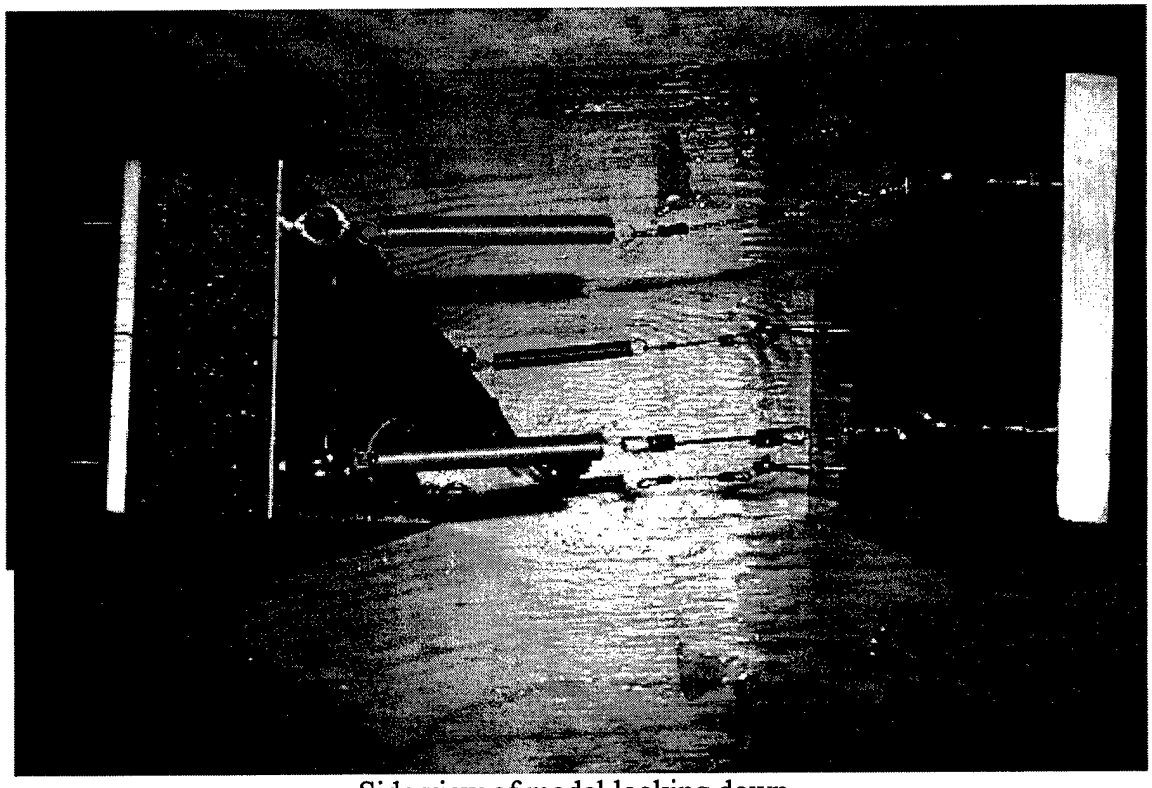

Side view of model looking down.

APPENDIX D
NATURAL PERIODS OF OSCILLATION

Configuration Description	Measured Natural Periods of Oscillation (s)		
	Surge	Heave	Pitch
Stiff moorings, no membrane	2.2	n/a*	n/a*
Stiff moorings, 1/4-length membrane	2.2	n/a*	n/a*
Stiff moorings, 1/2-length membrane	2.3	n/a*	n/a*
Stiff moorings, full-length membrane	3.1	n/a*	n/a*
Flexible moorings, no membrane	2.2	0.5	0.4
Flexible moorings, 1/4-length membrane	2.2	0.6	0.8
Flexible moorings, 1/2-length membrane	2.2	0.5	0.7
Flexible moorings, full-length membrane	1.6	0.8	0.5

* Measurement could not be made in laboratory due to high mooring stiffness.

LIST OF REFERENCES

Crull W.W. and Williams, A.N., 1993. Wave diffraction by array of thin-screened breakwaters. *Journal of Waterway, Port, Coastal, and Ocean Engineering, 119*(6), pp.606-617.

Lee, C., McDougal, W.G., Sollitt C.K. and Thomas, J.P., 1986. Mechanically coupled flap type breakwaters: theory and experiment. *Proceedings from the Ocean Structural Dynamics Symposium,* pp.730-757.

Chwang, A.T., 1983. A porous-wavemaker theory. *Journal of Fluid Mechanics*, 132, pp. 395-406.

Dalrymple, R.A. and Dean, R.G., 1991. *Water Wave Mechanics for Engineers and Scientists*, World Scientific Publishing Co., New Jersey.

Geiger, P.T., McDougal, W.G. and Williams, A.N., 1992. A submerged compliant breakwater. *Journal of Offshore Mechanics and Offshore Engineering,* 114, pp. 83-90.

Huang, Z., Lee, H.S. and Williams, A.N., 2000. Floating pontoon breakwater. *Ocean Engineering,* 27, pp. 221-240.

Leach, P.A., McDougal, W.G., Sollitt, C.K. and Lui, W., 1985. Hinged floating breakwaters. *Journal of Waterway, Port, Coastal, and Ocean Engineering,* 111(5), pp.895-909.

Lin, D.T. and Twu, S.W., 1991. On a highly effective wave absorber. *Coastal Engineering*, (15), pp. 389-405.

McDougal, W.G. and Williams, A.N., 2001. Floating porous membrane wave barrier. *Proceedings of OMAE 2001 20th International Conference on Offshore Mechanics and Arctic Engineering*, June 3-8, Rio de Janeiro, Brazil.

McDougal, W.G. and Williams, A.N., 1996. A dynamic submerged breakwater. *Journal of Waterway, Port, Coastal, and Ocean Engineering, 122*(6), pp.288-296.

McDougal, W.G., Sollitt, C.K. and Lui, W., 1992. Vertical membrane floating breakwater. *Acta Oceanologica Sinica*, 11(4), pp. 603-624.

McDougal, W.G. and Williams, A.N., 1991. Flexible floating breakwater. *Journal of Waterway, Port, Coastal, and Ocean Engineering,* 117(5), pp.429-450.

Rosner, J.C., 1992. A dynamic submerged breakwater. *M.S. thesis*, Oregon State University, Corvallis.

Williams, A.N., 1996. Floating membrane breakwater. *Journal of Offshore Mechanics and Offshore Engineering,* 118, pp. 46-50.

www.bellingham-marine.com/attenuators.html

www.oldcastle-precast.com/Oldcastle_Precast

BIOGRAPHICAL SKETCH

Michael Hermanson was born in Livermore, California and relocated with his family to Grants Pass, Oregon when he was 4 years of age where he spent the remainder of his youth. He graduated from North Valley High school in 1988 and started college in Fall of that year. After one year of college he decided to join the United States Navy. He competed 5 years of naval service before returning to college full-time. He graduated in 1998 with a Bachelor of Science degree in Civil Engineering from Oregon State University. While at OSU, he completed two Ocean Engineering classes that sparked his interest in the Ocean Engineering field. He returned to naval service upon graduation from OSU and was stationed in Twentynine Palms, California where he was assigned as the base Facilities Planning Officer for a Marine Corps base. Two years later he was reassigned to Great Lakes, Illinois where he managed construction projects for the Navy. In the winter of 2001, the author applied for graduate school to the Department of Civil and Coastal Engineering at the University of Florida. His application was accepted and he commenced his graduate studies at UF in the Fall of 2002. Upon graduation in December 2003, he will attend diving school at the Naval Diving and Salvage Center located in Panama City, Florida then report to the Navy's Underwater Construction Team Two located in Port Hueneme, California.